

SYNTHESIS AND ANALYTICAL STUDIES ON METAL COMPLEXES FOR C-H BOND ACTIVATION

A DISSERTATION
*Submitted in partial fulfillment of the
requirements for the award of the degree*
of
MASTER OF TECHNOLOGY
in
ADVANCED CHEMICAL ANALYSIS

By
SHILPI AGGARWAL



DEPARTMENT OF CHEMISTRY
INDIAN INSTITUTE OF TECHNOLOGY ROORKEE
ROORKEE - 247 667 (INDIA)
JUNE, 2008

CANDIDATE'S DECLARATION

I hereby certify that the work which is being presented in this dissertation entitled "**Synthesis and analytical studies on metal complexes for C-H bond activation**" in partial fulfillment of the requirement for the award of the degree of **Master of Technology in Advanced Chemical Analysis**, submitted in the Department of Chemistry of Indian Institute of Technology Roorkee, India, is an authentic record of my work carried out during the period from July, 2007 to June, 2008 under the supervision of **Dr U.P. Singh**, Professor, Department of Chemistry Indian Institute of Technology Roorkee, Roorkee.

The matter embodied in this dissertation has not been submitted by me for the award of any other degree.

I.I.T.Roorkee

Date: 26th June, 2008



(SHILPI AGGARWAL)

This is to certify that the above statement made by the candidate is correct to the best of our knowledge.



(Dr. U.P. Singh)

Professor

Department of Chemistry

Indian Institute of Technology, Roorkee

Roorkee-247667

ACKNOWLEDGEMENTS

Gratitude is the memory of heart and in carrying out this seminar work, persistent inspiration, unflinching support and encouragement of countless persons have served as the driving force.

I am completely indebted to my guide Dr. U.P. Singh, Professor, Department of Chemistry, Indian Institute of Technology Roorkee, Roorkee without whom this concept of working in the area of the "Synthesis and analytical studies on metal complexes for C-H bond activations" would not have taken birth in my mind. I would like to sincerely acknowledge his valuable guidance, relentless support, discerning thoughts and load of inspiration that led forward to develop deeper into the issue.

I am highly thankful to Dr. Kamaluddin, Professor and Head, Department of Chemistry, Indian Institute of Technology Roorkee, Roorkee and Dr. Ravi Bhushan, Professor and ex-Head, Department of Chemistry, Indian Institute of Technology Roorkee, Roorkee for providing me all the necessary facilities in the department to complete this work.

I would also like to thank my family for their continuous support and blessings throughout my education.

I would like to especially thank Ms. Sujata Kashyap for her kind cooperation and pleasant manner. Special thanks are due to Mrs. Pooja Tyagi, Mr. Vaibhave Aggarwal, Ms. Nidhi Goyal and Mr. Sandeep Singh of Bioinorganic Lab.

I am thankful to my friends Shailesh, Rahul, Payal Tyagi, Nidhi Tyagi, Himani, Shobha, Tanvi, Vaani, Nidhi and Susheela for their love, support and constant motivation.

Place: Roorkee

Date: 26th June, 2008

(SHILPI AGGARWAL)

I.I.T. Roorkee

ABSTRACT

The reaction of iron (II) chloride with 3,5-diisopropylpyrazole resulted in the formation of $[(3,5\text{-Pr}^i_2\text{pzH})_2\text{FeCl}_2]$. The same reaction mixture in presence of different para substituted benzoate ($p\text{-X-OBz}$) and excess amount of H_2O_2 gave mononuclear Fe(III) complex $[\text{Fe}(3\text{-OCMe}_2,5\text{-Pr}^i_2\text{pz})_3].2\text{X-OBz}$ (where X = H, Cl, F, CH_3 , OCH_3 , CHO, CN, NH_2 , NO_2). In these complexes one of the methine groups present in each of three 3,5-diisopropylpyrazole rings were oxidized during oxidation and coordinated to iron centre. These complexes were characterized by elemental analysis, IR, UV-Visible and thermal studies.

CONTENTS

CANDIDATE'S DECLARATION	i
ACKNOWLEDGEMENT	ii
ABSTRACT	iii
CONTENTS	iv
LIST OF FIGURES	vii
LIST OF TABLES	ix
LIST OF SCHEMES	x
1. Introduction	1
1.1. Introduction and literature survey	2
1.2. Aim and scope	28
2. Experimental Details	29
2.1. Reagents used	30
2.2. Make and model of the instruments	31
2.3. Methods used for synthesis of ligand and complexes	31
2.3.1. Synthesis of 3,5-diisopropyl pyrazole [3,5-Pr ⁱ ₂ pzH]	31
2.3.2. Synthesis of sodium salts of various p-substituted benzoic acids	32
2.3.3. Screening of different metals	32
2.3.4. Synthesis of Fe(3,5-Pr ⁱ ₂ pzH) ₃ Cl ₂	33
2.3.5. Synthesis of [Fe(3-OCMe ₂ -5-Pr ⁱ pzH) ₃].2OBz	33
2.3.6. Synthesis of [Fe(3-OCMe ₂ -5-Pr ⁱ pzH) ₃].2Cl-OBz	33
2.3.7. Synthesis of [Fe(3-OCMe ₂ -5-Pr ⁱ pzH) ₃].2F-OBz	34
2.3.8. Synthesis of [Fe(3-OCMe ₂ -5-Pr ⁱ pzH) ₃].2CH ₃ -OBz	34
2.3.9. Synthesis of [Fe(3-OCMe ₂ -5-Pr ⁱ pzH) ₃].2OCH ₃ -OBz	34
2.3.10. Synthesis of [Fe(3-OCMe ₂ -5-Pr ⁱ pzH) ₃].2CHO-OBz	34
2.3.11. Synthesis of [Fe(3-OCMe ₂ -5-Pr ⁱ pzH) ₃].2CN-OBz	34

2.3.12 Synthesis of $[\text{Fe}(3\text{-OCMe}_2\text{-5-Pr}^i\text{pzH})_3].2\text{NH}_2\text{-OBz}$	35
2.3.13 Synthesis of $[\text{Fe}(3\text{-OCMe}_2\text{-5-Pr}^i\text{pzH})_3].2\text{NO}_2\text{-OBz}$	35
3. Results and Discussion	36
3.1 Results and discussions	37
4. Spectra	47
4.1 IR spectrum of $\text{Fe}(3,5\text{-Pr}^i_2\text{pzH})_3\text{Cl}_2$	48
4.2 IR spectrum of $[\text{Fe}(3\text{-OCMe}_2\text{-5-Pr}^i\text{pzH})_3].2\text{OBz}$	49
4.3 IR spectrum of $[\text{Fe}(3\text{-OCMe}_2\text{-5-Pr}^i\text{pzH})_3].2\text{Cl-OBz}$	50
4.4 IR spectrum of $[\text{Fe}(3\text{-OCMe}_2\text{-5-Pr}^i\text{pzH})_3].2\text{F-OBz}$	51
4.5 IR spectrum of $[\text{Fe}(3\text{-OCMe}_2\text{-5-Pr}^i\text{pzH})_3].2\text{CH}_3\text{-OBz}$	52
4.6 IR spectrum of $[\text{Fe}(3\text{-OCMe}_2\text{-5-Pr}^i\text{pzH})_3].2\text{OCH}_3\text{-OBz}$	53
4.7 IR spectrum of $[\text{Fe}(3\text{-OCMe}_2\text{-5-Pr}^i\text{pzH})_3].2\text{CHO-OBz}$	54
4.8 IR spectrum of $[\text{Fe}(3\text{-OCMe}_2\text{-5-Pr}^i\text{pzH})_3].2\text{CN-OBz}$	55
4.9 IR spectrum of $[\text{Fe}(3\text{-OCMe}_2\text{-5-Pr}^i\text{pzH})_3].2\text{NH}_2\text{-OBz}$	56
4.10 IR spectrum of $[\text{Fe}(3\text{-OCMe}_2\text{-5-Pr}^i\text{pzH})_3].2\text{NO}_2\text{-OBz}$	57
4.11 UV-Visible spectrum of $\text{Fe}(3,5\text{-Pr}^i_2\text{pzH})_3\text{Cl}_2$	58
4.12 UV-Visible spectrum of $[\text{Fe}(3\text{-OCMe}_2\text{-5-Pr}^i\text{pzH})_3].2\text{OBz}$	58
4.13 UV-Visible spectrum of $[\text{Fe}(3\text{-OCMe}_2\text{-5-Pr}^i\text{pzH})_3].2\text{Cl-OBz}$	59
4.14 UV-Visible spectrum of $[\text{Fe}(3\text{-OCMe}_2\text{-5-Pr}^i\text{pzH})_3].2\text{F-OBz}$	59
4.15 UV-Visible spectrum of $[\text{Fe}(3\text{-OCMe}_2\text{-5-Pr}^i\text{pzH})_3].2\text{CH}_3\text{-OBz}$	60
4.16 UV-Visible spectrum of $[\text{Fe}(3\text{-OCMe}_2\text{-5-Pr}^i\text{pzH})_3].2\text{OCH}_3\text{-OBz}$	60
4.17 UV-Visible spectrum of $[\text{Fe}(3\text{-OCMe}_2\text{-5-Pr}^i\text{pzH})_3].2\text{CHO-OBz}$	61
4.18 UV-Visible spectrum of $[\text{Fe}(3\text{-OCMe}_2\text{-5-Pr}^i\text{pzH})_3].2\text{CN-OBz}$	61
4.19 UV-Visible spectrum of $[\text{Fe}(3\text{-OCMe}_2\text{-5-Pr}^i\text{pzH})_3].2\text{NH}_2\text{-OBz}$	62
4.20 UV-Visible spectrum of $[\text{Fe}(3\text{-OCMe}_2\text{-5-Pr}^i\text{pzH})_3].2\text{NO}_2\text{-OBz}$	62
4.21 DTA-DTG-TG curve of $[\text{Fe}(3\text{-OCMe}_2\text{-5-Pr}^i\text{pzH})_3].2\text{OBz}$	63
4.22 DTA-DTG-TG curve of $[\text{Fe}(3\text{-OCMe}_2\text{-5-Pr}^i\text{pzH})_3].2\text{Cl-OBz}$	64
4.23 DTA-DTG-TG curve of $[\text{Fe}(3\text{-OCMe}_2\text{-5-Pr}^i\text{pzH})_3].2\text{F-OBz}$	65
4.24 DTA-DTG-TG curve of $[\text{Fe}(3\text{-OCMe}_2\text{-5-Pr}^i\text{pzH})_3].2\text{CH}_3\text{-OBz}$	66

4.25 DTA-DTG-TG curve of [Fe(3-OCMe ₂ -5-Pr ⁱ pzh) ₃].2OCH ₃ -OBz	67
4.26 DTA-DTG-TG curve of [Fe(3-OCMe ₂ -5-Pr ⁱ pzh) ₃].2CHO-OBz	68
4.27 DTA-DTG-TG curve of [Fe(3-OCMe ₂ -5-Pr ⁱ pzh) ₃].2CN-OBz	69
4.28 DTA-DTG-TG curve of [Fe(3-OCMe ₂ -5-Pr ⁱ pzh) ₃].2NH ₂ -OBz	70
4.29 DTA-DTG-TG curve of [Fe(3-OCMe ₂ -5-Pr ⁱ pzh) ₃].2NO ₂ -OBz	71
5. Conclusion	72
References	74

LIST OF FIGURES

Fig. No.	Title	Page No.
Fig. 1.1	An iron protoporphyrin complex	17
Fig. 1.2	Generally accepted mechanism for C-H bond activation by cytochrome P450	18
Fig. 1.3	Active site structures of MMOH _{ox} and MMOH _{red}	19
Fig. 1.4	Active site structures of MMOH _{ox} and MMOH _{red}	21
Fig. 4.1	IR spectrum of Fe(3,5-Pr ⁱ ₂ pzH) ₃ Cl ₂	48
Fig. 4.2	IR spectrum of [Fe(3-OCMe ₂ -5-Pr ⁱ pzH) ₃].2OBz	49
Fig. 4.3	IR spectrum of [Fe(3-OCMe ₂ -5-Pr ⁱ pzH) ₃].2Cl-OBz	50
Fig. 4.4	IR spectrum of [Fe(3-OCMe ₂ -5-Pr ⁱ pzH) ₃].2F-OBz	51
Fig. 4.5	IR spectrum of [Fe(3-OCMe ₂ -5-Pr ⁱ pzH) ₃].2CH ₃ -OBz	52
Fig. 4.6	IR spectrum of [Fe(3-OCMe ₂ -5-Pr ⁱ pzH) ₃].2OCH ₃ -OBz	53
Fig. 4.7	IR spectra of [Fe(3-OCMe ₂ -5-Pr ⁱ pzH) ₃].2CHO-OBz	54
Fig. 4.8	IR spectra of [Fe(3-OCMe ₂ -5-Pr ⁱ pzH) ₃].2CN-OBz	55
Fig. 4.9	IR spectrum of [Fe(3-OCMe ₂ -5-Pr ⁱ pzH) ₃].2NH ₂ -OBz	56
Fig. 4.10	IR spectrum of [Fe(3-OCMe ₂ -5-Pr ⁱ pzH) ₃].2NO ₂ -OBz	57
Fig. 4.11	UV-Visible spectrum of Fe(3,5-Pr ⁱ ₂ pzH) ₃ Cl ₂	58
Fig. 4.12	UV-Visible spectrum of [Fe(3-OCMe ₂ -5-Pr ⁱ pzH) ₃].2OBz	58
Fig. 4.13	UV-Visible spectrum of [Fe(3-OCMe ₂ -5-Pr ⁱ pzH) ₃].2Cl-OBz	59

Fig. 4.14	UV-Visible spectrum of [Fe(3-OCMe ₂ -5-Pr ⁱ pzH) ₃].2F-OBz	59
Fig. 4.15	UV-Visible spectrum of [Fe(3-OCMe ₂ -5-Pr ⁱ pzH) ₃].2CH ₃ -OBz	60
Fig. 4.16	UV-Visible spectrum of [Fe(3-OCMe ₂ -5-Pr ⁱ pzH) ₃].2OCH ₃ -OBz	60
Fig. 4.17	UV-Visible spectra of [Fe(3-OCMe ₂ -5-Pr ⁱ pzH) ₃].2CHO-OBz	61
Fig. 4.18	UV-Visible spectra of [Fe(3-OCMe ₂ -5-Pr ⁱ pzH) ₃].2CN-OBz	61
Fig. 4.19	UV-Visible spectrum of [Fe(3-OCMe ₂ -5-Pr ⁱ pzH) ₃].2NH ₂ -OBz	62
Fig. 4.20	UV-Visible spectrum of [Fe(3-OCMe ₂ -5-Pr ⁱ pzH) ₃].2NO ₂ -OBz	62
Fig. 4.21	DTA-DTG-TG curve of [Fe(3-OCMe ₂ -5-Pr ⁱ pzH) ₃].2OBz	63
Fig. 4.22	DTA-DTG-TG curve of [Fe(3-OCMe ₂ -5-Pr ⁱ pzH) ₃].2Cl-OBz	64
Fig. 4.23	DTA-DTG-TG curve of [Fe(3-OCMe ₂ -5-Pr ⁱ pzH) ₃].2F-OBz	65
Fig. 4.24	DTA-DTG-TG curve of [Fe(3-OCMe ₂ -5-Pr ⁱ pzH) ₃].2CH ₃ -OBz	66
Fig. 4.25	DTA-DTG-TG curve of [Fe(3-OCMe ₂ -5-Pr ⁱ pzH) ₃].2OCH ₃ -OBz	67
Fig. 4.26	DTA-DTG-TG curve of [Fe(3-OCMe ₂ -5-Pr ⁱ pzH) ₃].2CHO-OBz	68
Fig. 4.27	DTA-DTG-TG curve of [Fe(3-OCMe ₂ -5-Pr ⁱ pzH) ₃].2CN-OBz	69
Fig. 4.28	DTA-DTG-TG curve of [Fe(3-OCMe ₂ -5-Pr ⁱ pzH) ₃].2NH ₂ -OBz	70
Fig. 4.29	DTA-DTG-TG curve of [Fe(3-OCMe ₂ -5-Pr ⁱ pzH) ₃].2NO ₂ -OBz	71

LIST OF TABLES

Table No.	Title	Page No.
Table 1.1.	Enzymes that are able to oxidize alkanes	3
Table 2.1	Reagents used	30
Table 3.1	UV-Visible data for compounds 14-23	42
Table 3.2	Thermal decomposition data for compounds 15-23	44
Table 3.3	Magnetic moment data of compounds 14-23	45

LIST OF SCHEMES

Table No.	Title	Page No.
Scheme 1.1.	Representative reactions catalyzed by alkane oxygenases	6
Scheme 3.1	Synthesis of 3,5-Pr ⁱ ₂ pzH	37
Scheme 3.2	Synthesis of sodium p-X benzoate salt	38
Scheme 3.3	Screening of metals	38
Scheme 3.4	Synthesis of [Fe(3,5-Pz ⁱ ₂ pzH) ₃ Cl ₂]	39
Scheme 3.5	Synthesis of [(Fe(3-OCMe ₂ -5-Pr ⁱ pz) ₃].2X-OBz]	40

1. INTRODUCTION

1.1 INTRODUCTION & LITERATURE REVIEW

Synthetic organic chemistry has developed intensely over the past fifty years. Organic synthesis involves transformation of functional groups or structural features exhibiting relatively high chemical reactivity. As a result, almost every class of organic compound can now be used as a source of starting materials for conversion to members of other classes which includes complicated materials such as polymers, biomolecules etc. Alkanes or the saturated hydrocarbons, an important class of organic compounds, represent an exception to this generalization. Thus, C-H bonds are generally not viewed as functional groups in regards to organic synthesis. Out of thousands of reagents that are regularly used in synthetic organic methods, only a few are capable of carrying out selective chemistry on alkanes.

The reason for the difficulty in converting alkanes to more useful products is alluded to by their other name 'paraffin' (meaning not enough affinity): alkanes are relatively inert. The chemical inertness of alkanes arises due to the fact that the constituent atoms of alkanes are all held by strong and localized C-C and C-H bonds, such that the molecules have no empty orbitals of low energy or filled orbitals of high energy that can readily participate in a chemical reaction, as is the case with unsaturated hydrocarbons such as olefins and alkynes [1]. Therefore, the lack of reactivity of alkane C-H bonds is often attributed to their high bond energies (typically 90-100 kcal/mol) and very low acidity (difficult to measure directly but estimated to have $pK_a = 45-60$) and basicity [2].

In spite of the fact that aliphatic C-H bonds are more difficult to break or transform, they are not completely inert. They do react at high temperatures, as seen in combustion but such reactions are not easily controllable and they usually result in thermodynamically stable but economically unattractive products i.e., carbon dioxide and water. At present the use of alkanes in combustion applications, utilizes their energy content but not their potential to be used as efficient precursors for the fine synthesis of important and economically important chemicals. Cracking and thermal dehydrogenation of alkanes converts them into valuable olefins but these reactions

require extreme conditions of high temperature and intensive energy. Alkanes have also been found to undergo a gas phase or solution phase reactions which involve exposure to either reactive species such as super acids or free radicals, but these species are usually expensive to make and also such processes pose a problem of relative unselectivity.

Aliphatic C-H bond activation or functionalisation has great practical implications. Usually the preparation of a certain class of compounds requires that there should be some heteroatom or unsaturation in the carbon backbone of the starting materials but this cannot be done in alkanes. In order to bring this conversion the reactive sites or functional groups are usually incorporated by means of multiple transformations but if the new functionality can be somehow introduced directly through transformation of C-H bonds, the same target molecule will be accessible in a single step by displacement of hydrogen atom. Moreover, the ability to selectively target a number of different C-H bonds in a complex substrate will permit direct access to multiple analogs from a common structural precursor. The C-H bond functionalization strategies if once successfully established will also be helpful in utilization of alkanes specially methane, which is principal constituent of natural gas. Most of the world's established natural gas resources are located in remote areas, at sites where the local demand is negligible, such as north slope of Alaska. The high cost of both transportation and methods prevalent for conversion of hydrocarbon gases into more readily transportable liquid impedes the exploitation of such resources [3]. Thus, development of efficient methodology for conversion of methane to other chemicals, methanol or liquid fuel will significantly improve methane utilization.

It has been found that in nature, several microorganisms are capable of performing functionalization of aliphatic C-H bonds continuously at ambient temperature and sometimes with great selectivity. Oxygenases are the oxidative enzymes that catalyze the selective oxidation of a wide range of organic compounds at physiological temperatures and pressures. Oxidation of a wide range of linear alkanes to corresponding alcohols is catalyzed by a group of oxidative enzymes:

multicomponent oxygenases, alkane hydroxylase and cytochrome P450 selectively. Different bacterial multicomponent monooxygenases catalyse the O₂ dependent hydroxylations of hydrocarbons. This family of enzymes includes methane/butane monooxygenases, four-component alkene/aromatic monooxygenases, phenol hydroxylases, alkene monooxygenases, hyperthermophilic toluene monooxygenases and tetrahydrofurn/propane monooxygenases. Different bacterial hydroxylases that are capable of being used in synthesis of fine chemicals using the whole cells are alkane monooxygenase, toluene monooxygenase, xylene monooxygenase, styrene monooxygenase and toluene dioxygenase. These enzymes are unique among diiron proteins for their ability to hydroxylate a variety of hydrocarbon substrates including alkanes, alkenes and aromatics Depending on the microorganism which produces it, these enzymes carry out oxidation of a wide range of alkanes [4 -6].

Table 1.1 Enzymes that are able to oxidize alkanes [7]

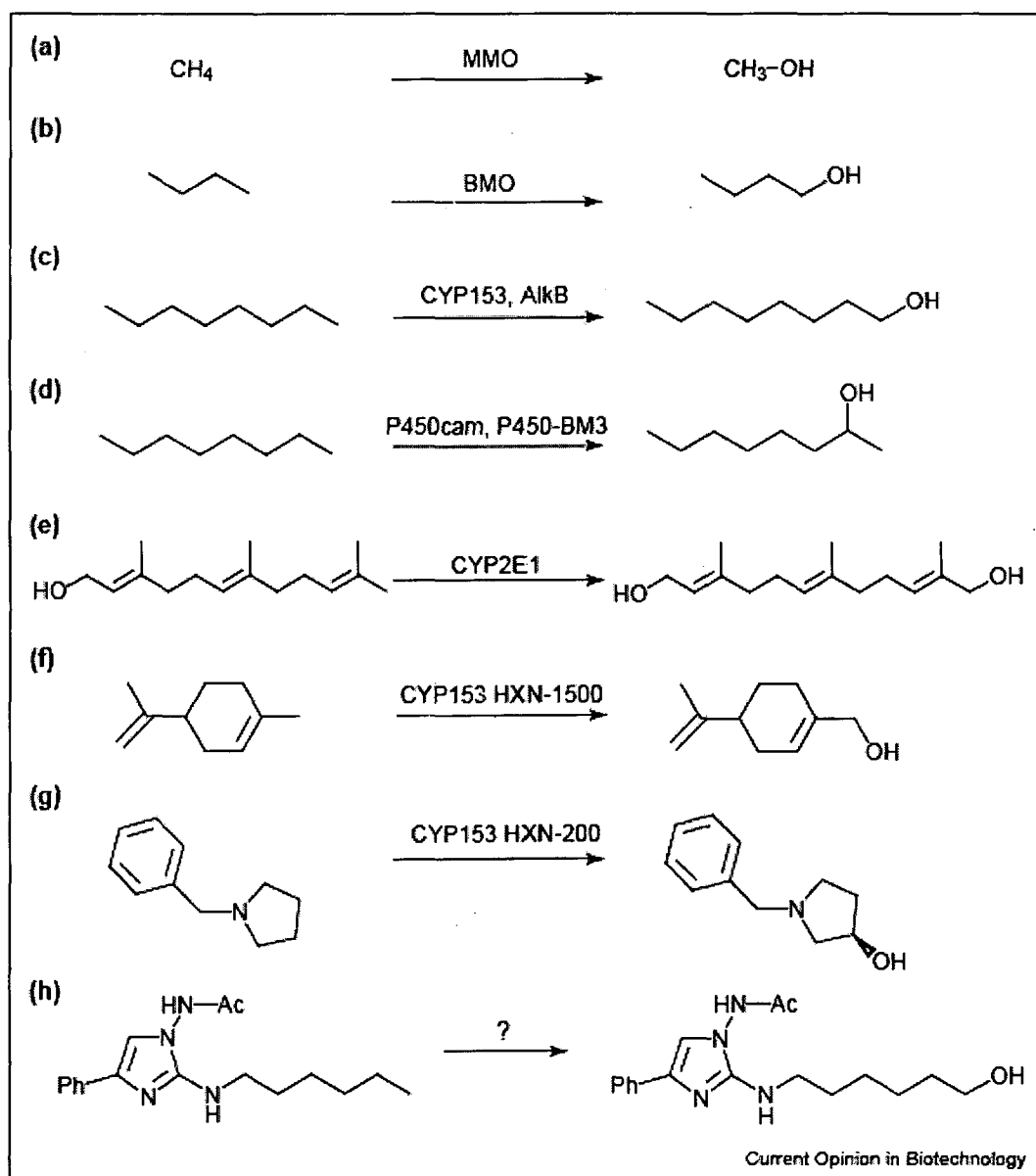
Enzyme	Composition and cofactors	Examples of host organisms	Substrate range
Class I P450 (CYP153)	P450 oxygenase: P450 heme Ferredoxin: [2Fe-2S] Ferredoxin reductase: FAD, NADH	<i>Sphingomonas</i> sp. HXN-200, <i>Mycobacterium</i> sp. HXN-1500, <i>Acinetobacter</i> sp. EB104	C ₄ -C ₁₆
Class II P450 (CYP52)	Microsomal oxygenase: P450 heme Reductase: FAD, FMN, NADPH	<i>Candida maltosa</i> , <i>Candida tropicalis</i> , <i>Yarrowia lipolytica</i>	C ₁₀ -C ₁₆
Class II P450 (CYP2E, CYP4B)	Microsomal oxygenase: P450 heme Reductase: FAD, FMN, NADPH	Humans and rabbits	C ₆ -C ₁₀
Integral membrane alkane hydroxylase	Membrane hydroxylase: dinuclear iron Rubredoxin: iron Rubredoxin reductase: FAD, NADH	<i>Acinetobacter</i> , <i>Alcanivorax</i> , <i>Burkholderia</i> , <i>Mycobacterium</i> , <i>Pseudomonas</i> , <i>Rhodococcus</i>	C ₅ -C ₁₆
Soluble methane monooxygenase	$\alpha_2\beta_2\gamma_2$ structure Hydroxylase: dinuclear iron Reductase: [2Fe-2S], FAD, NADH Regulatory subunit	<i>Methylinus trichosporium</i> OB3b, <i>Methylococcus capsulatus</i> (Bath)	C ₁ -C ₁₀
Particulate methane monooxygenase	Putative $\alpha_2\beta_2\gamma_2$ structure	All known methanotrophs	C ₁ -C ₅
Propane monooxygenase	Putative $\alpha_2\beta_2\gamma_2$ structure Reductase: NADH Regulatory subunit	<i>Gordonia</i> sp. TY-5	C ₃ and C ₁₅ -C ₂₂
Butane monooxygenase	$\alpha_2\beta_2\gamma_2$ structure Hydroxylase: dinuclear iron Reductase: [2Fe-2S], FAD, NADH Regulatory subunit	<i>Pseudomonas butanovora</i> ATCC 43655	C ₂ -C ₈
Engineered P450cam	P450 oxygenase: P450 heme Putidaredoxin: [2Fe-2S] Putidaredoxin reductase: FAD, NADH	<i>Pseudomonas putida</i> ATCC 29607	C ₃ -C ₁₀
Engineered P450BM-3	Single polypeptide: FAD, FMN, NADPH	<i>Bacillus megaterium</i> ATCC 14581	C ₃ -C ₈

These biological entities can be directly used for industrial alkane conversion in principle but in practice, these approaches may be primarily applicable to small-scale production of specialized chemicals as the large scale bioprocesses for alkane conversion present difficulty [6, 7].

Methane monooxygenase (MMOs) is found in methane oxidising bacteria (methanotrophs), a group of gram-negative bacteria, which are capable of utilizing methane as a source of energy and fuel. Methanotrophs are capable of converting methane to methanol. This key enzyme exists in two forms: the membrane bound, particulate methane monooxygenase (pMMO) and the cytoplasmic, soluble methane monooxygenase (sMMO). Particulate MMO contains an iron-copper cluster and is found in all methanotrophs. It is capable of transforming small chain linear alkanes with (C-1 –C-5) to corresponding alcohols. Soluble MMO contains a diiron cluster and is found in certain sub classes of methanotrophs such as *M. capsulatus*, *M. trichosporium*, *Methylosinus sporium*, *Methylocystis spp.*, *Methylomonas methanica*. It is capable of oxidizing a wide range of substrates including methane, linear alkanes with (C-5 – C-7), alkene, aromatics, alicyclic and heterocyclic compounds [8].

Alkane hydroxylase system is found in *Burkholderia cepacia*, *Pseudomonas*, *Acinetobacter* and *Rhodococcus* strains. It is an integral membrane protein and contains a diiron cluster [9]. This enzymatic complex is capable of oxidizing medium and long chain linear alkanes using reducing equivalents from NADH or NADPH. Alkane hydroxylase obtained from *Pseudomonas oleovorans* is capable of oxidizing medium chain length alkanes and alkenes (C-6 – C-12) [10]. This enzyme obtained from *Acinetobacter* sp. strain ADP 1 is capable of oxidizing longer alkanes (C-12 – C-18) [11] while the alkane hydroxylase synthesized by *Rhodococcus* sp. oxidizes alkanes with chain lengths ranging from dodecane to hexadecane [12]. The three alkane hydroxylases from *Acinetobacter* sp. strain M-1 can oxidize long alkanes (C-20 – C-44) that are found soluble in the cytosol or oil inclusion of the cell [13] while the two enzymes obtained from *Pseudomonas aeruginosa* PAO 1 can oxidize alkanes (C-12 – C-20 and C-15 – C-24) [14].

Cytochrome P450 is a monooxygenase enzyme which catalyses the incorporation of molecular oxygen into alkane. It is found in certain yeast as well as bacteria. It is a heme protein [15]. Cytochrome P 450 present in certain strains of the yeast *Candida* is able to carry out ω -oxidation of alkanes (C-11 – C-16) to corresponding alcohols which in turn is converted to α,ω -dicarboxylic acids by other enzymes [16]. The natural activity of this enzyme when present in *Bacillus megaterium* is to catalyze the enantioselective hydroxylation of alkanes with chain lengths ranging from dodecane to octadecane. However, certain mutants have been found which are able to carry out direct, regioselective and enantioselective hydroxylation of a wider range of alkanes from propanes to octadecanes [17].



Scheme 1.1 Representative reactions catalyzed by alkane oxygenases[7]

Despite the practical limitations, enzymatic transformations are much studied, to understand the underlying reaction mechanism and guide the design of synthetic catalysts mimicking the function, efficiency and selectivity of their biological counterparts. A number of structural and functional mimics of these monooxygenases have been developed to oxidize C-H bonds. Groves et al. discovered the first example of metalloporphyrin (iron tetraphenylporphyrin) in 1979, which catalysed the hydroxylation and epoxidation of different hydrocarbons using iodobenzene as a sacrificial oxidant. They found that chloro- $\alpha,\beta,\gamma,\delta$ -tetraphenylporphyrinatoiron (III) catalyzed the oxidation of cyclohexane to cyclohexanol in a solution of methylene chloride under nitrogen at room temperature, using iodobenzene as the oxygen source. Surprisingly the same complex catalysed the oxidation of cis-stilbene to cis-stilbene oxide while trans-stilbene was inert to this reaction with this catalyst. In fact, a mixture of the two olefins on oxidation by the same catalyst led to efficient isolation of cis-stilbene oxide and recovery of trans-stilbene. They also found that another complex chlorodimethylferritoporphyrin IX efficiently catalysed the oxidation of cis-stilbene and trans-stilbene to cis-stilbene oxide and trans-stilbene oxide respectively with iodobenzene as the oxidizing agent [18].

Wayland et al. carried out comparative kinetic and mechanistic studies for reaction of rhodium porphyrins in activating methane and toluene. The two rhodium complexes (tetramesitylporphyrinato)rhodium(II) monomer and (tetraxylporphyrinato)rhodium(II) dimer were reacted with the benzene solution of methane to give equal quantities of hydride and methyl derivatives of the rhodium complexes. The reactions were studied using ^1H NMR and were found to be reversible. The reaction proceeded to equilibrium position observable with ^1H NMR, the integration of which helped in evaluation of equilibrium constants. Reactions of the rhodium complexes were carried out under similar conditions but there was no evidence for activation of aromatic C-H bond activation in case of toluene. Instead the methyl group of toluene was found to react with the two rhodium porphyrins to produce hydride and benzyl derivatives without any evidence for aromatic C-H bond activation. The studies of rate laws, activation parameters and deuterium isotope effects suggested that the C-H bond activation reaction with rhodium (II) porphyrins involved the formation of a linear four-centered transition state. Kinetic studies suggested that the alkyl C-H bonds in both methane and toluene reacted with rhodium porphyrins by related mechanisms. However, the inability of these complexes to react with the aromatic C-H bonds can be ascribed to the

steric effects due to which the two bulky metalloradicals cannot be accommodated in the near-tetrahedral four centered transition state involved in this reaction. Thus, rhodium(II) porphyrins appear to have selectivity for carrying out activations of alkyl C-H bonds rather than aryl C-H bonds [19, 20].

Subsequently several metalloporphyrins were designed and studied for carrying out the oxidation of alkanes. Sakurai et al. studied the oxidation of cyclohexene using different metalloporphyrins i.e., Mn(TPP)Cl, Cr(TPP)Cl, VO(TPP)Cl and Cr(TPP)Cl. The reaction was carried out by allowing the metal porphyrins to react with cyclohexene dissolved in benzene in the presence of dibenzo-18-crown- and sodium borohydride under an atmosphere of 100% oxygen at 20°C in separate reactions. On carrying out these studies of the types and amounts of the products formed manganese porphyrins were found more efficient [21].

The biomimetic alkane oxidation systems carry out the reactions with the mechanisms similar to the enzymatic system. However, both yields and product distributions vary significantly with oxygen-transfer reagent, suggesting that a common oxometal complex is unlikely. In general these systems are neither as efficient nor as selective toward alkanes as natural systems, and more significant efforts have been lately focused upon their use as olefin epoxidation catalysts [2, 22]. As the approach of using the systems that mimic the structure of the active site of enzymes for regioselective C-H bond activations was not found successful another approach for designing artificial systems that mimic only the function of enzymes was explored to obtain C-H bond activation in the desired manner. As enzymes often involve transition metal complexes as cofactors, the application of these transition metals in construction of chemical models for activation of different substrates is supposed to be more productive. The controlled activation of small, relatively inert molecules has been practiced in transition metal chemistry since late 1950s. The binding to metal center has shown alterations or enhanced reactivity of a variety of molecules, through the changes in energies in their orbitals or their polarity. For instance, the coordination of the olefins and carbon monoxide to a metal centre renders them more susceptible to nucleophilic attack [1, 23], whereas the dioxygen when coordinated to a metal can react with an electrophile readily [1, 24]. The classic inert molecule, dinitrogen has also been shown to become activated on coordination to a metal and subsequently take part in chemical transformation [25]. Thus, looking at these activations with the help of transition metal coordination chemistry, it was anticipated that the aliphatic C-H bond can also be activated by the use of transition metal

complexes. Transition metal-mediated C-H activation holds promise for the preparation of functionalized products from readily available starting materials. Moreover, the transformations of C-H bonds of heteroaromatic substrates would provide potentially useful synthetic sequences due to the prevalence of heteroaromatic fragments in compounds of biological interest [2].

Shilov et al. for the first time demonstrated the possibility of activating methane and its homologs with Pt salts. According to their studies the addition of alkanes, including methane to a mixture of H_2PtCl_6 and Na_2PtCl_4 leads to the generation of both alkyl halides and alcohol. In an attempt to deduce the mechanism with the help proton NMR and chemical analysis they found that a complex of Pt(IV) containing a $\text{CH}_3\text{-Pt}$ is formed, which was isolated from the solution as an adduct of PH_3P [26].

Janowicz et al. reported direct C-H bond activation in completely saturated hydrocarbons. They reported the discovery of organotransition-metal systems capable of carrying out intermolecular oxidative addition to single C-H bonds in saturated hydrocarbon at room temperature in homogeneous solution. A dihydrido-iridium(III) complex, $(\text{Me}_5\text{C}_5)(\text{Me}_3\text{P})\text{Ir}(\text{H})_2$ was prepared by treatment of $[(\text{Me}_5\text{C}_5)\text{IrCl}_2]_2$ with trimethylphosphine followed by lithium triethylborohydride. This iridium complex on irradiation in benzene solution gave $(\eta^5\text{-pentamethylcyclopentadienyl})(\text{trimethylphosphine})\text{hydridophenyl iridium(III)}$ complex, while on irradiation in cyclohexane solution it gave $(\eta^5\text{-pentamethylcyclopentadienyl})(\text{trimethylphosphine})\text{hydridocyclohexyliridium(III)}$ complex and neopentane solution separately led to the formation of $(\eta^5\text{-pentamethylcyclopentadienyl})(\text{trimethylphosphine})\text{hydridoneopentyliridium(III)}$ complex. The structure of these products were studied and confirmed by NMR spectroscopic studies. The NMR data suggested that the hydridoalkyliridium complexes formed are the intermolecular C-H activation products [27].

Sen et al. studied the activation of different substrates including light alkanes (ethane, propane) in presence of species of platinum i.e., K_2PtCl_4 and Pt/O_2 in aqueous medium. They found that inactivated C-H bonds were activated by Pt(II) species while the C-H bonds adjacent to an oxygen atom were activated by metallic Pt. For instance, in the presence of Pt(II) the C-H bond of the substrate was oxidized only to alcohols i.e., ethanol and ethylene glycol while the presence of metallic Pt allowed further oxidation to corresponding

of C-H bond. The η^2 C-H activated complex was now unstable as the metal center was formally oxidized to three state. It was stabilized by rechelation of the pyrazolyl arm of the borate to give an alkyl hydride product $\text{TpRh}(\text{CO})(\text{R})(\text{H})$. Hence, the alkane was seen to be activated [31]. The formation of η^2 alkane complex at the room temperature activation of alkane by rhodium complex was confirmed by Periana et al. [32].

Backland et al. carried out the studies on the thione substituted derivatives of maltol which are of interest in applications of metal based drugs. During their studies they found unexpected C-H bond activation of the complexes of dithiomaltol with Ru(II) upon oxidation. The Ru complexes of 3-hydroxy-2-methyl-4-thiopyrone (thiomaltol or Htma) and 3-hydroxy-2-methyl-4H-thiopyran-4-thione (dithiomaltol or Httma), $[\text{Ru}(\text{bpy})_2(\text{tma})]^+$ and $[\text{Ru}(\text{bpy})_2(\text{ttma})]^+$ respectively were seen to undergo unexpected C-H bond activation upon oxidation. Oxidation of $[\text{Ru}(\text{bpy})_2(\text{ttma})]^+$ with different peroxidants C-H bond activation at its pendant methyl group to give an air-stable aldehyde $[\text{Ru}(\text{bpy})_2(\text{ttma-aldehyde})]^+$ through the formation of an intermediate oxidation product $[\text{Ru}(\text{bpy})_2(\text{ttma-alcohol})]^+$ which was characterized. The oxidation with different peroxidants i.e., oxone, m-chloroperbenzoic acid, urea hydrogen peroxide and 2,6-dicarboxypyridinium chlorochromate gave similar yields of around 15% while the yield of the aldehyde was found to be slightly higher with 2-iodoxybenzoic acid and $\text{Na}_2\text{Ir}(\text{IV})\text{Cl}_6$. Similar oxidations of analogous $[\text{Ru}(\text{bpy})_2(\text{ettma})]^+$ resulted in the formation of corresponding ketone $[\text{Ru}(\text{bpy})_2(\text{ettma-ketone})]^+$. All the complexes were characterized by UV-vis, ^1H NMR and IR spectroscopies. The structure of the aldehyde $[\text{Ru}(\text{bpy})_2(\text{ttma-aldehyde})]^+$ was confirmed by X-ray crystallography [33].

Uhl et al. reported C-H bond activation by hyperconjugation with Al-C bonds. Treatment of di(tert-butyl)butadiene with dialuminium hydride under different conditions resulted in formation of organoelement compounds which contained carbocations in solution. The three different types of carbocations obtained due to C-H bond activation were a butadienyl cation, a vinyl cation and an aliphatic cation. The hyperconjugation with Al-C at the adjacent C atoms activated the corresponding C-H bonds and diminished the positive charge at the inner carbon atoms which remains after the heterolytic cleavage of the C-H bond. Further the effective intramolecular coordination of the hydride ion by two coordinatively unsaturated aluminium atoms which act as a chelating Lewis acid, favours the formation of the cations over the formation of C-H bond formation [34].

Thiophenes can be activated by different metals. Paneque et al. reported the activation of C-H and C-S bonds of thiophene by rhodium complex. $[\text{TpRh}(\text{C}_2\text{H}_4)(\text{PMe}_3)]$ a mixed phosphine-ethylene derivative of Rh, was prepared by low temperature (-20°C) addition of phosphine (PMe_3) to a solution of $[\text{TpRh}(\text{C}_2\text{H}_4)_2]$. Irradiation of a solution $[\text{TpRh}(\text{C}_2\text{H}_4)(\text{PMe}_3)]$ in neat thiophene lead to the C-H and C-S bond activated products of thiophene $[\text{TpRh}(\text{H})(\text{C}_4\text{H}_3\text{S})(\text{PMe}_3)]$ and $[\text{TpRh}(\text{CHCHCHCHS})(\text{PMe}_3)]$ respectively. The study of the reaction was carried out by NMR spectroscopy. The photolysis reaction of thiophene with Rh complex gave both C-H and C-S activation products in almost the same yield while the reaction at elevated temperature $>60^\circ\text{C}$ gave a higher yield of the C-H activated product. Moreover, the reaction of thiophene with the related Rh species $[\text{TpRh}(\text{C}_2\text{H}_4)(\text{PEt}_3)]$ gave both C-H and C-S activated products in same proportion but again at the elevated temperature the reaction proceeded to give a higher yield of C-H activated product. However, the reaction of thiophene with CpRhL (Cp = cyclopentane, L = PMe_3 , C_2H_4) gave a higher yield of C-S oxidized product. Thus, the electronic and steric properties of the metal environment seemed to play an important role in deriving the reaction towards one or the other type of product [35]. The same group further reported that 2,5-dimethylthiophene undergoes complex transformations in its reaction with an iridium complex $\text{Tp}^{\text{Me}_2}\text{Ir}(\text{C}_2\text{H}_4)_2$. This transformation involved aliphatic C-H bond activation of one of the intermediates to give final products. 2,5-Dimethylthiophene and $\text{Tp}^{\text{Me}_2}\text{Ir}(\text{C}_2\text{H}_4)_2$ reacted at 60°C to give a mixture of two hydride products in the ratio 1:1, which were isolated by fractional crystallization and characterized by different spectroscopic techniques. From their structures it was inferred that one of the compound was formed by activation of one of the aromatic C-H bonds while the second compound involved the activation of aliphatic C-H bond of methyl group of 2,5-dimethylthiophene. NMR studies supported this formulation [36].

Heteroatomic systems are of biological significance. As a result the C-H bond transformations in heteroatomic systems would provide useful synthetic sequences. Several studies regarding the stoichiometric as well as catalytic C-H bond transformations in heteroatomic compounds which are mediated by transition metals such as thiophenes, furans, pyrroles have been made. Pittard et al. reported the stoichiometric as well as catalytic C-H bond activation in furan and thiophene compounds. A Ru(II) complex $\text{TpRu}(\text{CO})(\text{NCMe})(\text{Me})$, (Tp = hydridotris(pyrazolyl)borate) reacted with furan at 90°C to give methane and $\text{TpRu}(\text{CO})(\text{NCMe})(2\text{-furyl})$ by activation of C-H bond at 2 position in furan. The formation of methane was confirmed by the analysis of headspace of the reaction

in a gas-tight NMR tube using GC-MS technique. It was found that the C-H bond activation of furan in this reaction was regioselective and this regioselectivity of C-H bond activation was supported by the studies of the reaction using ^1H NMR and ^{13}C NMR spectroscopy. Homonuclear decoupling and NOE experiments were consistent with the regioselectivity of C-H bond activation i.e., activation at 2 position in furan. Further, the reaction of $\text{TpRu}(\text{CO})(\text{NCMe})(\text{Me})$ with thiophene at 90°C gave a mixture of methane and $\text{TpRu}(\text{CO})(\text{NCMe})(2\text{-thienyl})$ after approx. 19 hrs of continuous stirring. The reaction was studied with the help of NMR spectroscopy. The solid-state structure of $\text{TpRu}(\text{CO})(\text{NCMe})(2\text{-thienyl})$ was shown by x-ray diffraction studies. Moreover, it was observed that the same Ru complex $\text{TpRu}(\text{CO})(\text{NCMe})(\text{Me})$ catalyzed the addition of thiophene to ethylene at a temperature of 90°C and a pressure of 40 psi resulting in the formation of 2-ethylthiophene [37].

Organic synthesis is one of the main aims of C-H bond functionalization. In spite of modeling of a number of reaction systems which are capable of activating the otherwise inert aliphatic C-H bond, a few have been devised in a manner which find application in the field of synthesis feasibly. Bharath et al. reported the activation of a C-H bond of pendant phenyl ring of 2-(aryloxy)pyridine by a cobalt ion to produce a low spin complex which can be used as a precursor for further synthesis of rare low spin cobalt (II) complexes. The reaction of low-spin complexes $[\text{Co}(\text{II})\text{L}_3][\text{ClO}_4]\cdot\text{H}_2\text{O}$ ($\text{L} = 2\text{-(aryloxy)pyridine}$), $(\text{R})\text{C}_6\text{H}_4\text{N}=\text{NC}_5\text{H}_4\text{N}$ ($\text{R} = \text{H}$, *o*-Me/Cl, *m*-Me/Cl or *p*-Me/Cl) with *m*-chloroperbenzoic acid in a solution of acetonitrile at room temperature lead to the hydroxylation of *o*-carbon-hydrogen bond of pendant phenyl ring of both parent ligands selectively and spontaneously and resulted in another low spin complex $[\text{Co}(\text{III})\text{L}_2][\text{ClO}_4]\cdot\text{H}_2\text{O}$ ($\text{L} = \text{o-OC}_6\text{H}_4$ ($\text{R})\text{N}=\text{NC}_5\text{H}_4\text{N}$). During this transformation the Co ion is oxidized from +2 to +3 state. The reaction was studied with the help of ^1H NMR and ^{13}C NMR to establish the configuration of the product while the d-d transitions in the metal were studied with the help of UV spectroscopy. The hydroxylated complexes can act as precursors for chemical as well as electrochemical synthesis of rare octahedral low spin cobalt complexes [38].

Ito et al. proposed a reaction scheme for C-H bond activation which finds application in asymmetric synthesis. They gave an efficient method for the preparation of rhodium and iridium complexes by C-H bond activation and these complexes are capable of catalyzing asymmetric synthesis. It was shown that on heating a mixture 3,5-dimethyl-R-Phebox

(Phebox = bis(oxazolinyphenyl)) ligand, $\text{RhCl}_3(\text{H}_2\text{O})_3$ and NaHCO_3 at 50°C for 3hrs in a methanolic solution gave a rhodium complex $(3,5\text{-dimethyl-dimethylPhebox})\text{RhCl}_2(\text{H}_2\text{O})$ with a yield of 84%. The production of this rhodium complex involved aliphatic C-H bond activation. The rhodium complex $(3,5\text{-dimethyl-dimethylPhebox})\text{RhCl}_2(\text{H}_2\text{O})$ acts as a catalyst for asymmetric conjugate reduction of α,β -unsaturated carbonyl compounds and the asymmetric reductive aldol reaction of acralytes and aldehydes. Similarly, the iridium complex $(3,5\text{-dimethyl-dimethylPhebox})\text{IrCl}_2(\text{H}_2\text{O})$ was prepared by the C-H bond activation in the reaction that involved heating a mixture 3,5-dimethyl-R-Phebox (Phebox = bis(oxazolinyphenyl)) ligand, $\text{H}_2\text{IrCl}_6(\text{H}_2\text{O})_6$ and NaHCO_3 in a methanolic solution at 50°C for 3hrs. The iridium complex thus, obtained was also capable of catalyzing asymmetric conjugate reduction of α,β -unsaturated carbonyl compounds and the asymmetric reductive aldol reaction of acralytes and aldehydes. As a probe for testing the catalytic ability of these complexes in asymmetric conjugate reduction, (E)-ethyl 3-phenylbut-2-enoate was used as the substrate and it was found that in combination with diethoxymethylsilane gave a final yield of 90% of the reduction product while the iridium complex gave the reduction product with the yield of 63%. Similarly for testing the catalytic activities of these complexes, produced via this method, in asymmetric reductive aldol reaction, the symmetric coupling reaction of benzaldehyde and ter-butyl acralyte was examined. The rhodium complex in combination with diethoxymethylsilane gave reductive aldol product with 98% yield while the iridium product gave 19% yield. The structures of the two complexes were determined with the help of X-ray diffraction method [39].

Burling et al. reported that C-H bond activated complexes of ruthenium N-heterocyclic carbene can be used efficiently to catalyze a tandem oxidation / reduction reaction in conjugation with a Wittig reaction that allows for the formation of C-C bonds from alcohols. A number of N-alkyl-substituted heterocyclic carbene ruthenium hydride complexes have been studied for their catalytic activities for C-C bond formation from alcohols as substrates. All of the mono -NHC complexes of the type $\text{Ru}(\text{NHC})(\text{PPh}_3)_2(\text{CO})(\text{H})_2$ gave better catalyzed conversions of alcohols into C-C coupled products as compared to the $\text{Ru}(\text{PPh}_3)_3(\text{CO})\text{H}_2$ complexes. On intensive studies it was found that upon heating $\text{Ru}(\text{PPh}_3)_3(\text{CO})\text{H}_2$ with four equivalents of $\text{I}^i\text{Pr}_2\text{Me}_2$, a C-H bond activated isopropyl derivative $\text{Ru}(\text{I}^i\text{Pr}_2\text{Me}_2)(\text{PPh}_3)_2(\text{CO})\text{H}$ was obtained which gave more significant reaction results by being the most efficient catalyst. The C-H bond activated carbene complex of ruthenium showed the highest catalytic activity for C-C bond formation by allowing the

reaction of PhCH_2OH and $\text{Ph}_3\text{C=CHCN}$ to occur at a lower temperature of 70°C and even the reaction time was shortened to 3hrs. The reaction was studied with the help of NMR spectroscopy. Thus, it was finally concluded that the C-H bond activate complexes could be used as the precursors for the catalysis of the synthetic reactions [40].

Sakakura et al. reported a catalytic system for the carbonylation of hydrocarbons including alkanes to produce aldehydes via C-H bond activation steps. They showed that the rhodium complex $\text{RhCl}(\text{CO})(\text{PR}_3)_2$ on irradiation catalyzed the carbonylation of hydrocarbons including alkanes at ambient temperature under an atmospheric pressure of CO to yield aldehydes. However, the use of other complexes of Co, Ir and Ru resulted in much lower catalytic activities. The benzene was carbonylated to benzaldehyde mainly while benzophenone and benzyl alcohol were obtained as by-products. Even the monosubstituted benzenes were converted to meta-substituted benzaldehydes by $\text{RhCl}(\text{CO})(\text{PR}_3)_2$. In the study of reaction with n-alkanes, it was seen the terminal methyl group was selectively carbonylated to give a linear aldehyde. This regioselectivity was accounted for by the formation of thermodynamically stable hydridoalkyl intermediates. The linear aldehyde thus produced was seen to undergo further photoreaction (Norrish Type II) to give a terminal olefin and acetaldehyde. On irradiating the reaction with different wavelengths, it was seen that the catalytic activity, regioselectivity of the carbonylation and occurrence of Norrish Type II reaction were affected by irradiation wavelength. It was reported that on irradiation $\text{RhCl}(\text{CO})(\text{PR}_3)_2$ was seen to undergo CO dissociation to give $\text{RhCl}(\text{PR}_3)_2$ which in turn was proposed as the probable active species for C-H bond activation [41].

Bolig et al. reported highly selective activation and functionalization of sp^3 C-H bond with the help of a cobalt complex $[(\text{Cp})\text{Co}(\text{VTMS})_2]$ (VTMS = vinyltrimethyl silane). 1-(dimethyl(vinyl)silyl)azepane and 1-(dimethyl(vinyl)silyl)azocane were transformed to seven- and eight- membered N-protected enamines in a reaction catalyzed by this cobalt complex. The NMR studies suggested that the enamines were formed by activation of C-H bonds α to the protected nitrogen and involved an intramolecular hydrogen transfer. Enamines are versatile intermediates for organic synthesis, so this process of preparing enamines via the C-H bond activation process may find applications in organic synthesis [42].

Chen et al. reported an iron based small molecule catalyst which can oxidize aliphatic C-H bonds in a number of substrates using hydrogen peroxide as an oxidizing agent. $[\text{Fe}(\text{II})(\text{mep})(\text{CH}_3\text{CN})_2](\text{SbF}_6)_2$ complexes (mep = N,N'-dimethyl-N,N'-bis(2-pyridylmethyl)ethane, 1,2-diamine] under substrate limiting conditions converted only 1% pivalate to tertiary hydroxylated product with modest selectivity of 56%. However, on incorporation of methylamines into rigidifying pyrrolidine rings of this catalyst showed improvements in selectivity to 92% as well yield to 14%. The addition of acetic acid to the reaction further increased the catalytic activity of both these iron catalysts in epoxidation without affecting the selectivity. However, increment in initial catalyst loading alongwith an increase in either the equivalents of acetic acid or the equivalents of H_2O_2 gave better yield of the hydroxylated products. In all cases examined it was found that hydroxylation preferentially occur at the most electron-rich tertiary C-H bond and the stereochemistry of the substrate was retained. They further investigated the sensitivity of site of oxidation to the electronic environment of the 3° carbon atom. A series of dihydrocitronellol derivatives with electron withdrawing groups at α or β positions to one of the two 3° C-H centers. In substrates with no electronic bias hydroxylation with H_2O_2 occurred at both the 3° C-H centers but in presence of electron withdrawing group the hydroxylation occurred at the 3° C-H remote to the electron withdrawing group. To test for the effect of the steric environment of 3° C-H on selectivity of oxidation site, oxidation of acetoxy-p-ethane was performed in the presence of Fe(mep) catalyst with H_2O_2 . It was found that hydroxylation occurred at C-1 as was less sterically hindered. The selectivity for oxidation site was also affected by the presence of a directing group. Thus, selective C-H bond activation by using this iron complex can be used for synthetic purposes by determining the interplay between these three effects acting simultaneously [43].

In an attempt to create the chemical model of biological activation of the C-H bond in alkanes the possibilities of mimicking the natural processes by means of chemical catalysts and reaction systems involving same metals were studied. Iron has been found to be one of the most important metals in this respect [44]. Lipscomb in his review on metalloenzymes reported that enzymes with diiron clusters are capable of oxidizing C-H bonds in alkanes. Oxidation enzymes can be divided into two classes: the oxidases, which act through electron transfer with concomitant reduction of O_2 to water and the oxygenases, which catalyse the reaction of O_2 with organic- or inorganic substrates. The oxygenases can further be divided into monooxygenases and dioxygenases. A monooxygenase incorporates one of the oxygen

atoms from molecular oxygen into the substrate whereas the other oxygen is reduced to water. A dioxygenase incorporates both atoms from O₂ into the oxygenated product. Another subdivision can be made based on the ligands used to bind the metal ion. Enzymes that use heme prosthetic group for this purpose are called heme proteins. The enzymes that do not use a heme but instead bind the metal with ligands provided by the protein are called non-heme proteins [45]. Nature has evolved a number of iron-requiring enzymes that activate dioxygen and catalyze the oxidation of aliphatic C-H bonds. Among these are the heme-containing cytochrome P450 and the non-heme enzymes methane monooxygenase, alkane hydroxylase and fatty acid desaturases [46].

Cytochrome P 450 are membrane associated hemoproteins that are capable of metabolizing a number of substrates and catalyzing a number of biological reactions. Two of the most important reactions catalyzed by this enzyme are hydroxylation of C-H bond and epoxidation of C=C bonds. They are the monooxygenases which carry out hydroxylation of C-H bond with the help of molecular oxygen. It has been found that the enzyme contains an iron porphyrin complex with sulfur-bound cysteine, at the active site.

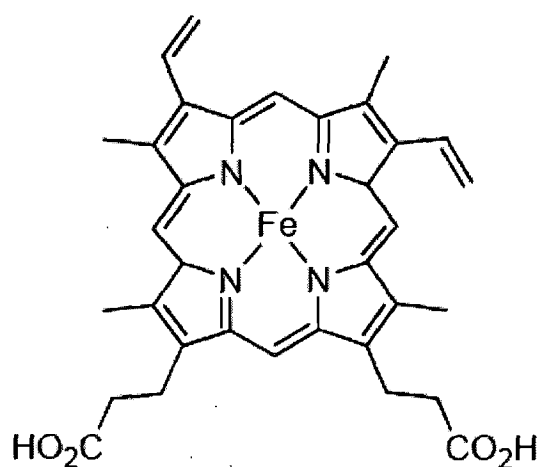


Fig 1.1 An iron protoporphyrin complex[47]

The catalytic cycle begins with the binding of substrate followed by introduction of first electron from NAD(P)H via an electron transfer cycle. In next step oxygen binds and accepts another electron to form a ferric peroxy anion. The ferric peroxy anion is protonated to form ferric hydroperoxy complex which undergoes subsequent

hydrolytic cleavage to generate an iron-oxo complex. The oxo complex is considered to be the active oxidant of C-H bonds in alkanes and it abstracts a hydrogen atom from C-H bond of alkane to give a cage shaped hydroxoiron(III) complex / alkyl radical pair. This is followed by oxygen rebound such that carbon radical combines with the hydroxide. As the mechanism involves the formation an alkyl free radical, cytochrome P-450 oxidations favor oxidation of the weaker tertiary C-H bonds over the primary and secondary CH bonds [47,48].

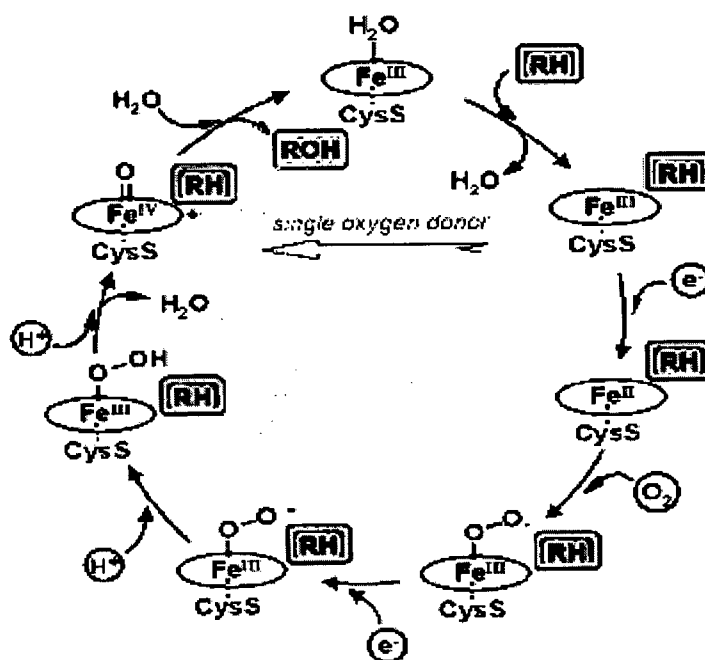


Fig 1.2 Generally accepted mechanism for C-H bond activation by cytochrome P450 [49]

In many, but not all, cytochrome P450s, an interesting so called “shunt” reaction has also been observed. In this type of reaction the substrate can be hydroxylated directly by peroxides such as hydrogen peroxide, cumene hydroperoxide and ter-butyl hydroperoxide without the requirement for activation of molecular oxygen by interaction with electron donating system. Thus, utilizing this peroxygenase activity,

cell free P450-dependent catalysis can be carried out without the need for NADPH regeneration, additional proteins or dioxygen [47,50].

Another class of enzymes, methane monooxygenase enzymes, is found in bacteria and catalyze selective oxidation of methane to methanol. It is found in methanotropic bacteria that use methane as their sole carbon source, like *Methylococcus capsulatus* and *Methylosinus trichosporium*. It consists of three components, a hydroxylase, which is responsible for the oxidation of methane, a reductase and a regulatory protein. Methane monooxygenase hydroxylase (MMOH) belongs to a class of non-heme iron proteins. It has been found to consist of two iron atoms in a carboxylate-rich ligand environment at the active site. These iron atoms are often bridged by an oxo group and / or bidentate carboxylates. The structure of both oxidized form of MMOH (MMOH_{ox}) and the reduced form (MMOH_{red}) as shown in figure 1.3

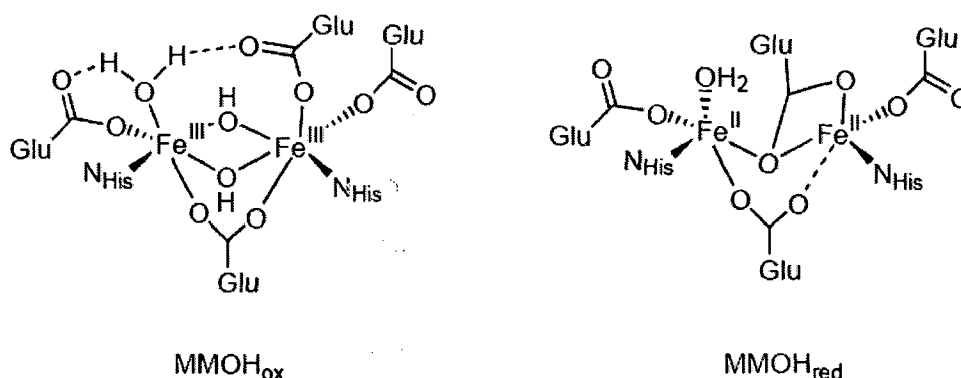


Fig 1.3 Active site structures of MMOH_{ox} and MMOH_{red} [51]

The two iron(III) centers in MMOH_{ox} are six coordinate, each having one nitrogen ligand (His) and five oxygen ligands like glutamic acid residues, bridging hydroxides /waters and a terminal water ligand. Upon reduction to MMOH_{red}, one of the glutamic acid ligands undergoes a carboxylate shift and becomes a monodentate bridging ligand. In addition a hydroxide bridge is lost and the other hydroxide / water bridge becomes a terminal instead of a bridging ligand. The consequence of these structural changes is one of the iron (II) center becomes effectively five coordinate and this is the form of cluster which is capable of reacting with molecular oxygen [51, 52].

The catalytic cycle of MMOH is believed to go through a number of intermediates. Mixing of MMOH_{red} with O_2 gives an intermediate P, which is proposed to be a μ -1,2-peroxo bridged diiron(III) species. The intermediate P converts to intermediate Q, which is believed to be the species responsible for methane hydroxylation. Spectroscopic studies suggest that MMPH-Q contains an bis- μ -oxo- Fe(IV)_2 cluster in which the two single atom oxygen bridged form a so-called “diamond core”. There are two mechanisms suggested for the reaction between compound Q and the alkane: radical and nonradical. The radical mechanism starts with abstraction of the hydrogen atom from the substrate to form QH (the rate determining step), hydroxyl bridged compound Q and the free alkyl radical. The nonradical mechanism implies a concerted pathway, occurring via a four-center transition state and leading to a “hydrido-alkyl-Q” compound. Some researchers suggested that the methane oxidation proceeds via a bound-radical mechanism. It was suggested that the transition state for the radical mechanism involves a torsion motion of the hydroxyl OH ligand before the methyl radical can add to the bridging hydroxyl ligand to form the alcohol. As the radical approaches, the H atom of the alkane leave the coplanar tricoordinate O environment and bends upward to create a tetrahedral tetracoordinate O environment. The final step for this reaction is the elimination of the alcohol and the regeneration of the catalysts. There are a few ways in which this can occur. It could be a stepwise mechanism that starts with the elimination of the alcohol and an intermediate Fe-O-Fe core, and the the latter can eliminate the water and regenerate the enzyme through a 2e- reduction. Alternatively, it can start with a 2e- reduction process of bridging the O1 atom to give a water molecule, followed by elimination of the alcohol and regeneration of the enzyme. In addition, it is possible that there is a concerted mechanism where the elimination of the methanol occurs spontaneously with 2e- reduction of the bridging O1 center and regeneration of the catalyst [51-55]. The generally accepted mechanism for oxidation of methane by methane monooxygenase enzyme is shown in figure 1.4.

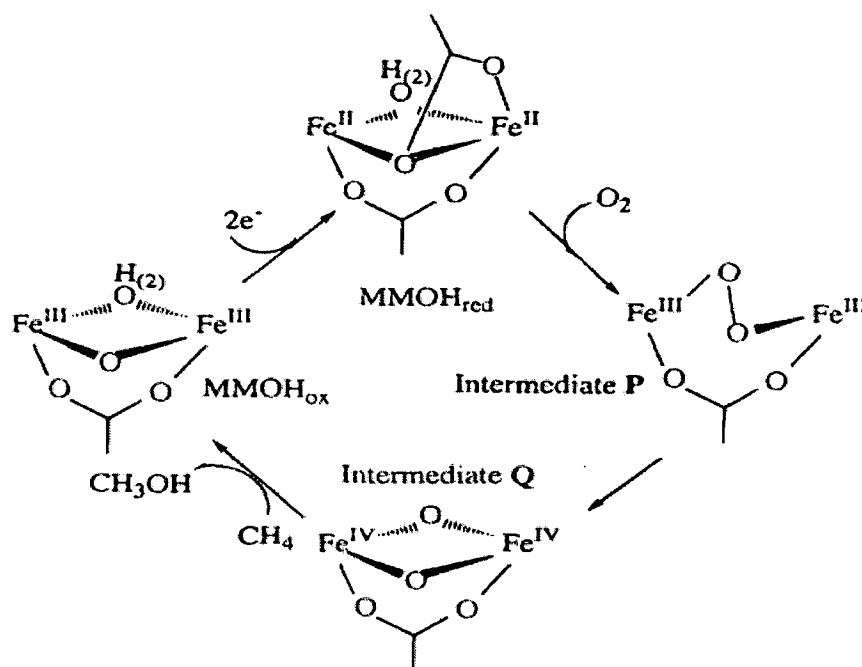


Fig 1.4 Catalytic cycle for methane oxidation by MMOH [56]

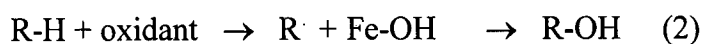
Lipoxygenases are mononuclear, non-heme iron enzymes that are found in both animals and plants and are known to catalyze the oxidative conversion of 1,4-diene-containing fatty acids to alkyl peroxides [57]. The rate determining step of the mechanism is generally accepted to be a hydrogen abstraction from substrate C-H bond to generate a substrate-radical which is subsequently trapped by dioxygen [58]. The species postulated to be responsible the hydrogen abstraction is a ferric-hydroxide complex, which is subsequently reduced by the H-atom to ferrous water complex [59]. Jonas et al. reported the activation of C-H bond by hydrogen abstraction by a ferric-methoxide complex based on the active iron complex in lipoxygenase enzyme. They designed a new ligand, 2,6-bis-((2-pyridyl)methoxymethane)pyridine (PY5) consisting of five pyridine units which can accommodate an iron metal in a nearly square pyramidal coordination to mimic specific attributes of iron coordination sites. On mixing Fe-OTf₂ (OTf = CF₃SO₃⁻) with the PY5 ligand in the ratio of 1:1 using methanol as a solvent, a 6-coordinate ferrous complex [Fe(PY5)(MeOH)]-(OTf)₂ (1). The complex 1 on oxidation with 0.5 eq. of either H₂O₂ or iodosobenzene in methanol yields the stable ferric complex

[Fe(PY5)(OMe)]-(OTf)₂ (**2**). The ferric-methoxide complex **2** when treated 1,4-cyclohexadiene abstracts a hydrogen atom from a weak C-H bond from it and itself gets reduced back to the ferrous-methanol complex **1**. Thus, a model capable of C-H bond activation was designed which represented the chemical species involved in rate determining step in the mechanism of lipoxygenase enzyme [60].

Groves discovered the first iron metalloporphyrin (iron tetraphenylporphyrin) catalyzed oxidation system as a biomimetic model of monooxygenases, in which cyclohexane was oxidized to cyclohexanol using iodosobenzene as a sacrificial oxidant [18]. In addition to these porphyrin-based monooxygenases mimics, a number of non-porphyrin systems perform similar alkane oxidation functions. It has been known since the last century that iron salts catalyze the oxidation of alkanes by peroxides (Fenton oxidation). These processes are considered to involve the iron-catalyzed homolysis of hydrogen peroxide followed by hydrogen abstraction and radical recombination (eq. 1).



The mechanism for alkane oxidation by an iron catalyst can be separated into two components: a C-H bond cleavage step and a C-O bond formation step (eq. 2)



The variation in the products observed for the catalysts may be rationalized by the relative timing of these two steps. At one extreme the two steps may occur in a concerted fashion, so the oxygen atom is effectively inserted into the C-H bond. Alternatively, the C-H bond is cleaved to form an alkyl radical that is very quickly trapped to form the C-O bond [61].

Barton et al. reported C-H bond activation using iron powder. They carried out oxidation of various aliphatic and alicyclic hydrocarbons by a system containing iron powder and a carboxylic acid in aqueous pyridine under an atmosphere of oxygen. A trace of hydrogen sulphide helped in initiating the reaction. In particular, the oxidation of adamantane was carried out in an aqueous pyridine solution containing

iron powder and tartaric acid under the atmosphere of oxygen. The reaction converted adamantane to a mixture of adamantan-1-ol, adamantan-2-ol and adamantanone. On carrying out the reaction in presence of different acids it was found that with increasing acid strength favors higher relative ratio of attack at the secondary methylene position of adamantane. Of all the acids used the highest yield was obtained in presence of tartaric acid [62].

The pyrazole nucleus is thermally and hydrolytically very stable. As a ligand, it coordinates to metals and metalloids through the 2-N. Due to these attractive features the coordination chemistry of pyrazole and of its derivatives have attracted much attention. When deprotonated, pyrazole becomes the pyrazolide ion, which can coordinate through both the nitrogen atoms as an exobidentate ligand of C_{2v} symmetry. On conducting electronic spectral studies of $[Ni(Hpz)_6]^{2+}$ complex both in solution as well as of single crystal it was suggested that pyrazole occupies a position similar to that of pyridine or ammonia in spectrochemical series. The nucleophilicity of the nitrogens and their steric accessibility may be varied through appropriate ring substitution. Pyrazoles and its derivatives have biological activity which is well studied [63]. 3,5-diisopropyl pyrazole which has an electron releasing group should thus, be stronger coordinating ligand. The presence of a substituent at 3 position of pyrazole introduces steric hindrance and makes it difficult to have six-3-substituted pyrazoles coordinated via the 2-N to a metal. This difficulty can be circumvented by coordination through a tautomeric 5-substituted structure, where steric hindrance is minimized. Several substituted pyrazoles both at 3 and 5-positions have been synthesized.

Most of the synthesized substituted pyrazoles have wide application in coordination chemistry, bioinorganic and organometallic chemistry. The utilizations of these compounds extend from the role as inhibitor of the alcohol dehydrogenase to their potential antiallergic action. Some pyrazole derivatives may even inhibit the induction of mutations of some carcinogens. On the other hand, metal ions, especially transition metal ions, play an important role in biological systems. For example,

4. Water is the only by-product obtained in oxidation by hydrogen peroxide. Thus, hydrogen peroxide is used as a preferred oxidizing agent in several reactions. Several examples of aliphatic C-H bond oxidation using hydrogen peroxide as the oxidizing agent have been reported [66].

Cho et al. reported oxidation of a methyl group in a complex of Ni using H₂O₂ to give a ligand based carboxylate group and an alkoxide as the final product. In particular, the reaction of [Ni₂(OH)₂(Me₂-tpa)₂]²⁺ (**3**) (Me₂-tpa = bis(6-methyl-2-pyridylmethyl)(2-pyridylmethyl)amine) with H₂O₂ lead to the oxidation of a methylene group on the Me₂-tpa ligand to give an N-dealkylated ligand and oxidation of a methyl group to afford a ligand-based carboxylate and an alkoxide as the final oxidation products. A series of sequential reaction intermediates produced in the oxidation pathways: a bis(μ-oxo) dinickel(III) ([Ni₂(O)₂(Me₂-tpa)₂]²⁺ (**4**), a bis(μ-superoxo) dinickel(II) ([Ni₂(O₂)₂(Me₂-tpa)₂]²⁺ (**5**), a (μ-hydroxo)(μ-alkylperoxo) dinickel(II) ([Ni₂(OH)(Me₂-tpa)(Me-tpa-CH₂OO)]²⁺ (**6**), and a bis(μ-alkylperoxo) dinickel(II) ([Ni₂(Me-tpa-CH₂OO)₂]²⁺ (**6**), were isolated and characterized by various physicochemical measurements including X-ray crystallography, and their oxidation pathways were investigated. Reaction of **3** with H₂O₂ in methanol at -40°C generates **4**, which is extremely reactive with H₂O₂, producing **5**. Complex **4** was isolated only from disproportionation of the superoxo ligands in **5** in the absence of H₂O₂ at -40°C. The thermal studies carried out in an atmosphere of nitrogen suggested that a ligand-based radical Me-tpa-CH₂ is generated as a reaction intermediate, probably by H-atom abstraction by the oxo group. Although there is a possibility that the Me-tpa-CH₂OO species could undergo various reactions, one of the possible reactive intermediates, **6**, was isolated from the decomposition of **5** under O₂ at -20 °C. The alkylperoxo ligands in **6** and **7** can be converted to a ligand-based aldehyde by either homolysis or heterolysis of the O-O bond, and disproportionation of the aldehyde gives a carboxylate and an alkoxide via the Cannizzaro reaction [67].

Hikichi et al. reported oxidation of an aliphatic C-H bond in an isopropyl chain of the ligand in a Co complex to an alkoxo ligand using H₂O₂ as an oxidizing agent. A dinuclear Co(II)-μ-peroxo complex, {Co[HB(3,5-Prⁱpz)₃]}₂(μ-O₂) (**9**), is yielded by reaction of the bis(μ-hydroxo)-Co(II) complex, {Co(OH)[HB(3,5-Prⁱpz)₃]}₂ (**8**), with an equimolar amount of H₂O₂. Spontaneous decomposition of the μ-peroxo complex **9** yields a mono-oxygenated μ-alkoxo-μ-hydroxo complex, Co₂(μ-OH)[HB(μ-3-OCMe₂-5-Prⁱpz)(3,5-Prⁱpz)₂][HB(3,5-Prⁱpz)₃] (**11**), in which one of the six 3-isopropyl methane carbon atoms is oxygenated and the resulting alkoxo ligand bridges the two Co(II) centers. In contrast, decomposition of **9** in the presence of an excess amount of H₂O₂ results in further oxygenation to give a mixture of the dinuclear Co(II)-bis(μ-alkoxo) complex, {Co[HB(μ-3-OCMe₂-5-Prⁱpz)(3,5-Prⁱpz)₂]}₂ (**12**), and the mononuclear Co(II)-hydroxo alcohol complex, Co(OH)[HB(3-Me₂COH-5-Prⁱpz)(3-Me₂COH-5-Prⁱpz)₂] (**13**). In the bis(μ-alkoxo) complex **12**, one of the three 3-isopropyl groups in each ligand is functionalized to give the alkoxide group, which bridges the two metal centers. In the mononuclear hydroxo alcohol complex **13**, all of the three 3-isopropyl groups are oxygenated. The Co(II) center is coordinated by the resulting alcohol ligand as well as an hydroxide. Reaction of **8** with 2 equiv of ROOH (R = Buⁱ and PhMe₂C) at low temperature yields the blue thermally unstable alkylperoxo compound **10**. The HB(3-But-5-Prⁱpz)₃ derivative, Co(OOCMe₂-Ph)[HB(3-But-5-Prⁱpz)₃] (**9**), characterized successfully by X-ray crystallography contains the tetrahedral Co center. The monomeric alkylperoxo complexes **10** also decomposes to give the bis(μ-alkoxo) complex **12**, but neither mono-oxygenated **11** nor fully oxygenated **13** is obtained. These observations suggest that the present aliphatic C-H bond oxygenations may proceed via homolysis of the O-O bond of the Co(II)-peroxo species [68].

In a number of examples intramolecular activation of both sp² and sp³ hybridized C-H bonds in a variety of ligands has appeared [69-70]. Thyagarajan et al. reported intramolecular C-H bond activation in isopropyl group of the Tp-ligand attached to Co in its five-coordination complex with a Tp^{i-Pr,Me}-ligand, a trimethylsilylamido group and one of the isopropyl group of the Tp-ligand through the formation of a

terminal cobalt imido intermediate [71]. Zhao et al reported spontaneous self-assembly by a mononuclear complex of platinum $\text{Pt}(\text{NPA})(\text{CH}_3)_2$ [NPA = N-(2'-pyridyl)-7-azaindole] into an organoplatinum Pt_4 macrocycle $\text{Pt}_4(\text{N,C,N-NPA})_4(\text{CH}_3)_4$ via a cyclometallation driven self assembly process at ambient temperature [72].

1.2 AIM AND SCOPE

The aim and scope of this work is to activate secondary aliphatic C-H bond of isopropyl group present on 3,5-diisopropylpyrazole ring in metal complexes with iron as central metal atom. For this the complex of iron with 3,5-diisopropylpyrazole have been prepared and the oxidation of the one methine carbon of isopropyl groups present on each of the three 3,5-diisopropylpyrazole rings attached to iron center have been carried out using hydrogen peroxide as the oxidizing agent. Further the effect of the presence of various p-substituted sodium benzoates on the oxidation of the C-H bond of isopropyl chains in this complex has been studied. Our strategy of using 3,5-diisopropylpyrazole has drawn inspiration from several papers reported in literature according to which the secondary C-H bond in isopropyl group present in 3,5-diisopropylpyrazole ring has a great capability of getting oxidized to an OH bond which in turn has a tendency of forming metal oxygen bond. We have been inspired to study the effect of presence of benzoates by the papers reported in literature that the presence of organic acids facilitates the oxidation of C-H bond using iron metal center catalysts or complexes.

2. EXPERIMENTAL DETAILS

Table 2.1 Reagents used:

S. No	Chemicals	Grade	Make
1	Methanol [MeOH]	A.R	Rankem
2	Acetonitrile [CH ₃ CN]	A.R	Rankem
3	Dichloromethane [CH ₂ Cl ₂]	A.R	Rankem
4	Iron(II) chloride [FeCl ₂]	A.R	Himedia
5	Anhydrous sodium sulphate [Na ₂ (SO) ₄]	A.R	Himedia
6	Diethyl ether [Et ₂ O]	A.R	Rankem
7	Benzoic acid	AR	Loba Chemie Pvt. Ltd.
8	4-Chloro benzoic Acid	AR	Spectro chem.
9	4-Cyano benzoic Acid	AR	Reidel-de Haën
10	4-Methoxy benzoic Acid	AR	Merck
11	4-Amino benzoic Acid	AR	Aldrich
12	4-Nitro benzoic Acid	LR	Reidel-de Haën
13	4-Methyl benzoic Acid	AR	Merck
14	4-Flouro benzoic Acid	LR	Aldrich
15	4-Formyl benzoic Acid	AR	Aldrich
16	Tertiarybutylamine [Me ₃ CNH ₂]	A.R	Aldrich
17	Lithium amide [LiNH ₂]	A.R	Aldrich
18	Isopropylmethylketone [Me ₂ CHCOMe]	A.R	Aldrich
19	Methylisobutyrate [Me ₃ CCOO ⁻]	A.R	Aldrich
20	Hydrochloric Acid [HCl]	A.R.	Rankem
21	Bromoacetaldehydediethylacetal	A.R.	Aldrich
22	Sodium bicarbonate [Na ₂ CO ₃]	A.R	Fluka
23	Potassium thiocyanate [KSCN]	A.R.	S.d. Fine
24	Sodium sulfate [Na ₂ SO ₄]	A.R.	S.d. Fine

25	Hydrazine monohydrate [NH ₂ NH ₂ .H ₂ O]	A.R.	Fluka
26.	Hydrogen peroxide	A.R.	Rankem

2.2 Make and model of the instruments:

IR spectra were recorded on a Nexus FT-IR (Thermonicolet). Solid samples were recorded as KBr pellet and liquid samples as film between NaCl plates. Elemental Analysis were performed at Vario EL elemental. All the UV-Vis spectra were recorded by Perkin Elmer Lambda 35 spectrometer. The room temperature magnetic measurements were performed on Princeton applied research vibrating sample magnetometer Model 155. Thermal analyses were recorded by Perkin Elmer Pyris Diamond. Powder X-Ray diffraction spectra were recorded on Bruker Axs D8 Advanced diffractometer. Lyophilizer was used for removing water during the synthesis of various sodium salts of p-substituted benzoic acids.

2.3 Method used for synthesis of ligand and complexes:

2.3.1 Synthesis of 3,5-diisopropyl pyrazole [3,5-Prⁱ₂pzH]:

Diisobutyrylmethane used for the preparation of 3,5-diisopropylpyrazole was synthesized by the following method:

Lithium amide (25.00g, 1.08mol) and diethyl ether (80ml) were placed in three necked flask round bottom flask. To the mixture was added a dropwise solution of isopropylmethylketone (58.82g, 0.68mol) over a 60 min. period. Methylisobutyrate (56.62g, 0.55mol) was then added dropwise to the above mixture over a period of 90 min. After being refluxed for 10 hrs., a dilute HCl solution was added to the mixture to hydrolyze the unreacted lithium amide and the water layer was extracted with diethyl ether (3 x 100ml). The ether layer was washed three times with a saturated NaCl aqueous solution. After drying over MgSO₄, the diethyl ether was removed by evaporation. The resulting solution was distilled under reduced pressure at 140 °C affording 44.96g diisobutyrylmethane.

In a two-necked round bottom flask having diisobutyrylmethane (42.49g, 0.27mol) in 60ml ethanol, the aqueous hydrazine monohydrate (23.00g, 0.46mol) was added

dropwise to a solution over a period of 90 minutes. After refluxing for 10 hrs, the mixture was allowed to cool at room temperature, 100 ml saturated NaCl aqueous solution was added and the compound was extracted with diethyl ether (3 x 100ml). The organic layer was washed with saturated NaCl solution (three times). After being dried over MgSO₄ for 6 hrs. the solvent was evaporated to dryness. The resultant white solid was recrystallized from acetonitrile, affording 3,5-diisopropylpyrazole as white needles (yield 28.24%). Anal. Calcd. (%) for C₉H₁₆N₂; C, 71.01; H, 10.59; N 18.40; Found: C, 70.83; H, 10.49; N, 17.75. IR (KBr, cm⁻¹) (ν_{N-H}) 3415, (ν_{C-H}) 2961, (ν_{C=C}) 1677.

2.3.2 Synthesis of sodium salts of various p-X benzoic acids [*p*-XC₆H₄COO⁺Na⁻]:

Sodium salts of various para-X benzoic acids (X = H, Cl, F, CH₃, OCH₃, CHO, CN, NH₂, NO₂) were prepared by reaction of corresponding p-benzoic acids and sodium hydroxide in equivalent amount. In a particular experiment 40 mmol of p-X benzoic acid was added to an aqueous solution of 40 mmol of sodium benzoate and the solution was stirred for 6 hrs. The resultant solution was filtered and lyophilized till solid powder was obtained.

2.3.3 Screening different metals for aliphatic C-H bond activation:

Different metal salts were screened to test their ability for being used in intramolecular aliphatic C-H bond activation. In particular, to the methanolic solution of (0.5 mmol) metal salt MY₂ (M = Ni²⁺, Cu²⁺, Mn²⁺, Fe²⁺, ...) (Y = Cl⁻) was added dichloromethane solution (12ml) of (0.237g, 1.5mmol) 3,5-diisopropylpyrazole and the reaction mixture was stirred for 1 hour. To this solution, the methanolic solution (4ml) of (0.162g, 1.0 mmol) sodium p-fluorobenzoate was added. To the resultant reaction mixture was added 30eq. of aqueous 30% H₂O₂ (2.15ml, 21.0 mmol) at room temp., the solution was allowed to stir at -50°C for 20 minutes. The water layer formed was separated with the help of separating funnel while the organic layer containing the product was retained. The organic layer was then stirred with anhydrous sodium sulfate to remove any remaining water. The resultant mixture was

filtered and the solvent was evaporated under vacuum. The IR was recorded for each product.

2.3.4 Synthesis of $Fe(3,5-Pr^i_2pzH)_3Cl_2$ (**14**):

To the methanolic solution of (0.064 g, 0.5 mmol) ferrous chloride was added dichloromethane solution (12ml) of (0.237 g, 1.5 mmol) 3,5-diisopropylpyrazole and the reaction mixture was stirred for 1 hour. The resultant mixture was filtered and the solvent was evaporated under vacuum. Yield = 45.23%. Anal. Calcd for $C_{29}H_{54}Cl_2FeN_6$: C, 56.77; H, 8.87; N, 13.70. Found: C, 56.10; H, 9.12; N, 13.81. UV-Vis (methanol, λ_{max} , nm, $\epsilon/M^{-1}cm^{-1}$) 238 (5050), 388 (269). IR (KBr, cm^{-1}) (ν_{N-H}) 3478, (ν_{C-H}) 2979 ($\nu_{C=C}$)1678.

2.3.5 Synthesis of $[Fe(3-OCMe_2-5-Pr^i_2pzH)_3].2OBz$ (**15**) :

To the methanolic solution of (0.064 g, 0.5 mmol) ferrous chloride was added dichloromethane solution (12ml) of (0.237 g, 1.5 mmol) 3,5-diisopropylpyrazole and the reaction mixture was stirred for 1 hour. To the mixture the methanolic solution (4ml) of (0.144g, 1mmol) sodium benzoate was added drop by drop. To the resultant mixture H_2O_2 was added drop by drop at room temperature till the colour of the solution turned brown. The solution was allowed to stir at $-50^\circ C$ for 1 hour. The water layer was separated with the help of separating funnel while the organic layer containing the product was retained. The organic layer was dried over anhydrous sodium sulfate. The organic mixture was filtered and the solvent was evaporated under vacuum. Yield = 46.05%. Anal. Calcd for $C_{37}H_{58}FeN_6O_5$: C, 61.49; H, 8.09; N, 11.63. Found: C, 61.70; H, 7.95; N, 11.08. UV-Vis (acetonitrile, λ_{max} , nm, $\epsilon/M^{-1}cm^{-1}$) 240 (5200), 378(475).. IR (KBr, cm^{-1}) (ν_{N-H}) 3406, (ν_{C-H}) 2970, ($\nu_{C=C}$) 1670, (ν_{Fe-O}) 627.

2.3.6 Synthesis of $[Fe(3-OCMe_2-5-Pr^i_2pzH)_3].2Cl-OBz$ (**16**) :

Compounds **16-23** were obtained in similar manner applied to **15**. Yield = 50.25%. Anal. Calcd for $C_{37}H_{57}ClFeN_6O_5$: C, 58.69; H, 7.59; N, 11.10. Found: C, 58.80; H,

7.86; N, 10.91. UV-Vis (acetonitrile, λ_{\max} , nm, $\epsilon/M^{-1}\text{cm}^{-1}$) 220 (5480), 424 (361). IR (KBr, cm^{-1}) ($\nu\text{N-H}$) 3406, ($\nu\text{C-H}$) 2976, ($\nu\text{C=C}$) 1681, ($\nu\text{Fe-O}$) 611.

2.3.7 Synthesis of [Fe(3-OCMe₂-5-PrⁱpzH)₃].2F-OBz (17):

Yield = 49.72%. Anal. Calcd for C₃₇H₅₇FFeN₆O₅: C, 59.99; H, 7.76; N, 11.35. Found: C, 59.60; H, 7.450; N, 11.20. UV-Vis (acetonitrile, λ_{\max} , nm, $\epsilon/M^{-1}\text{cm}^{-1}$) 238 (5190), 402 (204). IR (KBr, cm^{-1}) ($\nu\text{N-H}$) 3434, ($\nu\text{C-H}$) 2968, ($\nu\text{C=C}$) 1670, ($\nu\text{Fe-O}$) 612.

2.3.8 Synthesis of [Fe(3-OCMe₂-5-PrⁱpzH)₃].2CH₃-OBz (18):

Yield = 51.63%. Anal. Calcd for C₃₈H₆₀FeN₆O₅: C, 61.95; H, 8.21; N, 11.41. Found: C, 61.59; H, 7.95; N, 11.81. UV-Vis (acetonitrile, λ_{\max} , nm, $\epsilon/M^{-1}\text{cm}^{-1}$) 237 (5309), 462 (162). IR (KBr, cm^{-1}) ($\nu\text{N-H}$) 3415, ($\nu\text{C-H}$) 2965, ($\nu\text{C=C}$) 1679, ($\nu\text{Fe-O}$) 616.

2.3.9 Synthesis of [Fe(3-OCMe₂-5-PrⁱpzH)₃].2OCH₃-OBz (19):

Yield = 48.45%. Anal. Calcd for C₃₈H₆₀FeN₆O₆: C, 60.63; H, 8.03; N, 11.16. Found: C, 61.09; H, 8.15; N, 11.81. UV-Vis (acetonitrile, λ_{\max} , nm, $\epsilon/M^{-1}\text{cm}^{-1}$) 220 (5080), 397 (401). IR (KBr, cm^{-1}) ($\nu\text{N-H}$) 3430, ($\nu\text{C-H}$) 2967, ($\nu\text{C=C}$) 1685, ($\nu\text{Fe-O}$) 619.

2.3.10 Synthesis of [Fe(3-OCMe₂-5-PrⁱpzH)₃].2CHO-OBz (20):

Yield = 43.63%. Anal. Calcd for C₃₈H₅₈FeN₆O₆: C, 60.79; H, 7.79; N, 11.19. Found: C, 59.97; H, 8.90; N, 10.96. UV-Vis (acetonitrile, λ_{\max} , nm, $\epsilon/M^{-1}\text{cm}^{-1}$) 231 (5120), 460 (145). IR (KBr, cm^{-1}) ($\nu\text{N-H}$) 3418, ($\nu\text{C-H}$) 2965, ($\nu\text{C=C}$) 1697, ($\nu\text{Fe-O}$) 625.

2.3.11 Synthesis of [Fe(3-OCMe₂-5-PrⁱpzH)₃].2CN-OBz (21):

Yield = 46.66%. Anal. Calcd for C₃₈H₅₇FeN₇O₅: C, 61.04; H, 7.68; N, 13.11. Found: C, 61.19; H, 7.39; N, 13.52. UV-Vis (acetonitrile, λ_{\max} , nm, $\epsilon/M^{-1}\text{cm}^{-1}$) 243 (5220), 372 (492). IR (KBr, cm^{-1}) ($\nu\text{N-H}$) 3437, ($\nu\text{C-H}$) 2970, ($\nu\text{C=C}$) 1672, ($\nu\text{Fe-O}$) 625.

2.3.12 Synthesis of [Fe(3-OCMe₂-5-Prⁱpzh)₃].2NH₂-OBz (22):

Yield = 39.11%. Anal. Calcd for C₃₇H₅₉FeN₇O₅: C, 60.24; H, 8.06; N, 13.29. Found: C, 59.91; H, 7.89; N, 12.93. UV-Vis (acetonitrile, λ_{max}, nm, ε/M⁻¹cm⁻¹) 223 (4980), 420 (209). IR (KBr, cm⁻¹) (νN-H) 3420, (νC-H) 2981, (νC=C) 1678, (νFe-O) 620.

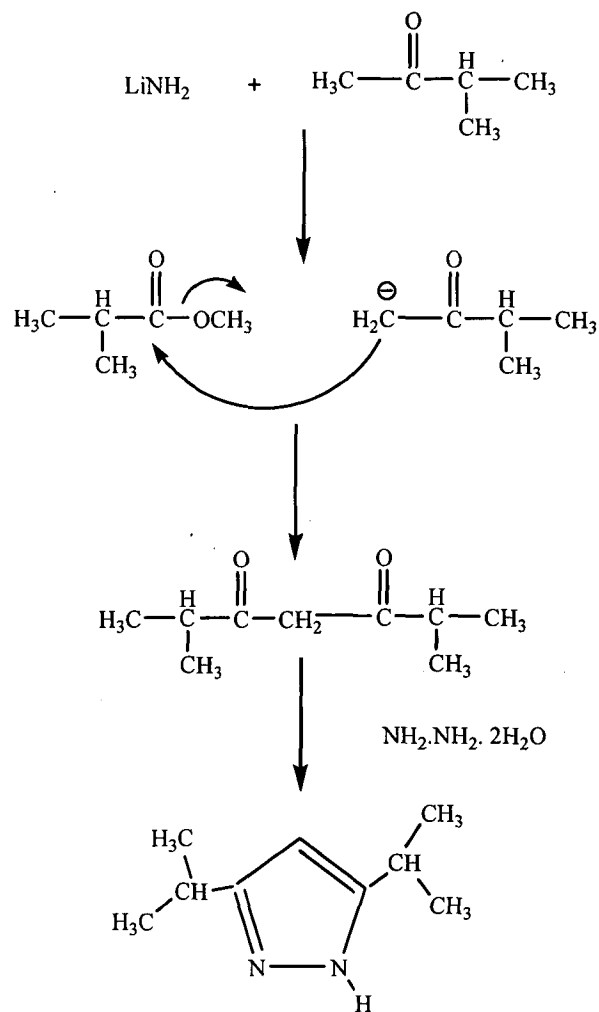
2.3.13 Synthesis of [Fe(3-OCMe₂-5-Prⁱpzh)₃].2NO₂-OBz (23):

Yield = 47.33%. Anal. Calcd for C₃₇H₅₇FeN₇O₇: C, 57.88; H, 7.48; N, 12.77. Found: C, 57.91; H, 6.99; N, 12.25. UV-Vis (acetonitrile, λ_{max}, nm, ε/M⁻¹cm⁻¹) 242 (5330), 391 (253). IR (KBr, cm⁻¹) (νN-H) 3406, (νC-H) 2970, (νC=C) 1671, (νFe-O) 627.

3. RESULTS AND DISCUSSION

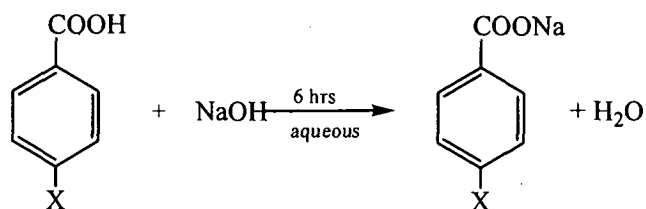
3. RESULTS AND DISCUSSION

The ligand used in present work i.e., 3,5-diisopropylpyrazole was synthesized by scheme 3.1.



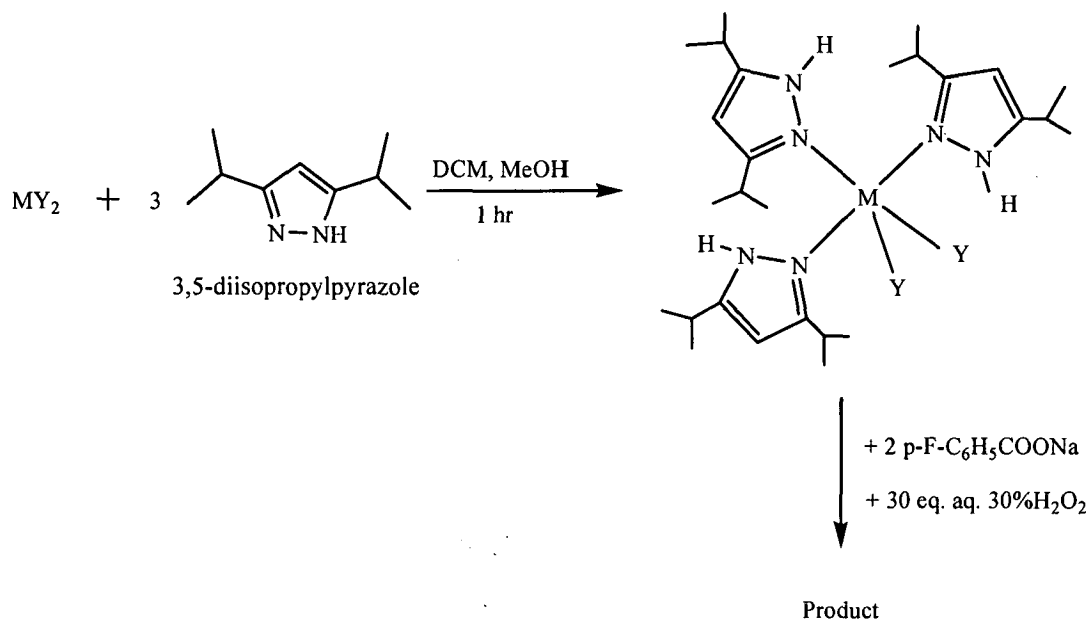
Scheme 3.1. Synthesis of 3,5- Pr^i_2pzH

Various sodium *p*-X benzoate salts (X= H, F, Cl, CH₃, OCH₃, CN, CHO, NH₂, NO₂) were synthesized according to the scheme 3.2.



*Scheme 3.2. Synthesis of sodium *p*-X benzoate salt*

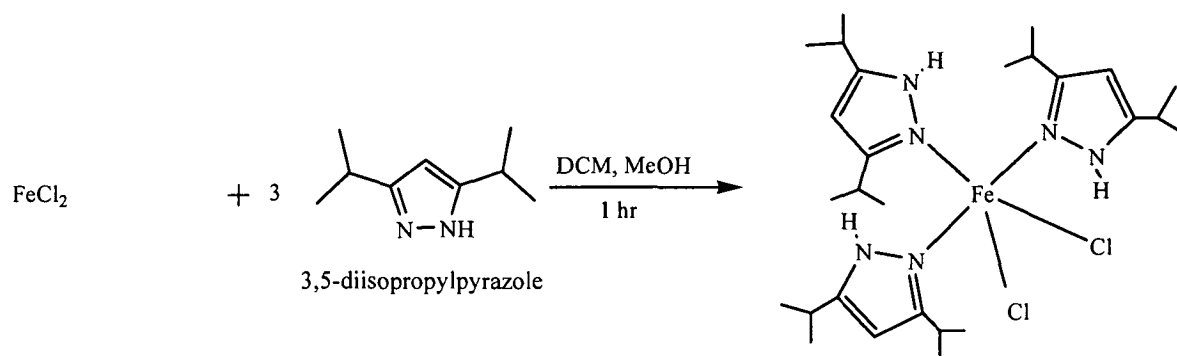
Various metal salt of the MY₂ type (M = Ni, Mn, Cu, Fe) (Y = Cl) were screened for their ability to be used in activation of C-H bond. The method that we tried is according to the scheme 3.3.



Scheme 3. 3. Screening of metals

The results show that out of these metal ions, only iron is able to activate the C-H bond in 3,5-diisopropylpyrazole.

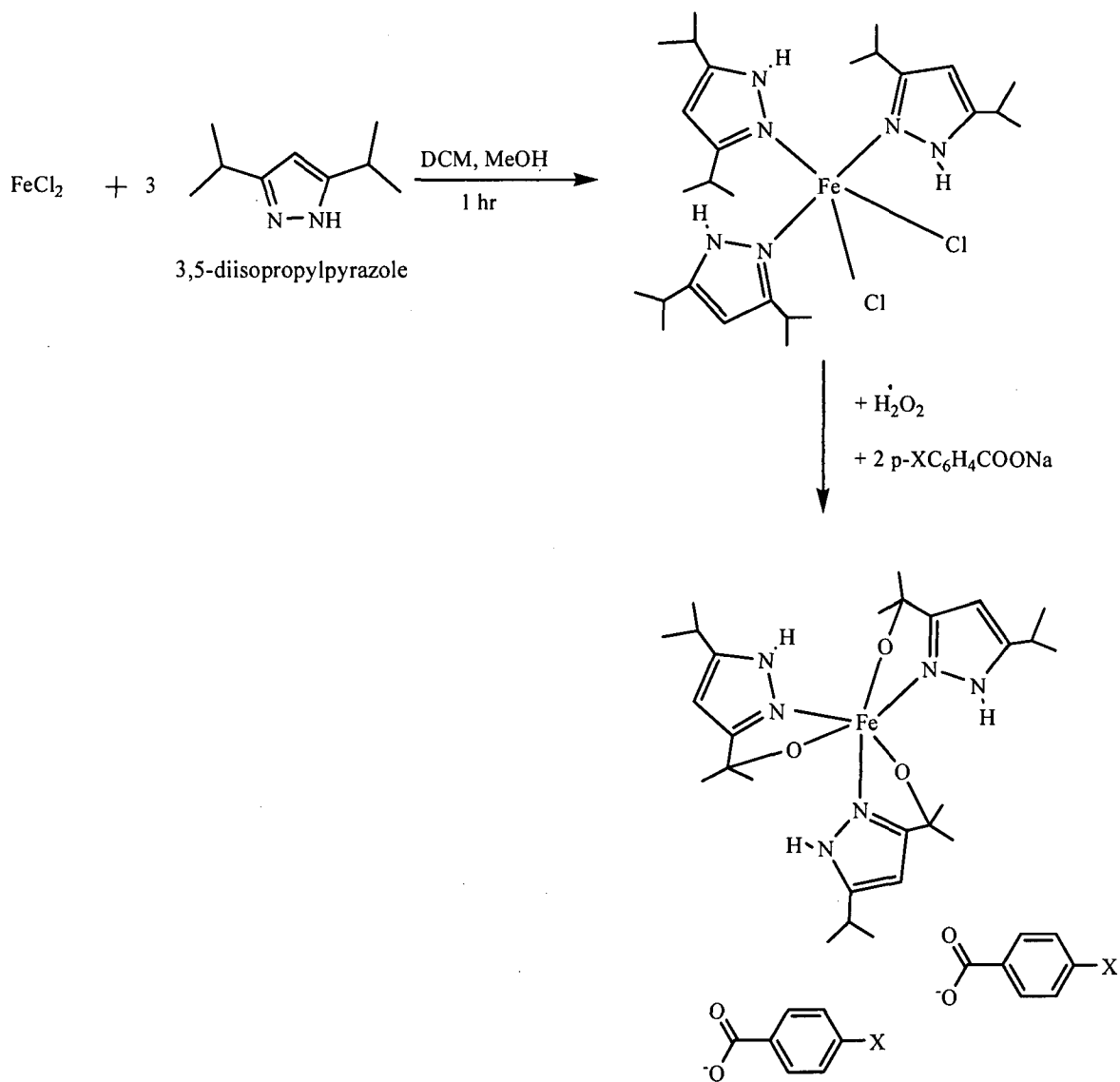
The complex $[\text{Fe}(3,5\text{-Pz}^i_2\text{pzH})_3\text{Cl}_2]$ (**14**) was synthesized according to the scheme 3.4.



Scheme 3.4. Synthesis of $[\text{Fe}(3,5\text{-Pz}^i_2\text{pzH})_3\text{Cl}_2]$

Scheme for synthesis of [(Fe(3-OCMe₂-5-PrⁱpzH)₃].2X-OBz] (15-23):

The compounds [(Fe(3-OCMe₂-5-Prⁱpz)₃].2X-OBz] (X= H, F, Cl, CH₃, OCH₃, CN, CHO, NH₂, NO₂)(15-23) were synthesized according to the scheme 3.5.



Scheme.3.5. Synthesis of [(Fe(3-OCMe₂-5-Prⁱpz)₃].2X-OBz]

3.2 Screening of metals:

In case of Mn, the solution of $[\text{Mn}(3,5\text{-Pz}_2\text{pzH})_3\text{Cl}_2]$ obtained after stirring for 1 hr was slightly pink (Mn^{+2}) but on addition of 30eq of aqueous 30% H_2O_2 the solution turned light brown (Mn^{+3}) in colour but on stirring at -50°C the colour changed back to light pink. This observation can be attributed to the fact that oxidation using H_2O_2 results in formation of H_2O as byproduct and in the presence of water Mn^{+3} undergoes a disproportionation reaction to give Mn^{+2} and MnO_2 . Moreover Mn^{+2} is highly stable owing to the fact that this state corresponds to exactly half filled d-sub shell.

In case of Cu, the solution of $[\text{Cu}(3,5\text{-Pz}_2\text{pzH})_3\text{Cl}_2]$ obtained after stirring for 1 hr was green (Cu^{+2}) and on addition of 30eq of aqueous 30% H_2O_2 the colour of the solution did not show any appreciable change and on stirring at -50°C the colour intensified. This observation can be attributed to the fact that Cu shows a stable oxidation state of +2 while +3 oxidation state is uncommon.

In case of Ni, the solution of $[\text{Ni}(3,5\text{-Pz}_2\text{pzH})_3\text{Cl}_2]$ obtained after stirring for 1 hr was light green (Ni^{+2}) but on addition of 30eq of aqueous 30% H_2O_2 the solution did not show any colour change and no change was seen even after stirring at -50°C as Ni shows stable oxidation state of +2 only.

In case of Fe, the solution of $[\text{Fe}(3,5\text{-Pz}_2\text{pzH})_3\text{Cl}_2]$ obtained after stirring for 1 hr was light yellowish green (Fe^{+2}) and on addition of 30eq of aqueous 30% H_2O_2 the colour of the solution turned brown (Fe^{+3}) and on stirring at -50°C the colour intensified. This observation can be attributed to the fact that Fe shows a stability in both oxidation states of +2 and +3 although +3 is highly stable owing to exactly half filled d-sub shell.

On the basis of these observations Fe was chosen as the preferred metal as it could undergo oxidation from +2 to +3 to suit our reaction strategy. The choice of Fe metal was further supported by the papers which reported that Fe metal plays key role in enzymes involved in carrying out hydroxylation of aliphatic C-H bonds.

3.3 Elemental Analysis:

The ligand 3,5-Prⁱ₂pzH and the complexes **14-23** were subjected to elemental analysis for the % determination of C, H and N content. The elemental analysis was performed on samples carefully dried under vacuum for several hours. The results obtained were within the error range of $\pm 3\%$.

3.4 Infra-red Spectra:

IR spectra of ligand 3,5-Prⁱ₂pzH and complexes **14-23** were recorded as KBr discs in the range of 4000cm⁻¹ to 400 cm⁻¹. For ligand 3,5-Prⁱ₂pzH, peaks are obtained at 3415 (ν N-H), 2961 (ν C-H), 1617 (ν C=N). The IR spectra of compounds **14-23**, showed peaks in the region 3400-3450 (ν N-H), 2950-2990 (ν C-H), 1600-1630 (ν C=C) for the stretching of N-H bonds, C-H bands and C=C bonds respectively. For compounds **15-23** the peaks in the region 1550-1590 (ν asCOO) and 1400-1450 (ν sCOO) have been obtained due to the carboxylate group present in the benzoate. In compounds **15-23** an additional peak in the region 610-630 (ν Fe-O) was obtained.

3.5 UV-Visible Spectra:

Electronic absorption spectroscopy is a powerful tool for the elucidation of the structure of transition metal complexes and also for the organic compounds. The UV-vis spectra of complexes **14-23** were recorded. The ligand being colorless does not exhibit any UV-vis spectrum. The high energy absorption in the 245-220 nm is most likely due to transition involving metal-ligand orbital. The absorption peaks in the region 370-460 nm were obtained due to the d-d transitions. The data for UV-Visible studies has been shown in Table 3.1.

Table 3.1 UV-Visible data for complexes 14-23.

Complexes	Electronic Bands, nm ($M^{-1}cm^{-1}$)
Fe(3,5-Pr ⁱ ₂ pzH) ₃ Cl ₂	238 (5050), 388 (269)

[Fe(3-OCMe ₂ -5-Pr ⁱ pzh) ₃].2OBz	240 (5200), 378 (475)
[Fe(3-OCMe ₂ -5-Pr ⁱ pzh) ₃].2Cl-OBz	220 (5480), 424 (361)
[Fe(3-OCMe ₂ -5-Pr ⁱ pzh) ₃].2F-OBz	238 (5190), 402 (204)
[Fe(3-OCMe ₂ -5-Pr ⁱ pzh) ₃].2CH ₃ -OBz	237 (5309), 462 (162)
[Fe(3-OCMe ₂ -5-Pr ⁱ pzh) ₃].2OCH ₃ -OBz	220 (5080), 397 (401)
[Fe(3-OCMe ₂ -5-Pr ⁱ pzh) ₃].2CHO-OBz	231 (5120), 460 (145)
[Fe(3-OCMe ₂ -5-Pr ⁱ pzh) ₃].2CN-OBz	243 (5220), 372 (492)
[Fe(3-OCMe ₂ -5-Pr ⁱ pzh) ₃].2NH ₂ -OBz	223 (4980), 420 (209)
[Fe(3-OCMe ₂ -5-Pr ⁱ pzh) ₃].2NO ₂ -OBz	242 (5330), 391 (253)

3.6 TGA/ DTA Spectra:

Thermal analysis studies were carried out for compounds **15-23** in the air using DTA, TGA and DTG techniques in the temperature range of 25-900 °C at the heating rate of 10 °C min⁻¹. As seen from the TGA curves for complexes **15-23**, the thermal decomposition of complexes can be divided into two stages. The first stage involves weight loss due to the removal of p-substituted benzoates anions in the temperature range of 140-250 °C while the weight loss in second stage corresponds to the removal of three 3,5-diisopropylpyrazole rings in the temperature range of 280-520°C . The data for thermal decomposition studies has been shown in Table 3.2.

Table 3.2 Thermal decomposition data for compounds 15-23

Compound	Stage	TG temp. range (C)	% Wt. Loss observed	% Wt. Loss calculated	Constituents lost
15	I	149-249	35.23	30.52	Two benzoate anions
	II	349-484	50.73	52.86	Three 3,5-diisopropylpyrazole rings
16	I	148-230	31.21	34.20	Two p-chloro benzoate anions
	II	350-524	52.00	33.12	Three 3,5-diisopropylpyrazole rings
17	I	149-249	29.36	33.40	Two p-flouro benzoate anions
	II	349-484	51.51	51.60	Three 3,5-diisopropylpyrazole rings
18	I	148-230	31.00	31.00	Two p-methyl benzoate anions
	II	350-524	51.64	52.02	Three 3,5-diisopropylpyrazole rings
19	I	150-248	33.42	34.00	Two p-methoxy benzoate anions
	II	250-473	50.39	51.24	Three 3,5-diisopropylpyrazole rings
20	I	150-241	28.05	32.56	Two p-formyl benzoate anions
	II	248-473	52.89	49.59	Three 3,5-diisopropylpyrazole rings
21	I	147-193	34.24	32.66	Two p-cyano benzoate anions
	II	253-457	51.81	50.76	Three 3,5-diisopropylpyrazole rings
22	I	147-230	35.43	30.96	Two p-amino benzoate anions
	II	350-524	49.84	51.96	Three 3,5-diisopropylpyrazole rings
23	I	149-250	35.69	35.54	Two p-nitro benzoate anions
	II	255-468	51.03	48.57	Three 3,5-diisopropylpyrazole rings

3.6 Magnetic measurement:

Magnetic measurements were carried out for complexes **14-23**. The formula used for calculation of magnetic moment is

$$\mu_{\text{eff}} = 2.84 [(\mu_2 - \mu_1)MT / (w_2 - w_1)H]^{1/2}$$

where, $T = 24 + 273 = 297 \text{ K}$

$H = 5000 \text{ Gauss}$

$M = \text{molecular weight of the complex}$

Table 3.3 Magnetic moment data of complexes

S.No.	Compounds (mol. wt.)	μ of Empty holder (emu) * 10^{-2}	Wt. Of holder (gm)		μ of Filled holder (emu) * 10^{-2}	Wt. of sample (gm)	μ_{eff} (B.M.)
			Empty	Filled			
1	$\text{Fe}(3,5\text{-Pr}^i\text{pzH})_3\text{Cl}_2$ (631.0)	0.063	1.04903	1.06883	0.151	0.01980	4.23
2	$[\text{Fe}(3\text{-OCMe}_2\text{-5-Pr}^i\text{pzH})_3].2\text{OBz}$ (858.0)	0.065	1.03695	1.04893	0.153	0.01198	5.53
3	$[\text{Fe}(3\text{-OCMe}_2\text{-5-Pr}^i\text{pzH})_3].2\text{Cl-OBz}$ (912.0)	0.045	1.12671	1.13661	0.124	0.00991	5.91
4	$[\text{Fe}(3\text{-OCMe}_2\text{-5-Pr}^i\text{pzH})_3].2\text{F-OBz}$ (880.0)	0.063	1.08101	1.09091	0.139	0.00990	5.64
5	$[\text{Fe}(3\text{-OCMe}_2\text{-5-Pr}^i\text{pzH})_3].2\text{CH}_3\text{-OBz}$ (872.0)	0.104	0.97423	0.98569	0.187	0.01146	5.15
6	$[\text{Fe}(3\text{-OCMe}_2\text{-5-Pr}^i\text{pzH})_3].2\text{OCH}_3\text{-OBz}$ (888.0)	0.90	1.09412	1.10352	0.164	0.00940	5.82
7	$[\text{Fe}(3\text{-OCMe}_2\text{-5-Pr}^i\text{pzH})_3].2\text{CHO-OBz}$ (915.0)	0.067	0.97165	0.98145	0.158	0.00980	6.30
8	$[\text{Fe}(3\text{-OCMe}_2\text{-5-Pr}^i\text{pzH})_3].2\text{CN-}$	0.085	1.08716	1.09406	0.149	0.00690	6.28

	OBz (894.0)						
9	[Fe(3-OCMe ₂ -5-Pr ⁱ pzh) ₃].2NH ₂ - OBz (872.0)	0.054	0.95382	0.96511	0.136	0.01129	5.73
10	[Fe(3-OCMe ₂ -5-Pr ⁱ pzh) ₃].2NO ₂ - OBz (934.0)	0.058	1.09216	1.10350	0.129	0.01134	5.51

4. SPECTRA

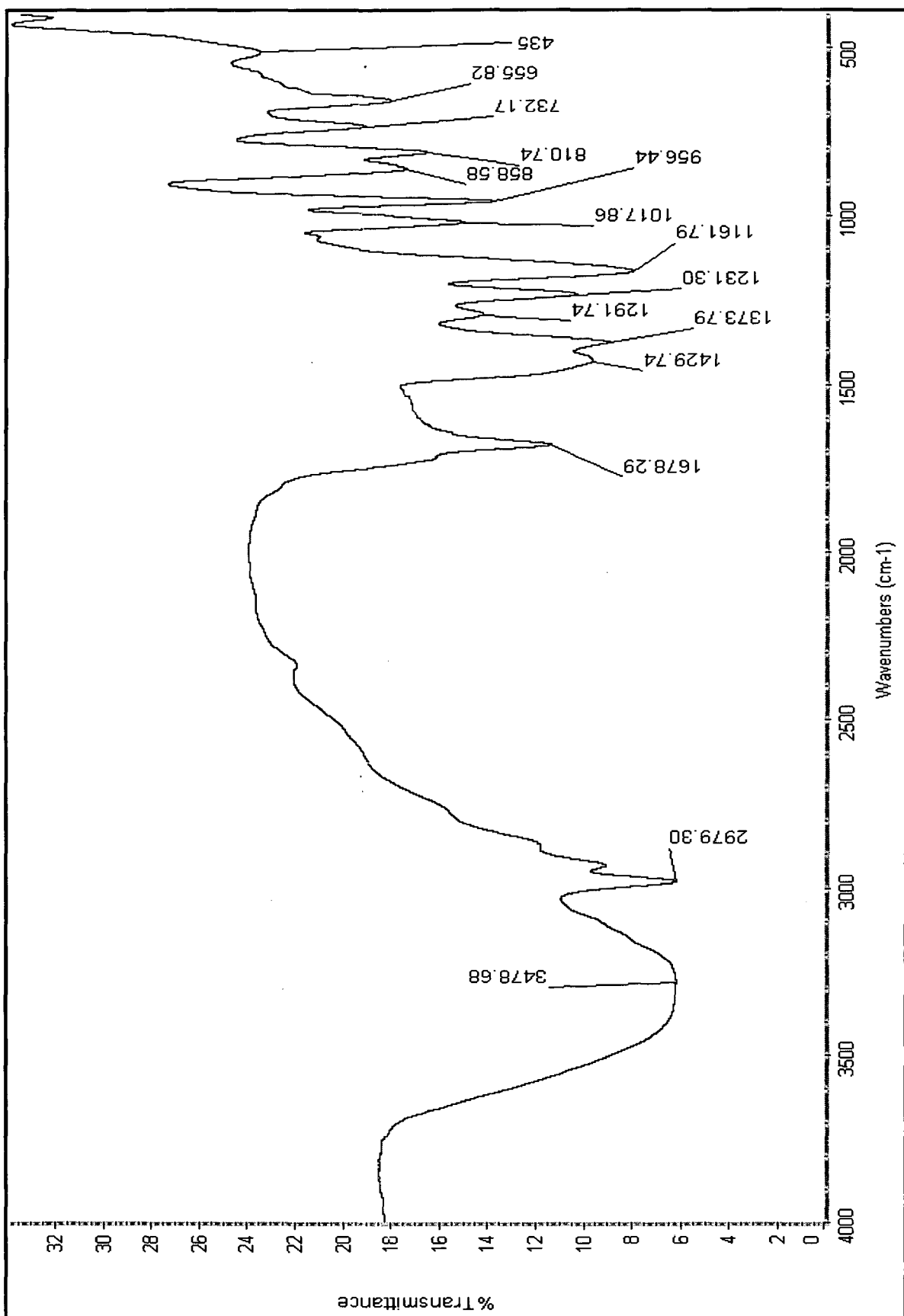


Fig 4.1 IR spectrum of $\text{Fe}(\text{3,5-Pr}_7\text{pzH})_2\text{Cl}_2$

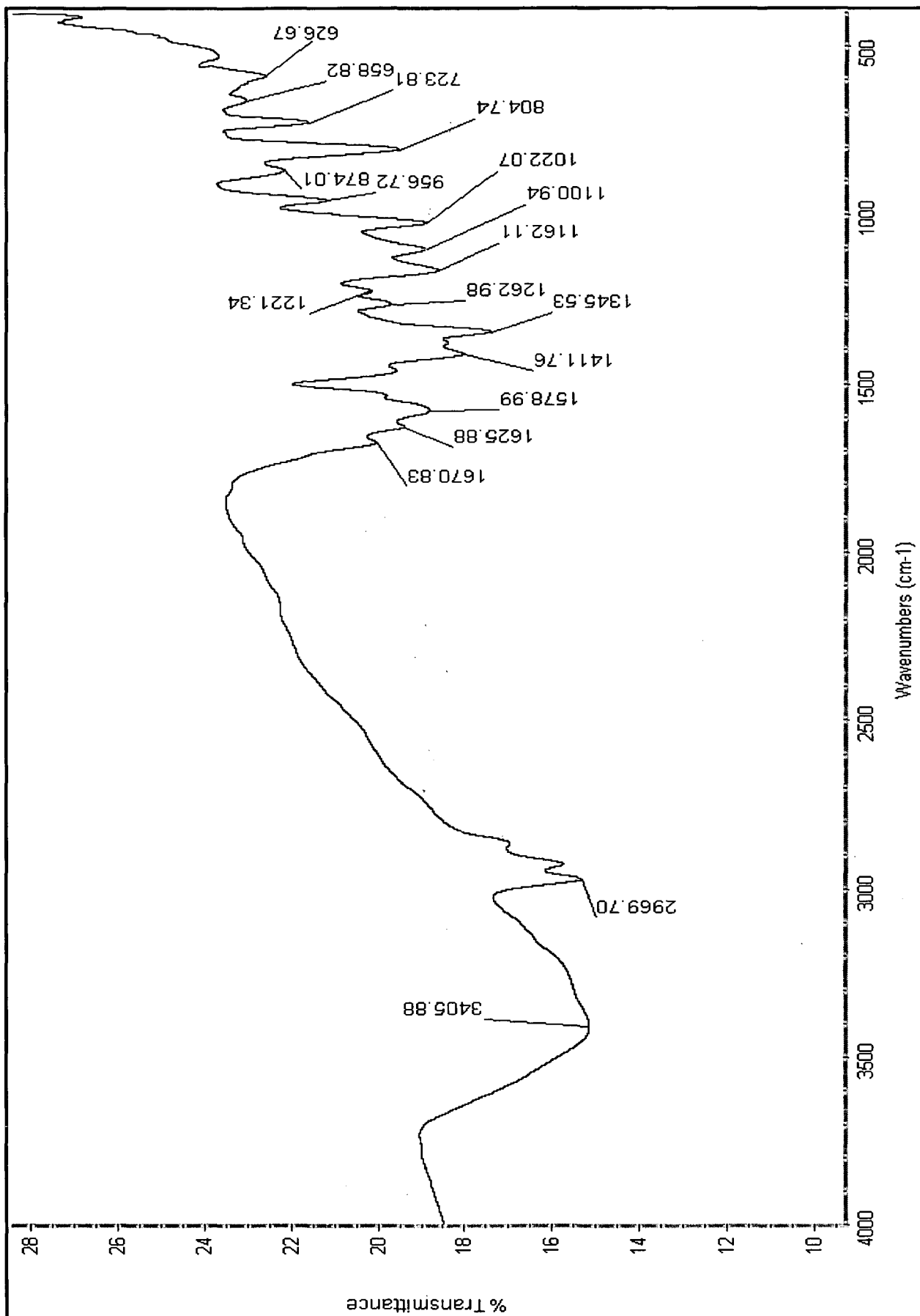


Fig 4.2 IR spectrum of $[\text{Fe}(\text{3-OCMe}_2\text{-5-Pr'pzH})_3] \cdot 2\text{OBz}$

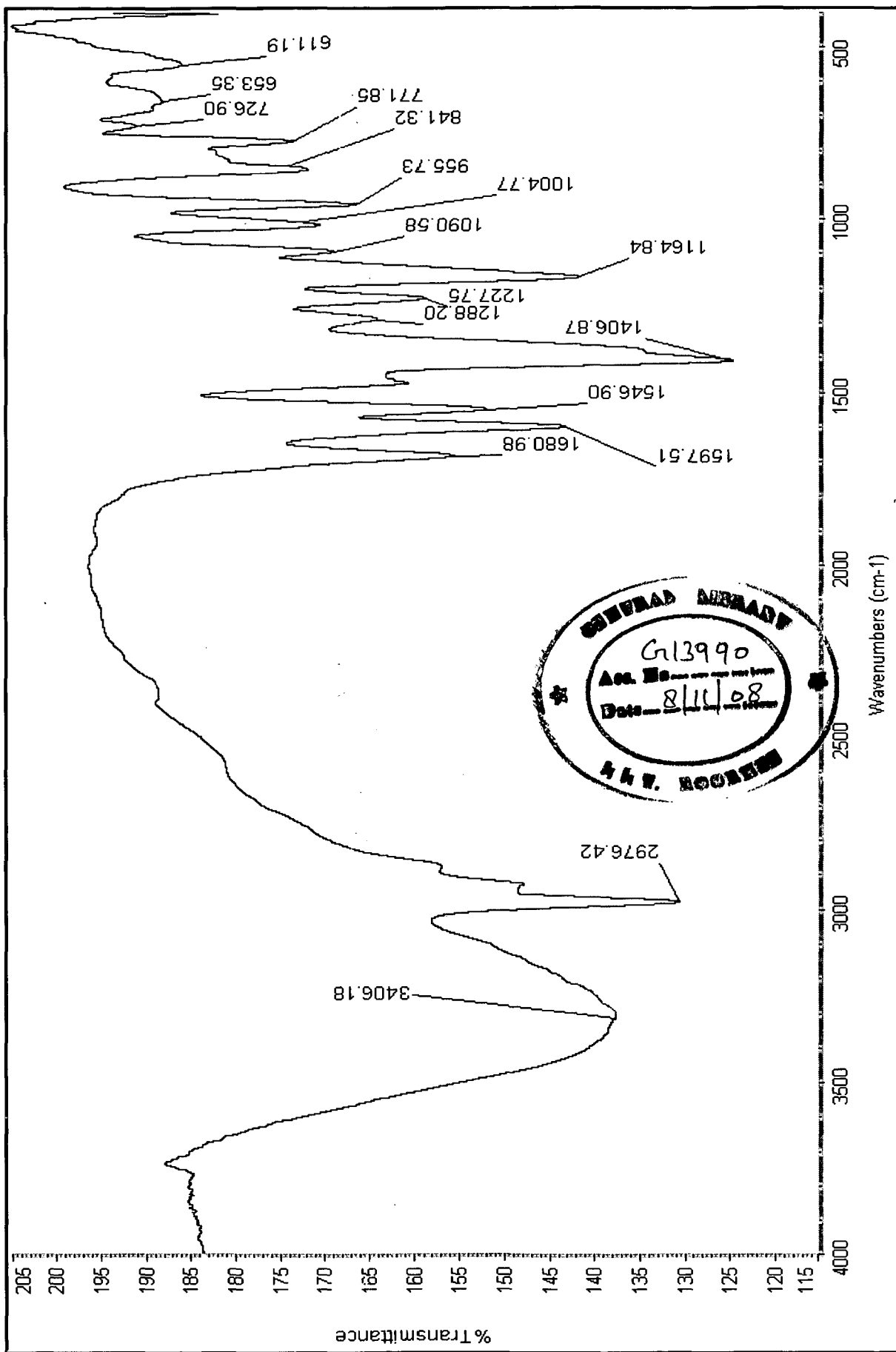


Fig. 4.3 IR spectrum of $[\text{Fe}(\text{3-OCMe}_2\text{-5-Pr'pzH})_3] \cdot 2\text{Cl} \cdot \text{OBz}$

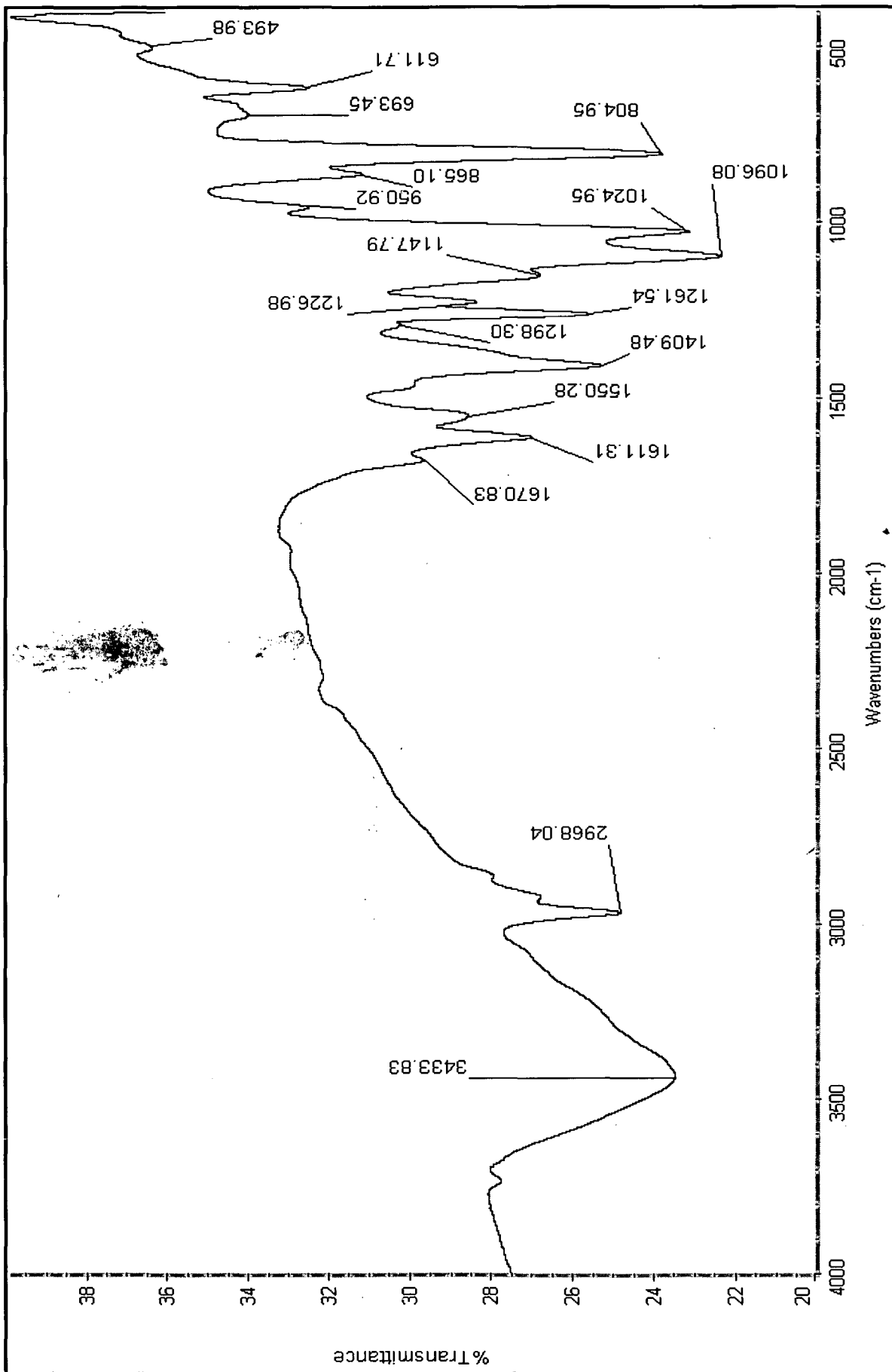


Fig 4.4 IR spectrum of $[\text{Fe}(\text{3-OCMe}_2\text{-5-Pr'pzH})_3] \cdot 2\text{F-OBz}$

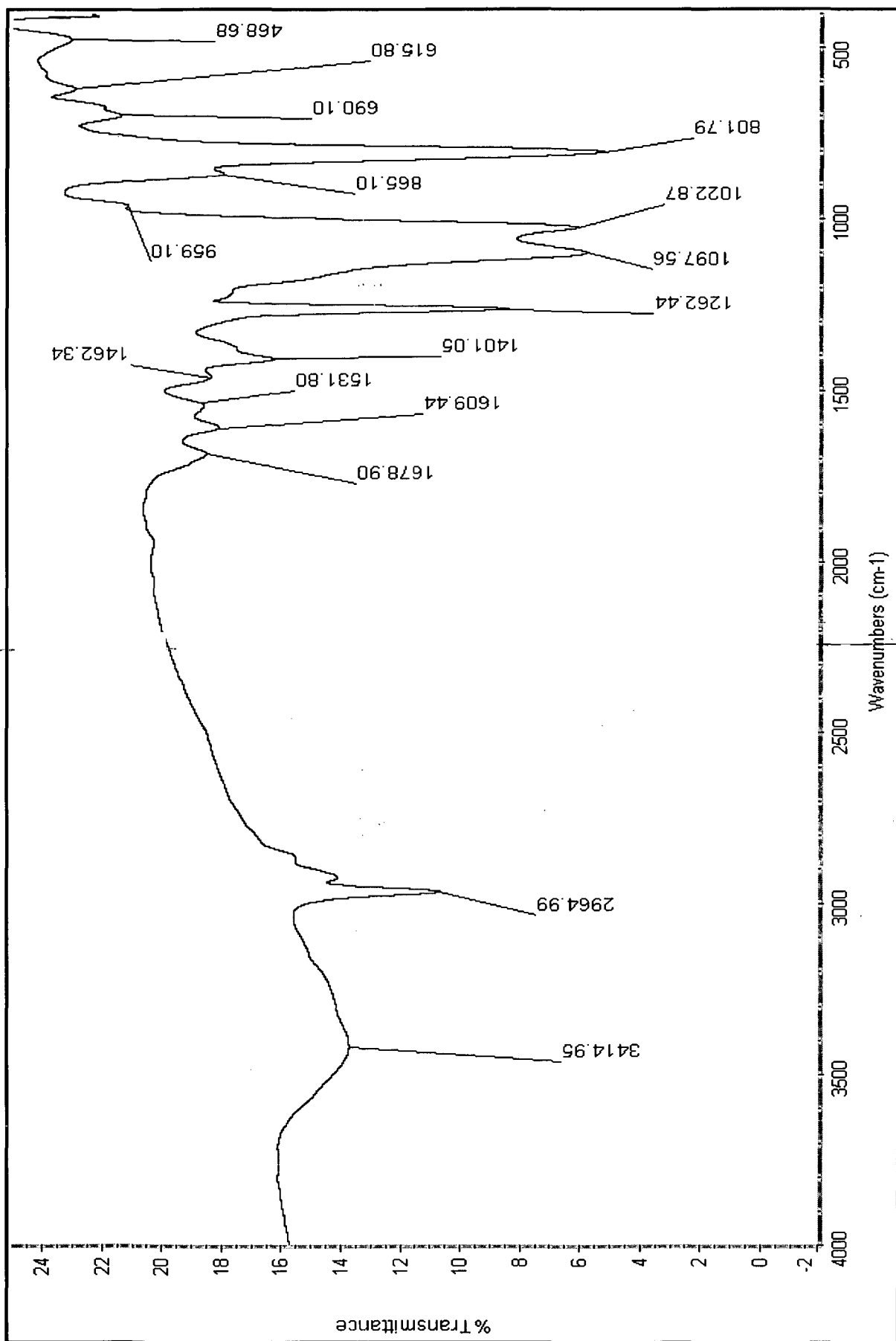


Fig 4.5 IR spectrum of $[\text{Fe}(\text{3-OCMe}_2\text{-5-Pr'pzH})_3] \cdot 2\text{CH}_3\text{-OBz}$

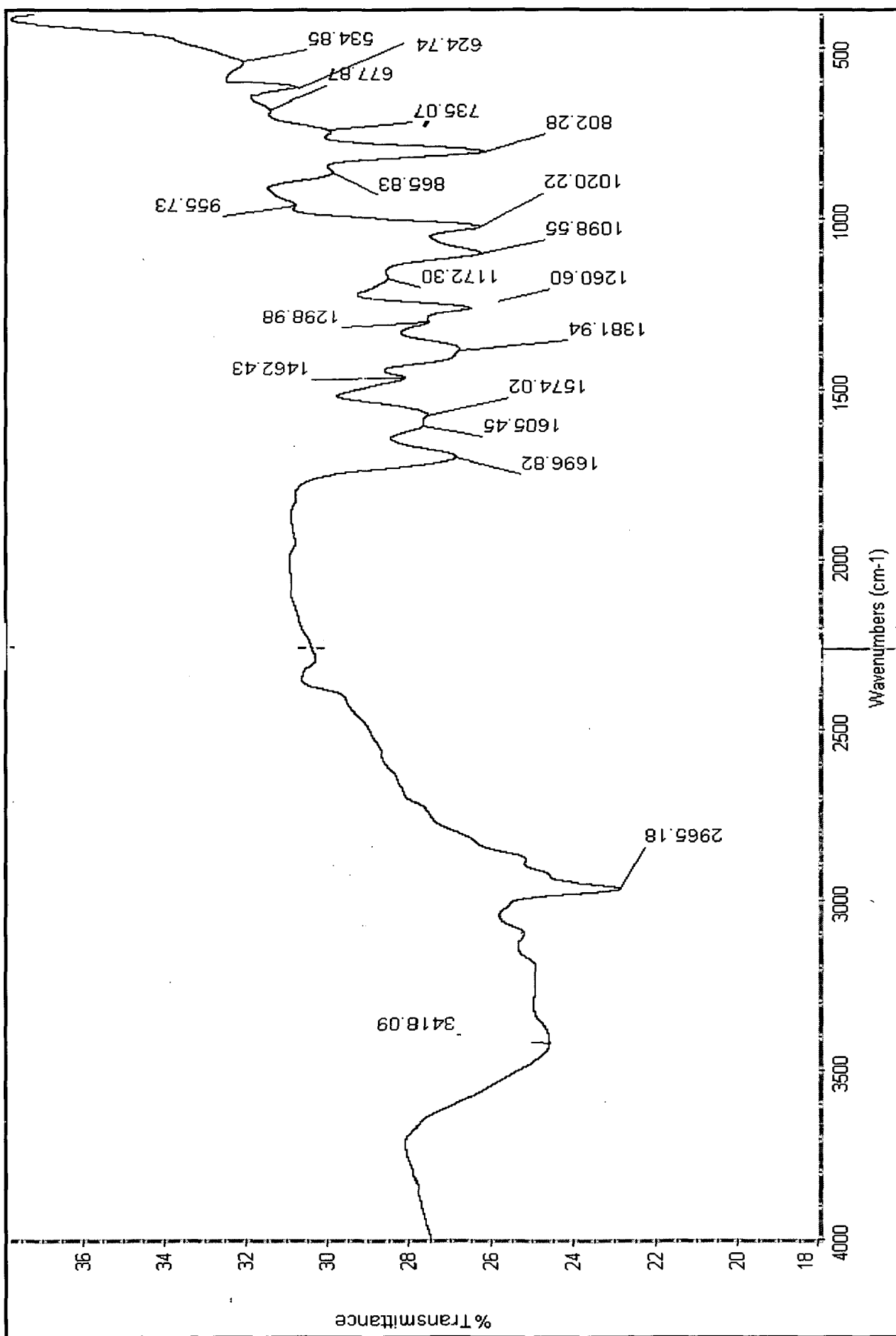


Fig 4.7 IR spectra of $[\text{Fe}(\text{3-OCMe}_2\text{-5-Pr}^1\text{pzH})_3] \cdot 2\text{CHO-OBz}$

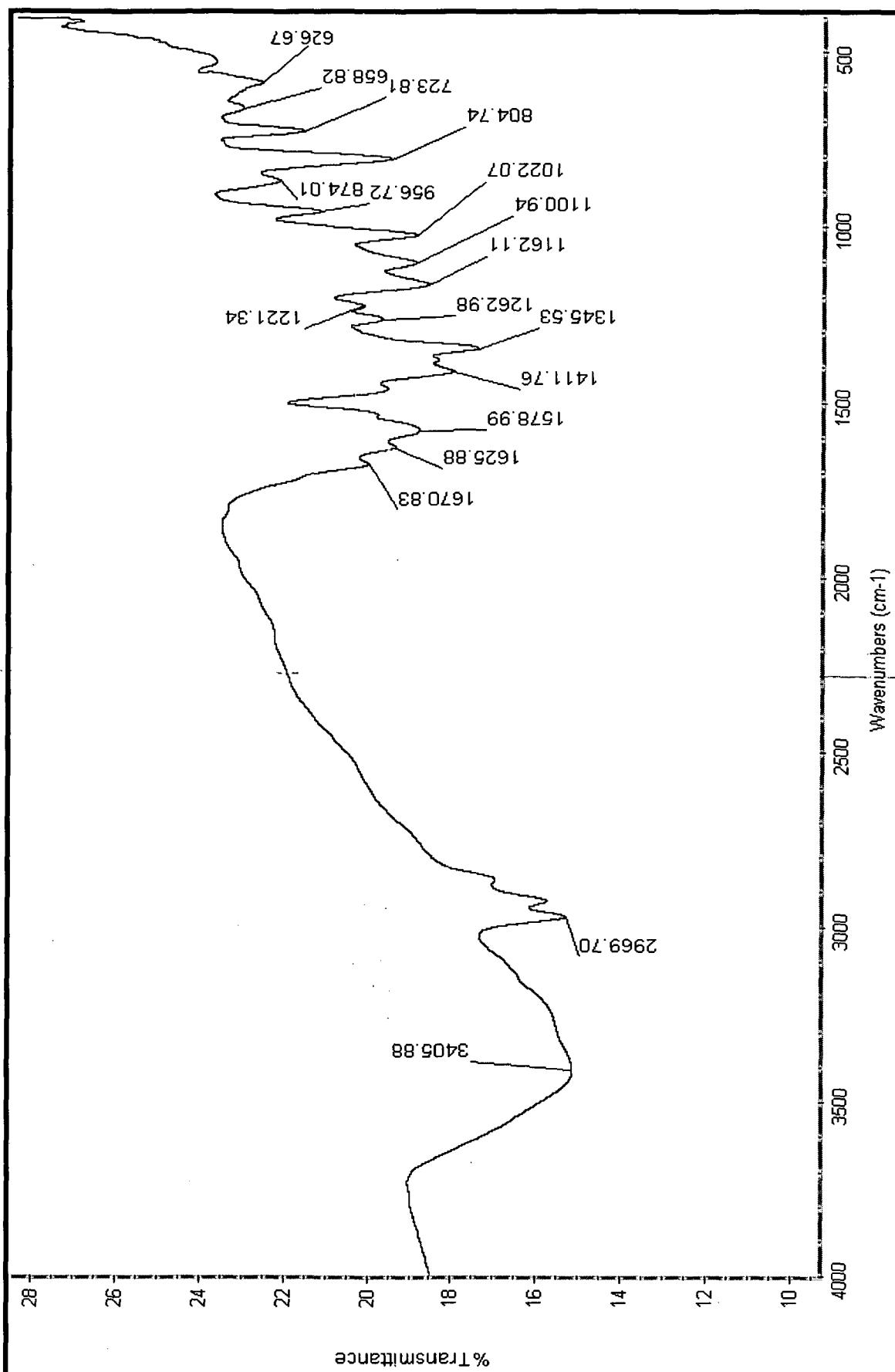


Fig 4.8 IR spectra of $[\text{Fe}(\text{3-OCMe}_2\text{-5-Pr}^1\text{pzH})_3]_{1.2}\text{CN-OBz}$

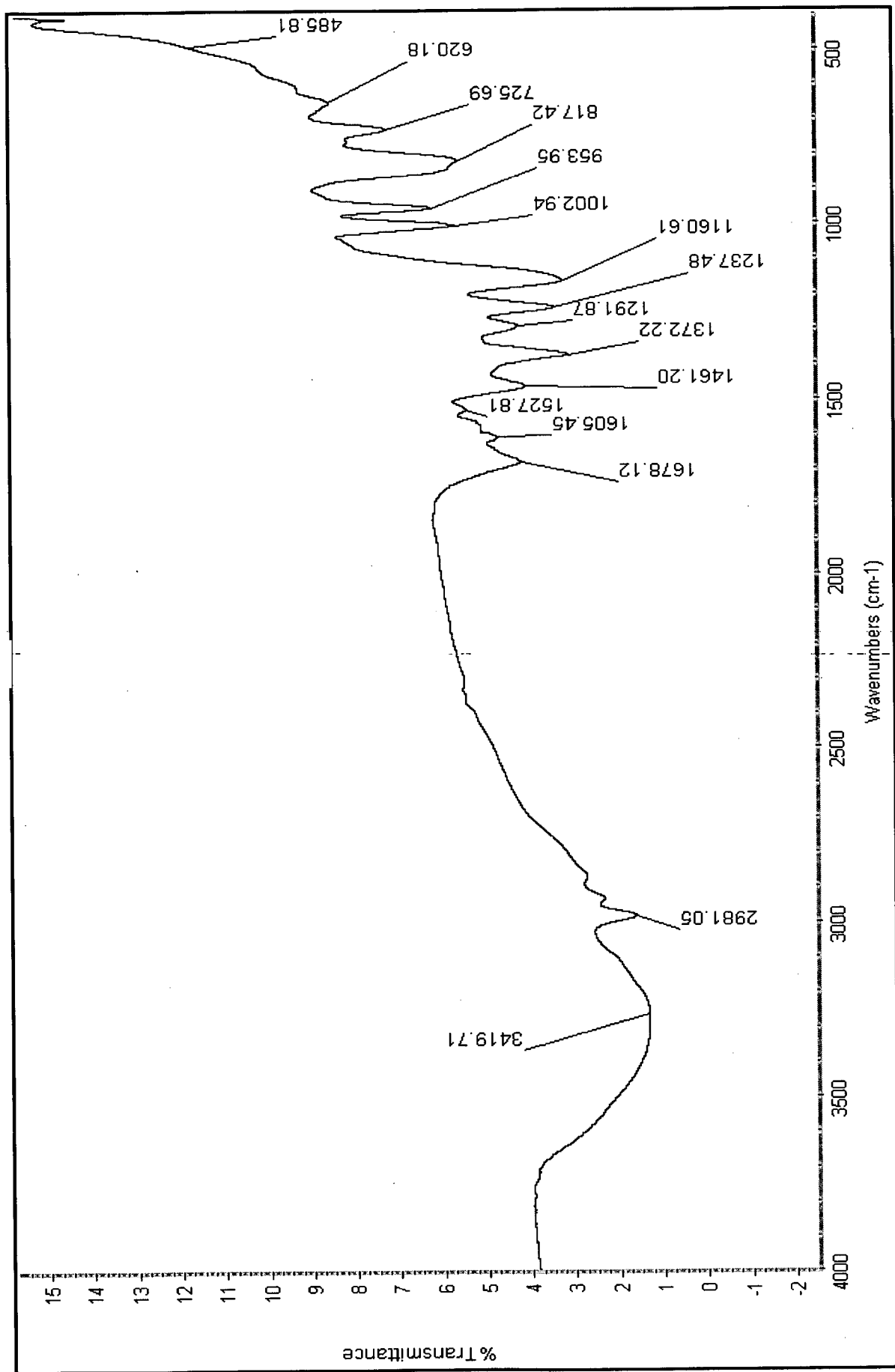


Fig 4.9 IR spectrum of $[\text{Fe}(\text{3-OCMe}_2\text{-5-Pr'pzH})_3] \cdot 2\text{NH}_2\text{-OBz}$

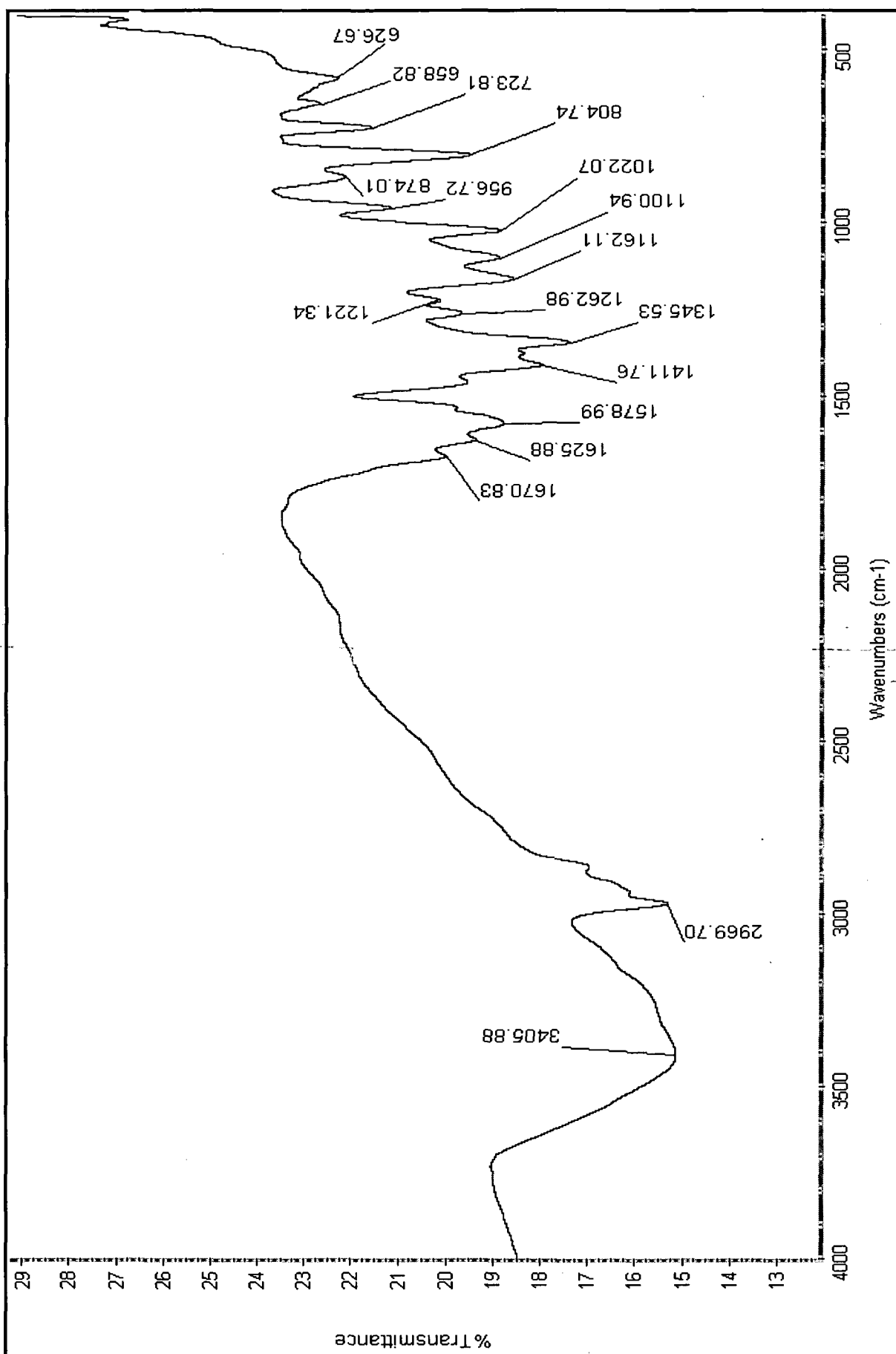


Fig 4.10 IR spectrum of $[\text{Fe}(\text{3-OCMe}_2\text{-5-Pr'pzH})_3] \cdot 2\text{NO}_2\text{-OBz}$

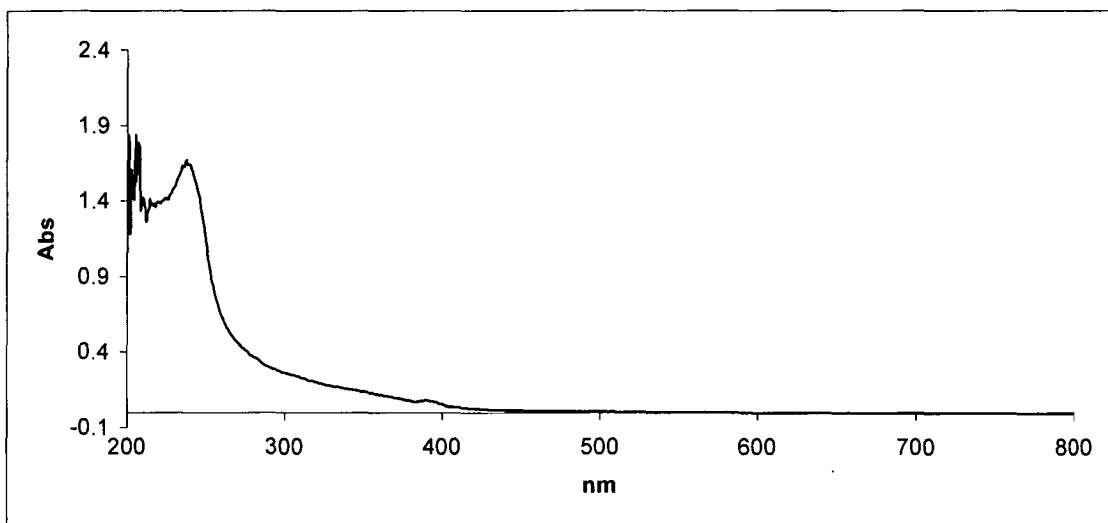


Fig 4.11 UV-Visible spectrum of $\text{Fe}(3,5\text{-Pr}^i_2\text{pzH})_3\text{Cl}_2$

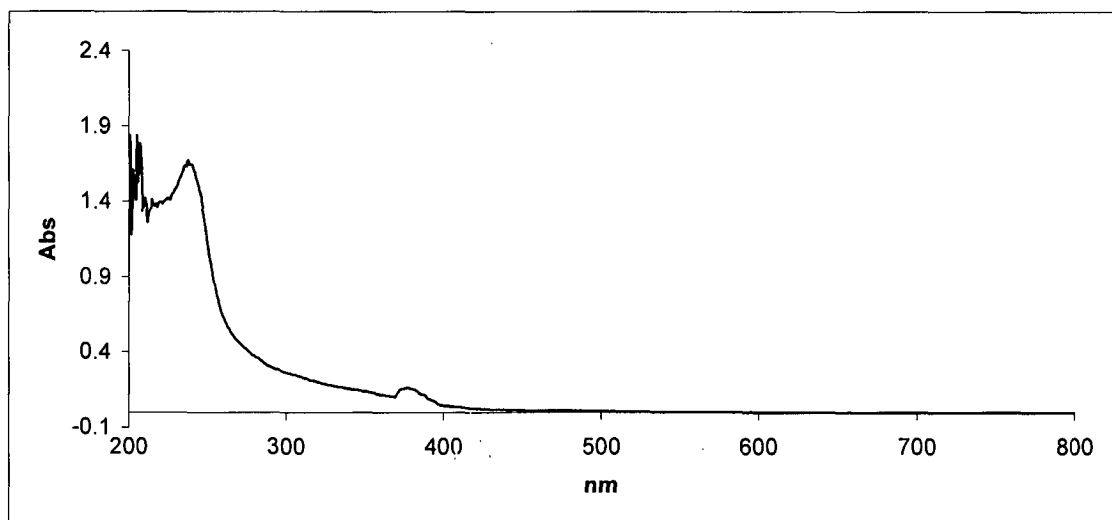


Fig 4.12 UV-Visible spectrum of $[\text{Fe}(3\text{-OCMe}_2\text{-5-Pr}^i\text{pzH})_3].2\text{OBz}$

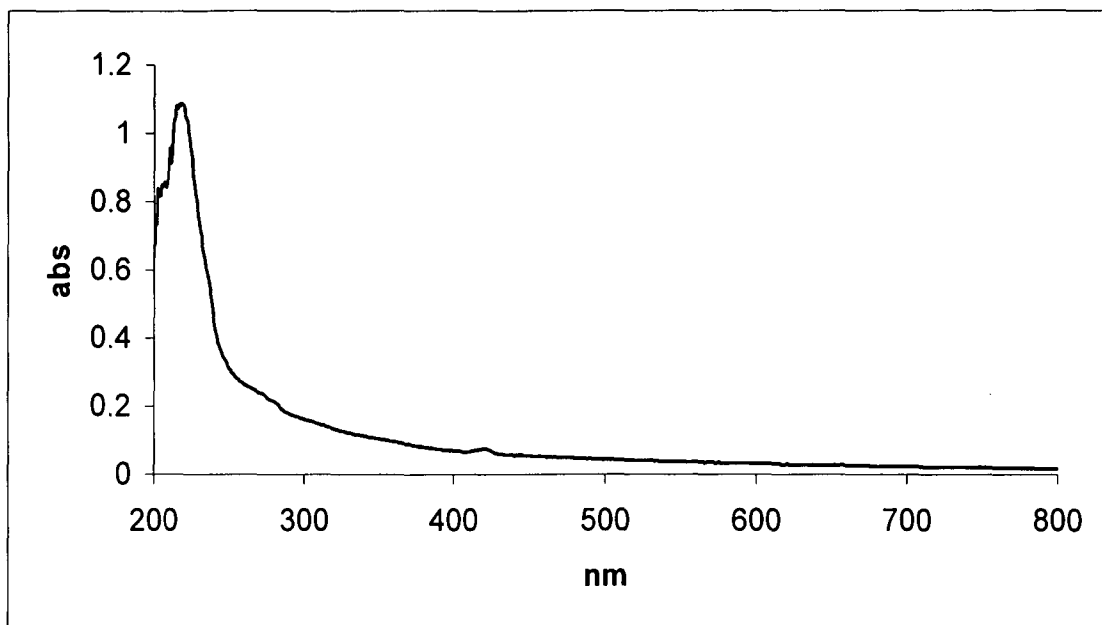


Fig 4.13 UV-Visible spectrum of $[\text{Fe}(3\text{-OCMe}_2\text{-5-Pr}^i\text{pzh})_3]\cdot 2\text{Cl-OBz}$

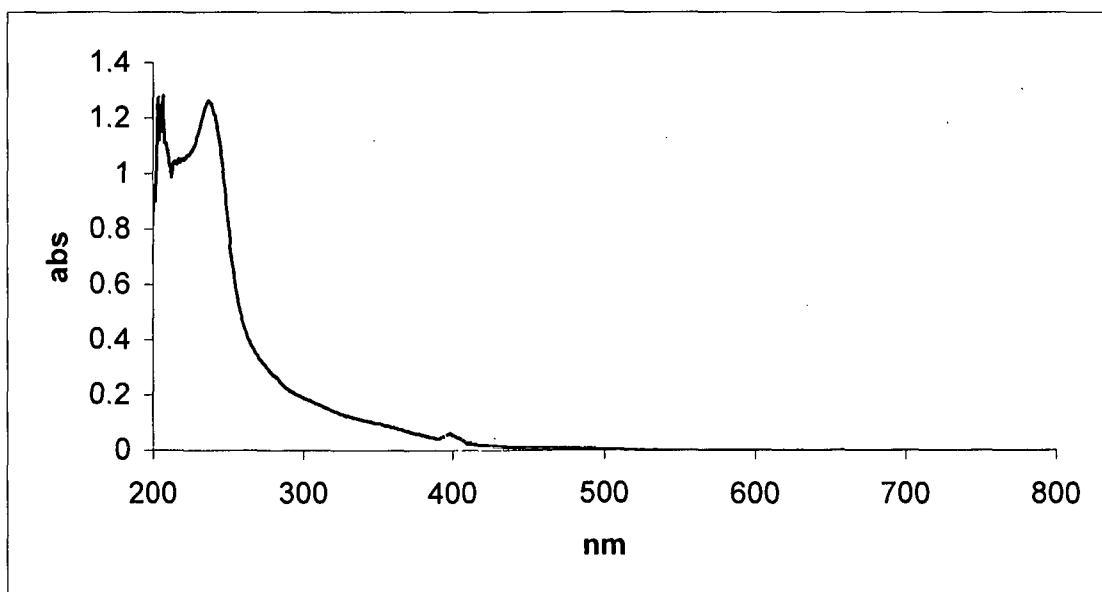


Fig 4.14 UV-Visible spectrum of $[\text{Fe}(3\text{-OCMe}_2\text{-5-Pr}^i\text{pzh})_3]\cdot 2\text{F-OBz}$

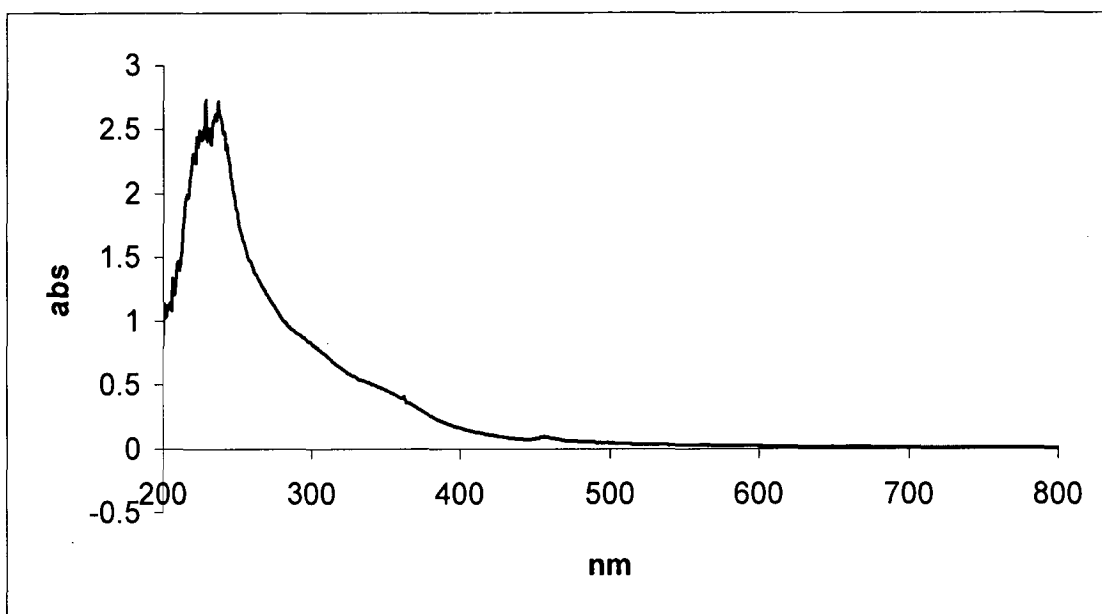


Fig 4.15 UV-Visible spectrum of $[\text{Fe}(\text{3-OCMe}_2\text{-5-PrpzH})_3] \cdot 2\text{CH}_3\text{-OBz}$

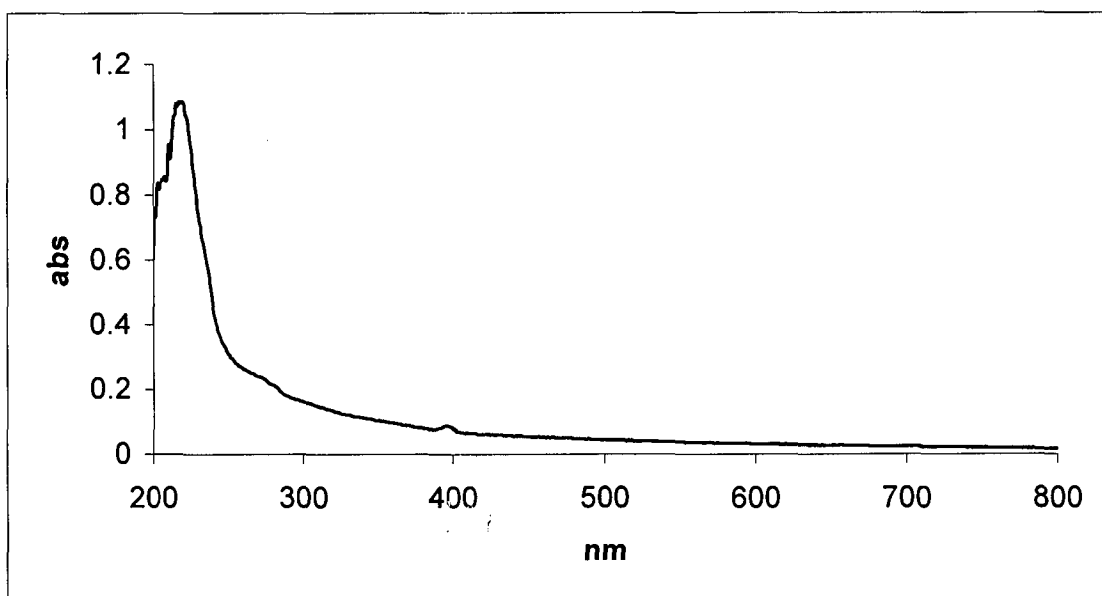


Fig 4.16 UV-Visible spectrum of $[\text{Fe}(\text{3-OCMe}_2\text{-5-Pr}^i\text{pzH})_3] \cdot 2\text{OCH}_3\text{-OBz}$

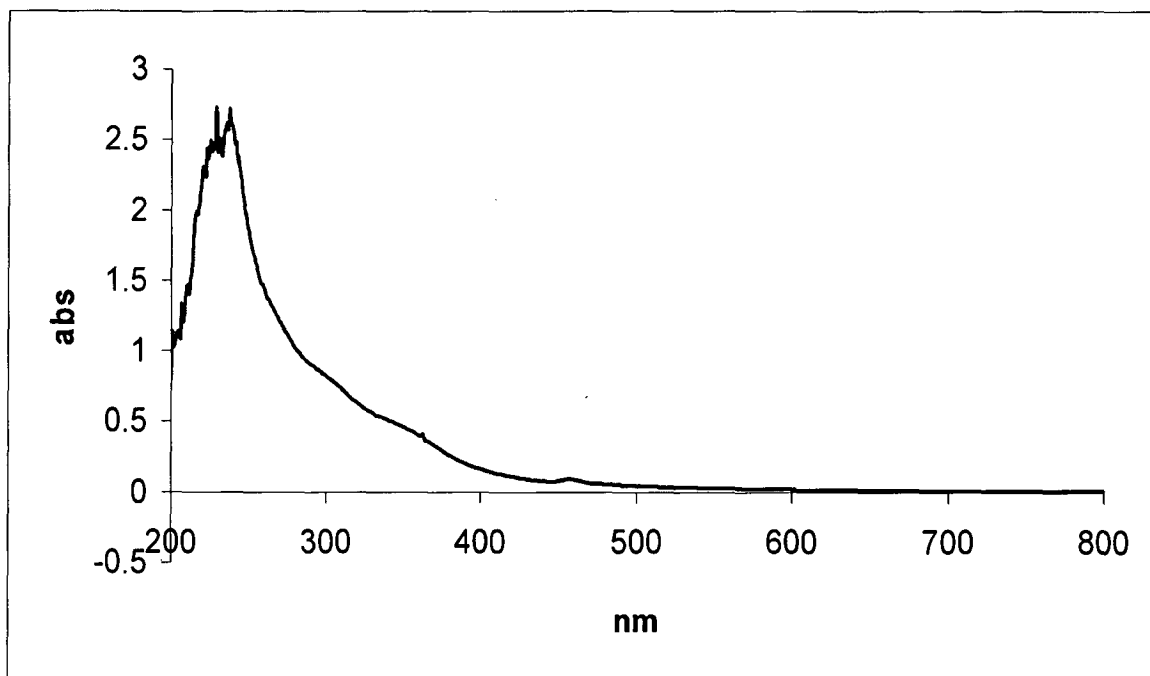


Fig 4.17 UV-Visible spectrum of $[\text{Fe}(3\text{-OCMe}_2\text{-5-Pr}^1\text{pzH})_3]\cdot 2\text{CHO-OBz}$

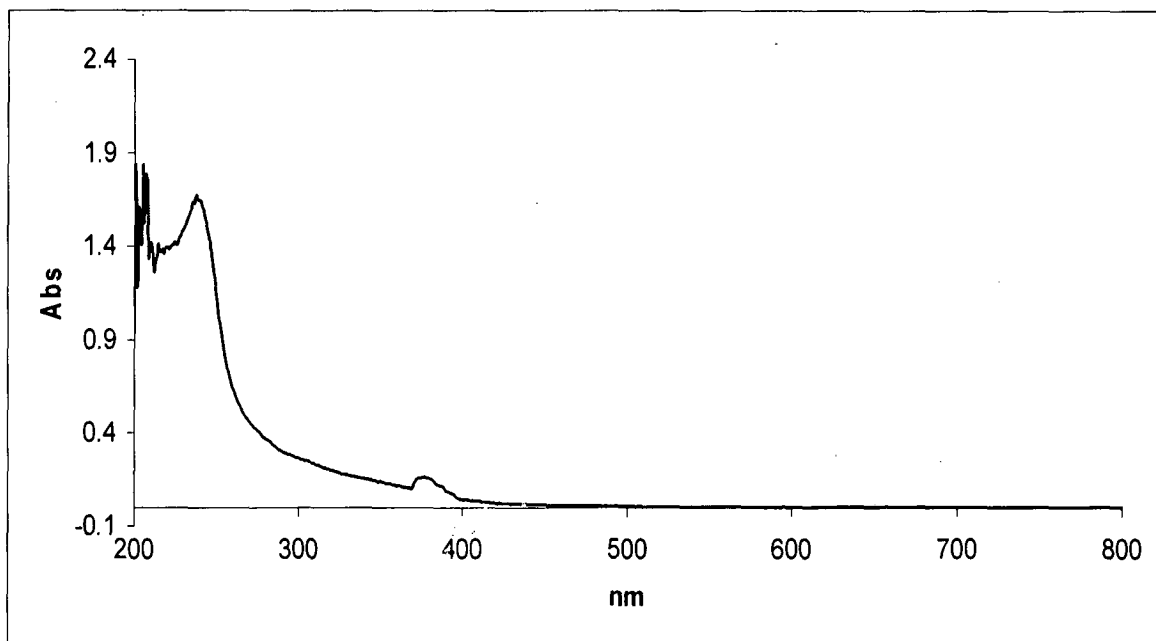


Fig 4.18 UV-Visible spectrum of $[\text{Fe}(3\text{-OCMe}_2\text{-5-Pr}^1\text{pzH})_3]\cdot 2\text{CN-OBz}$

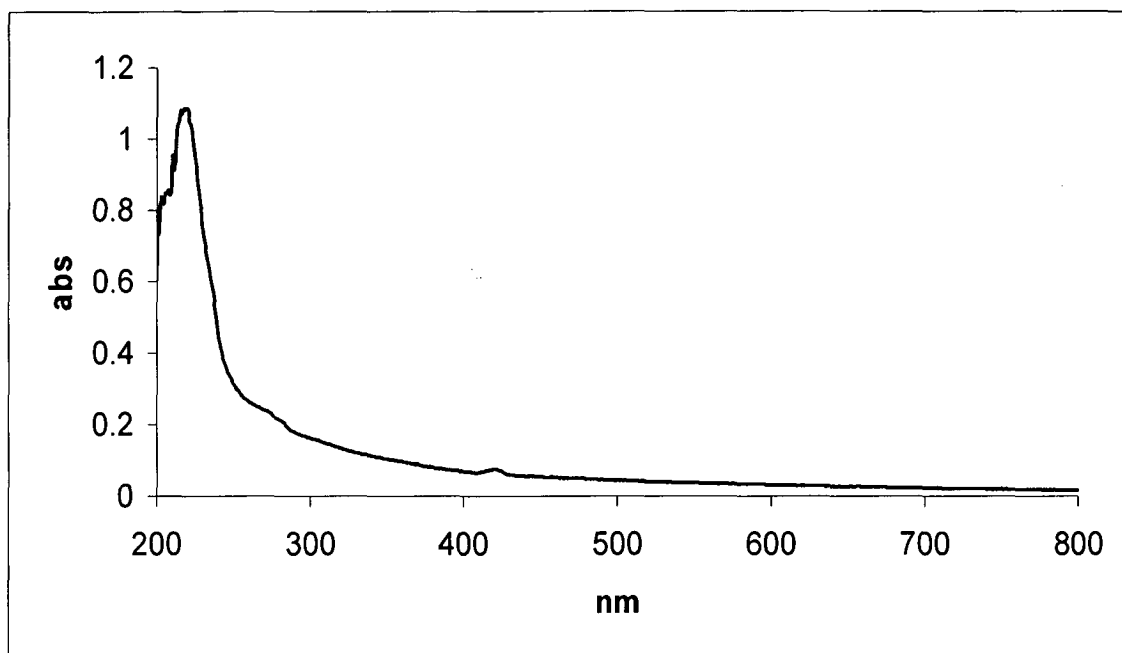


Fig 4.19 UV-Visible spectrum of $[\text{Fe}(3\text{-OCMe}_2\text{-5-Pr}^i\text{pzH})_3]\cdot 2\text{NH}_2\text{-OBz}$

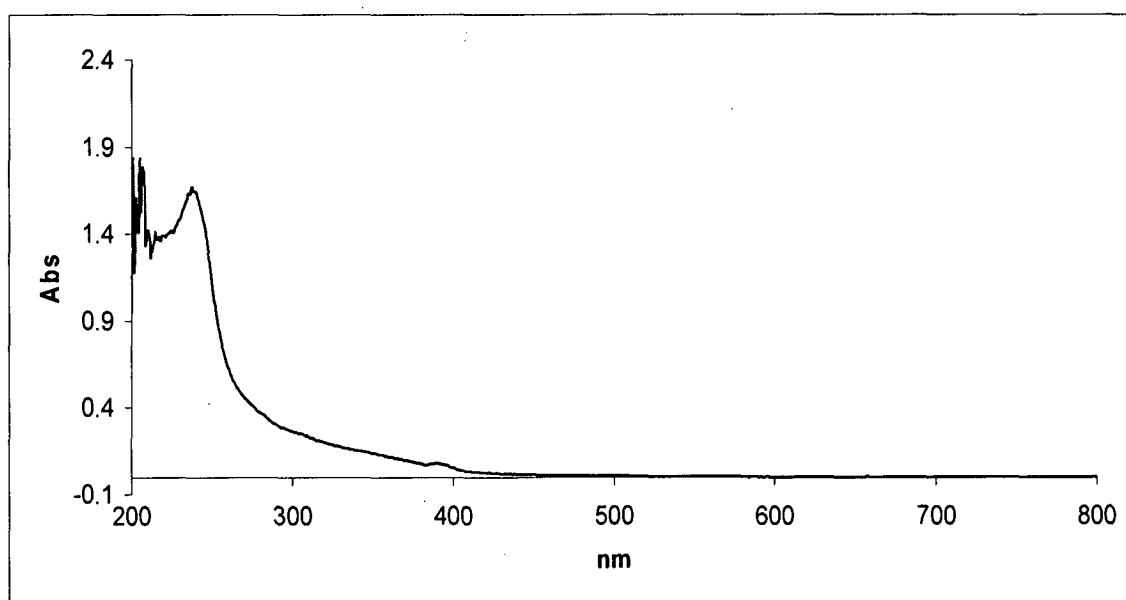


Fig 4.20 UV-Visible spectrum of $[\text{Fe}(3\text{-OCMe}_2\text{-5-Pr}^i\text{pzH})_3]\cdot 2\text{NO}_2\text{-OBz}$

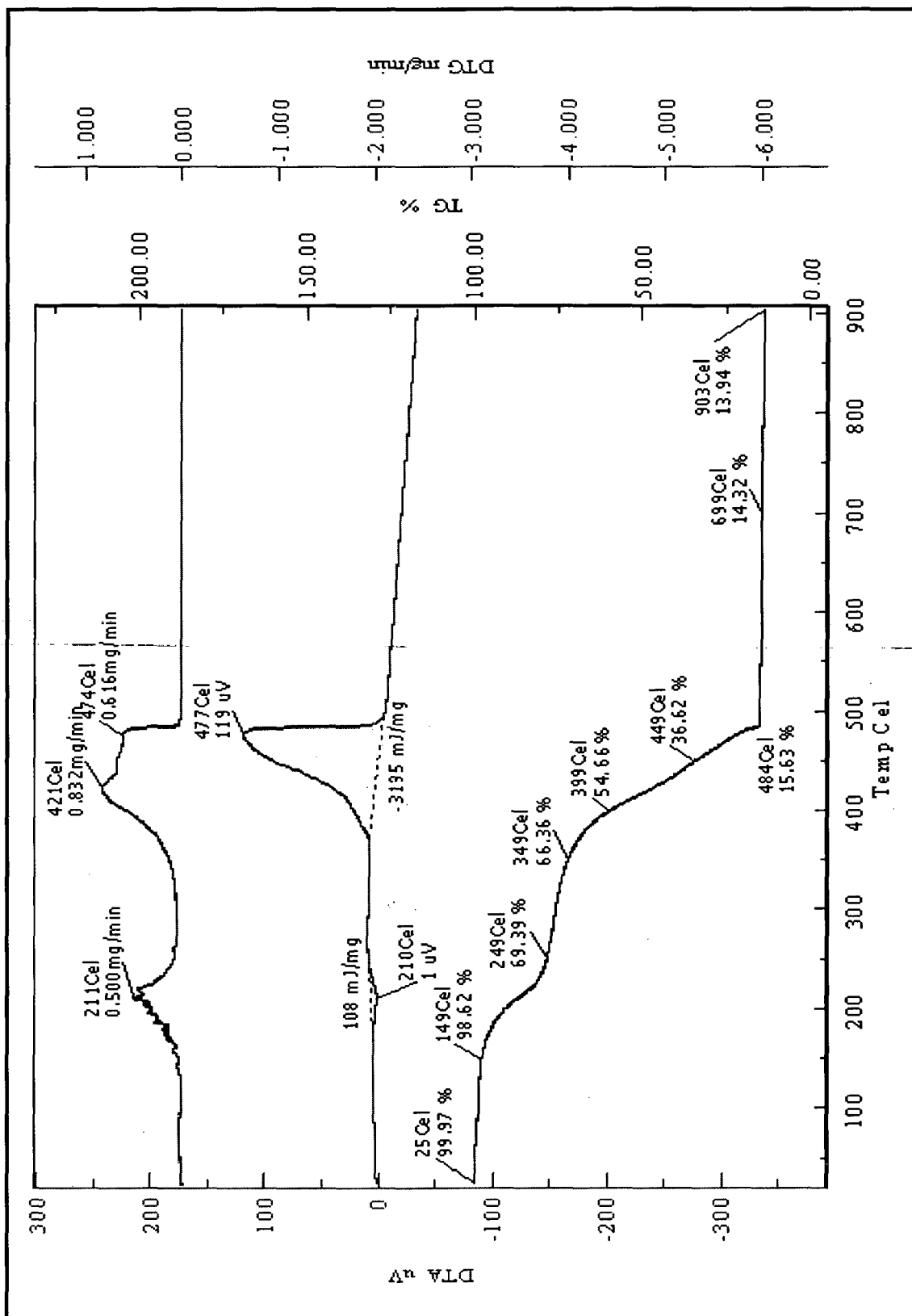


Fig 4.22 DTA-DTG-TG curve of $[Fe(3-OCMe_2-5-Pr'pzhH)_3] \cdot 2OBz$

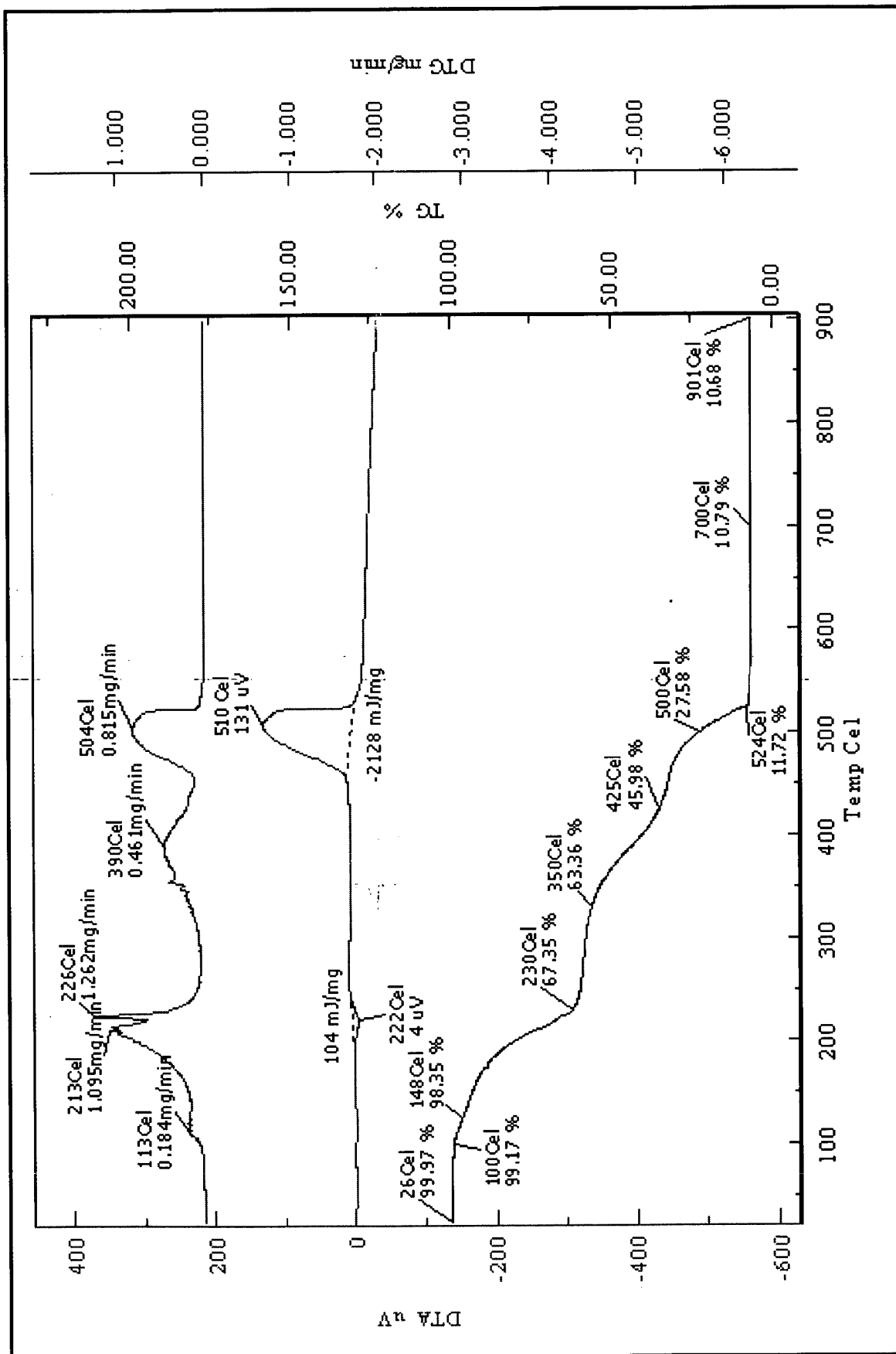


Fig 4.22 DTA-DTG-TG curve of $[\text{Fe}(\text{3-OCMe}_2\text{-5-Pr'pzH})_3] \cdot 2\text{Cl} \cdot \text{OBz}$

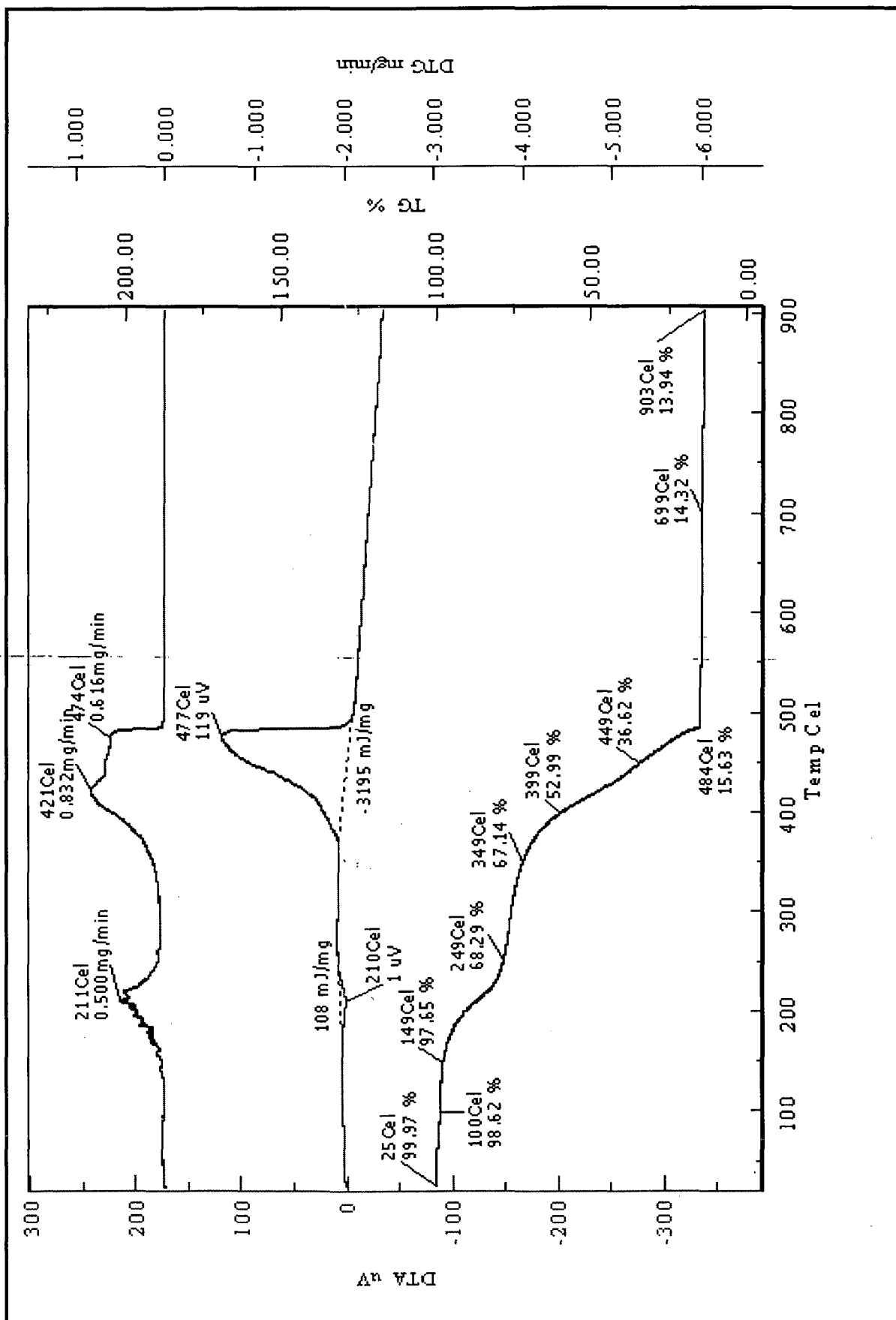


Fig 4.23 DTA-DTG-TG curve of $[\text{Fe}(\text{3-OCMe}_2\text{-5-Pr'pzH})_3]_2\text{F-OBz}$

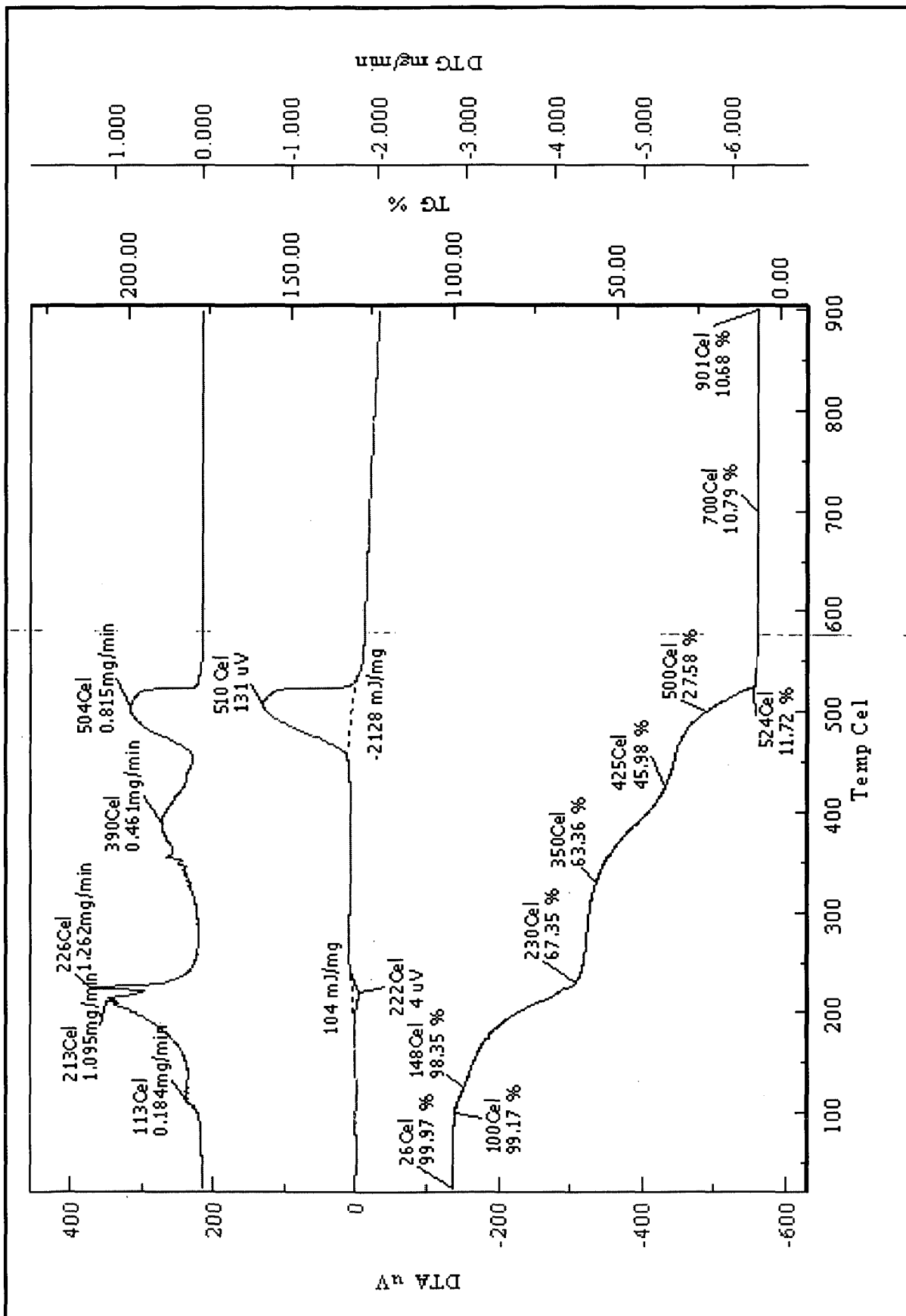


Fig 4.24 DTA-DTG-TG curve of $[\text{Fe}(\text{3-OCMe}_2\text{-5-Pr}^1\text{pzH})_3] \cdot 2\text{CH}_3 \cdot \text{OBz}$

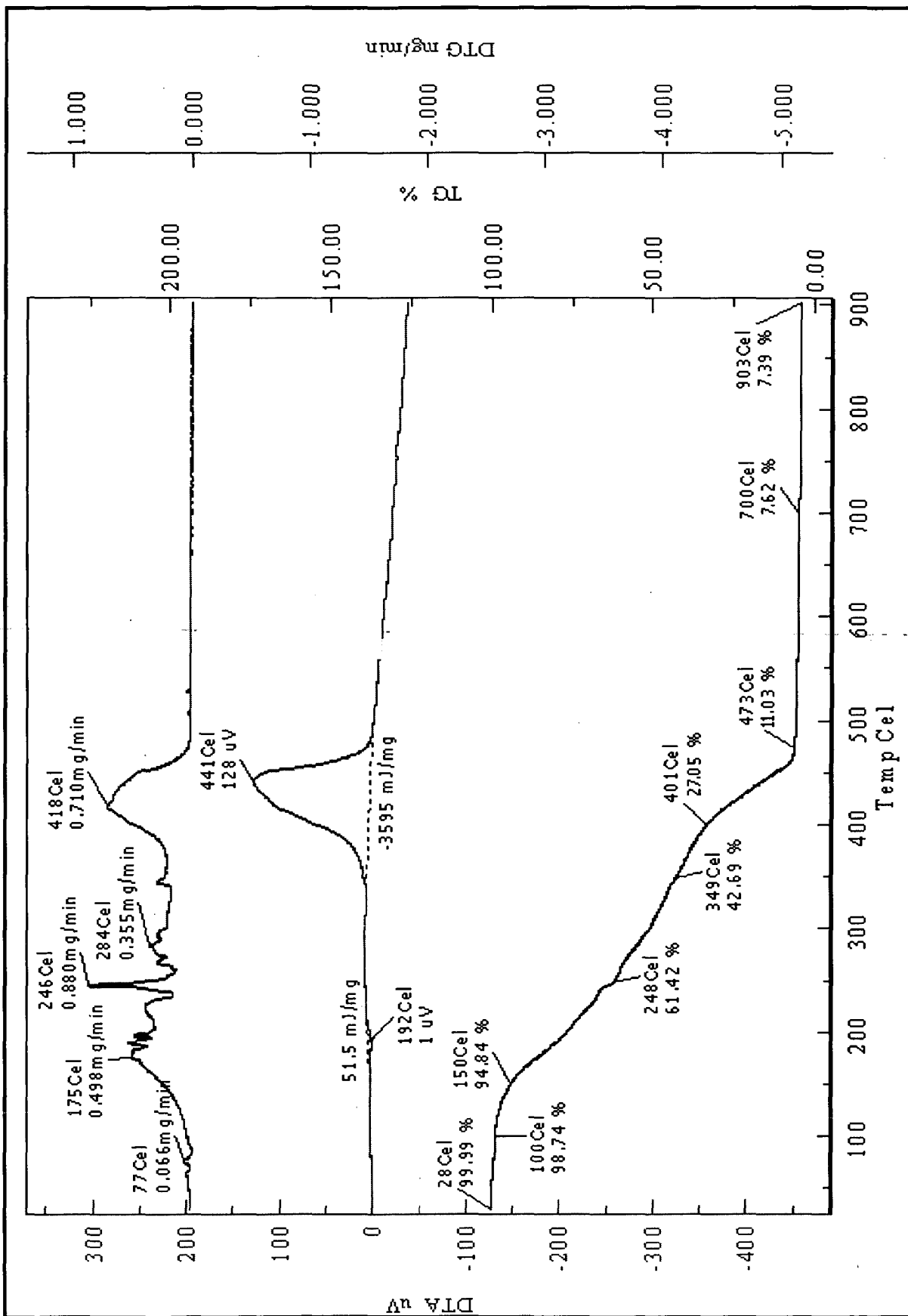


Fig 4.25 DTA-DTG-TG curve of $[\text{Fe}(\text{3-OCMe}_2\text{-5-Pr-pzH})_3] \cdot 2\text{OCH}_3 \cdot \text{OBz}$

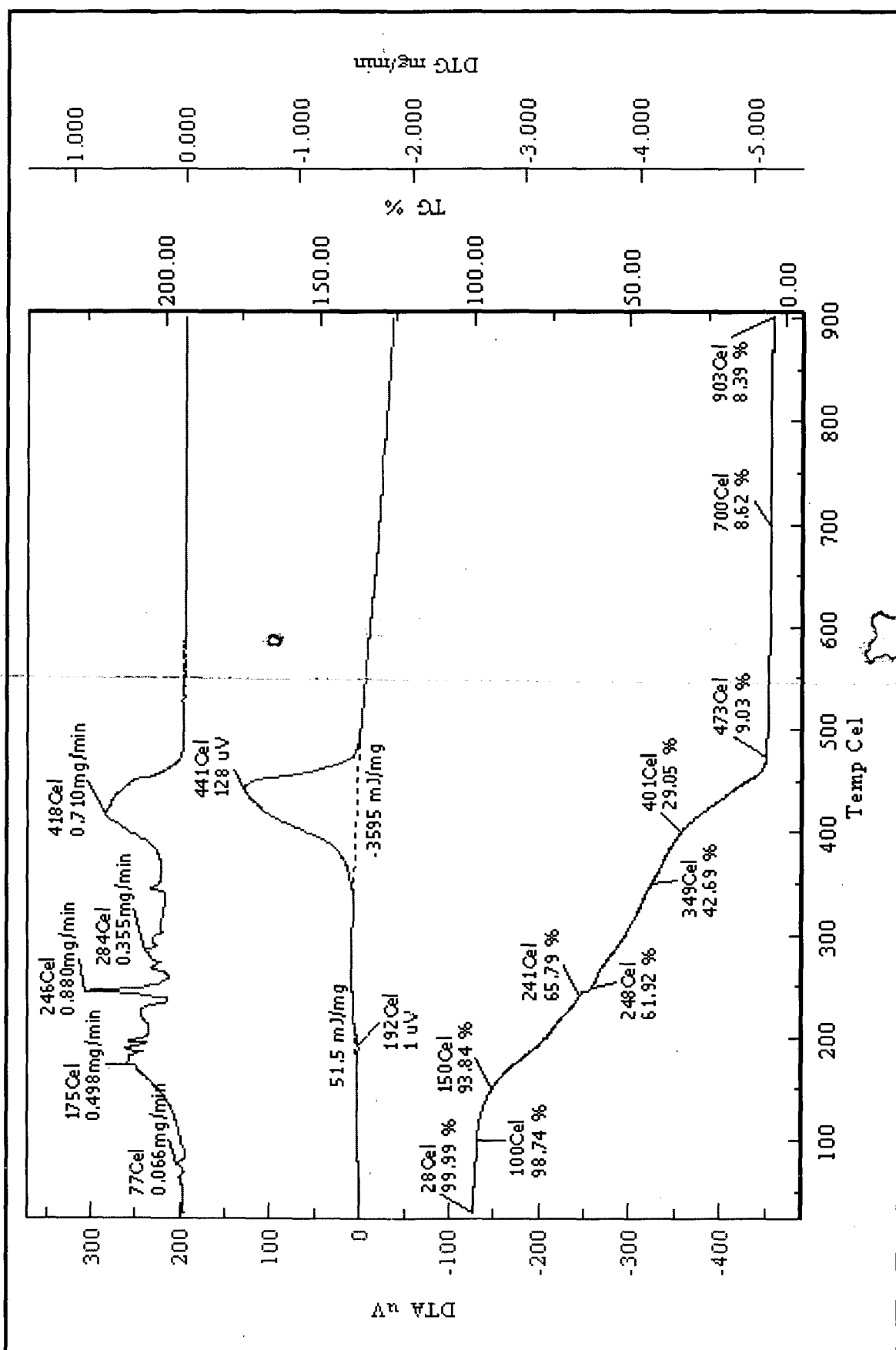


Fig 4.26 DTA-DTG-TG curve of $[Fe(3-OCMe_2-5-Pr^1pzH)_3] \cdot 1.2CHO-OBz$

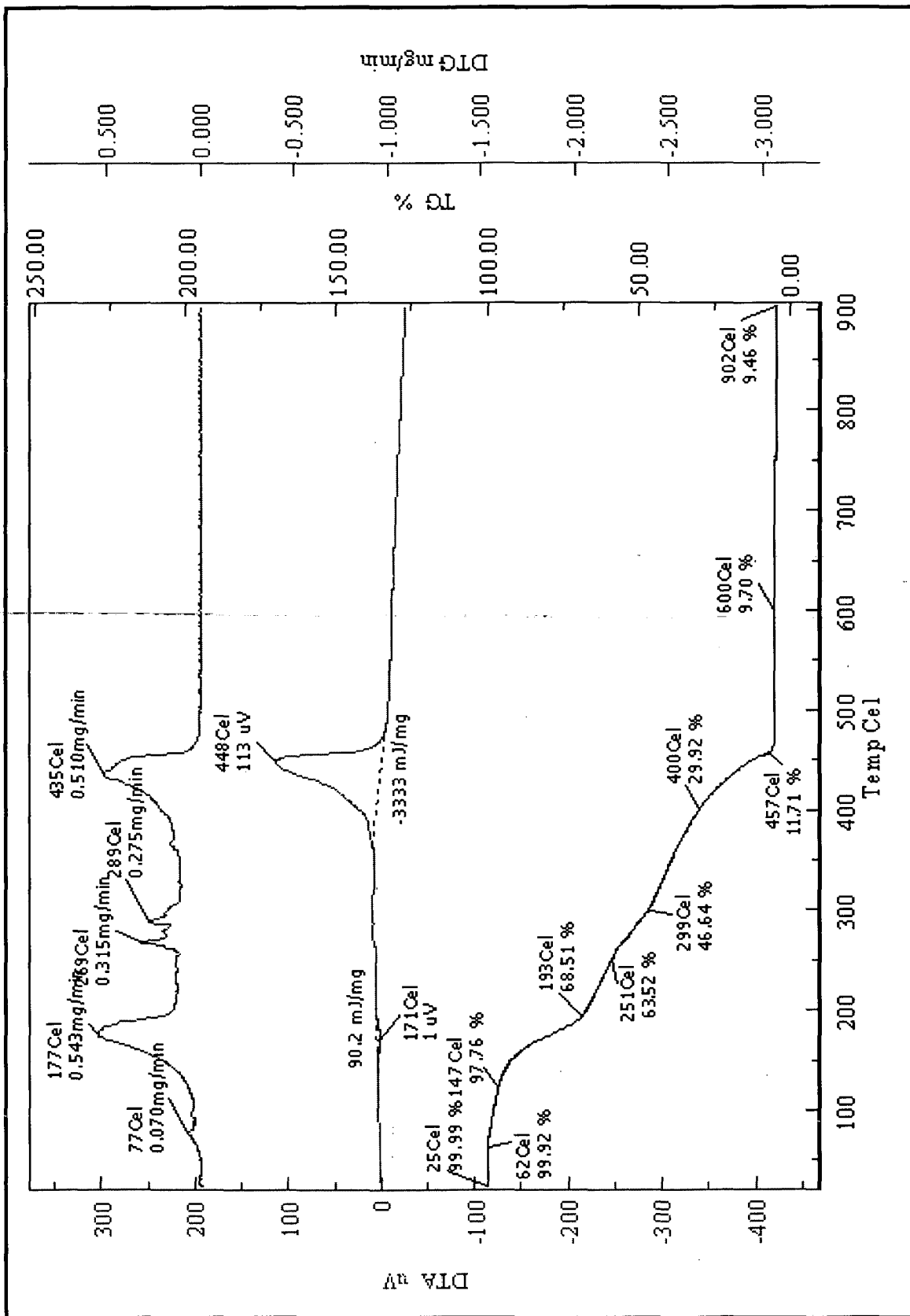


Fig 4.27 DTA-DTG-TG curve of $[\text{Fe}(\text{3-OCMe}_2\text{-5-Pr}^1\text{pzH})_3] \cdot 2\text{CN-OBz}$

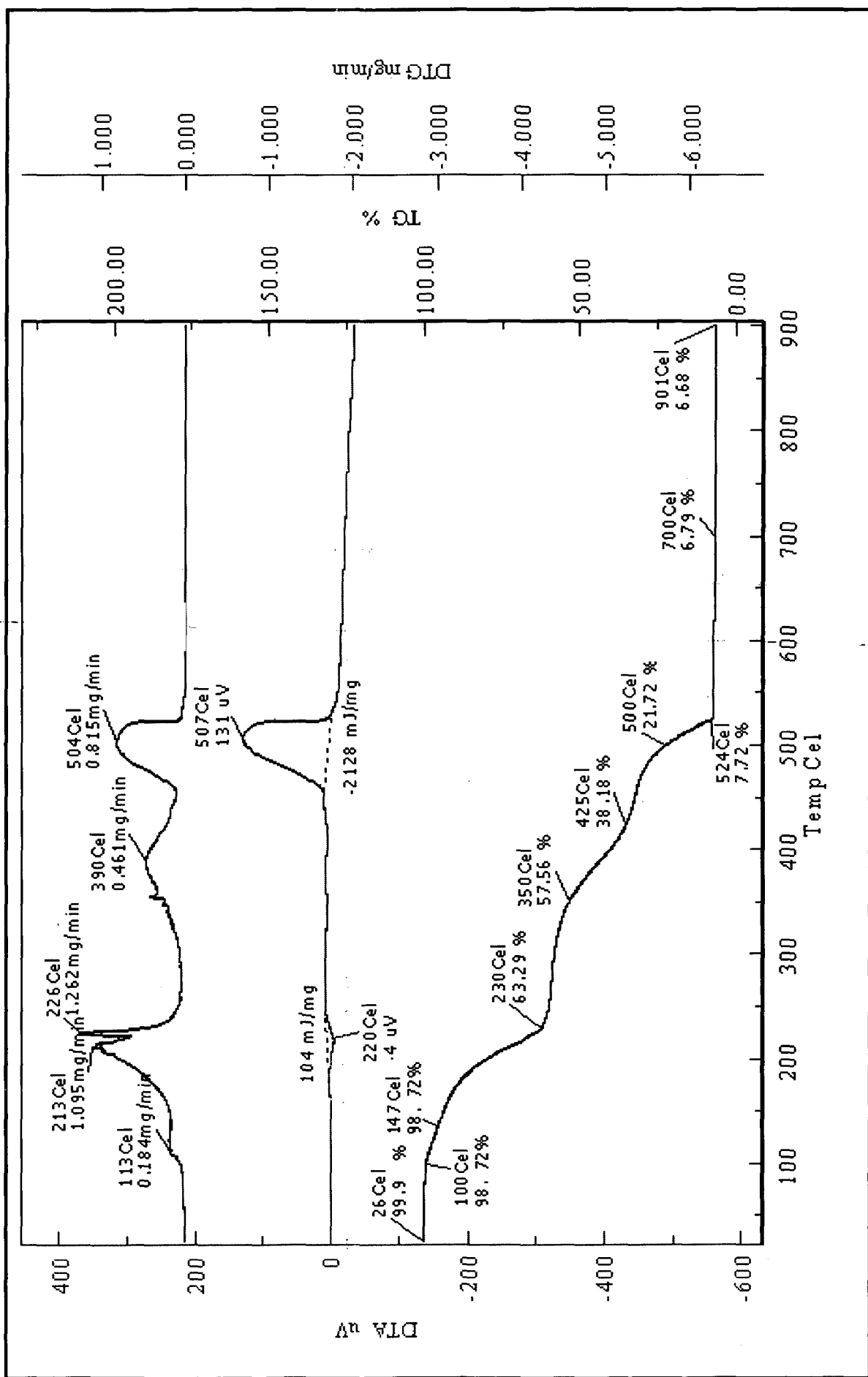


Fig 4.28DTA-DTG-TG curve of $[Fe(3-OCMe_2-5-Pr(pzH)_3)_2NH_2-OBz]$

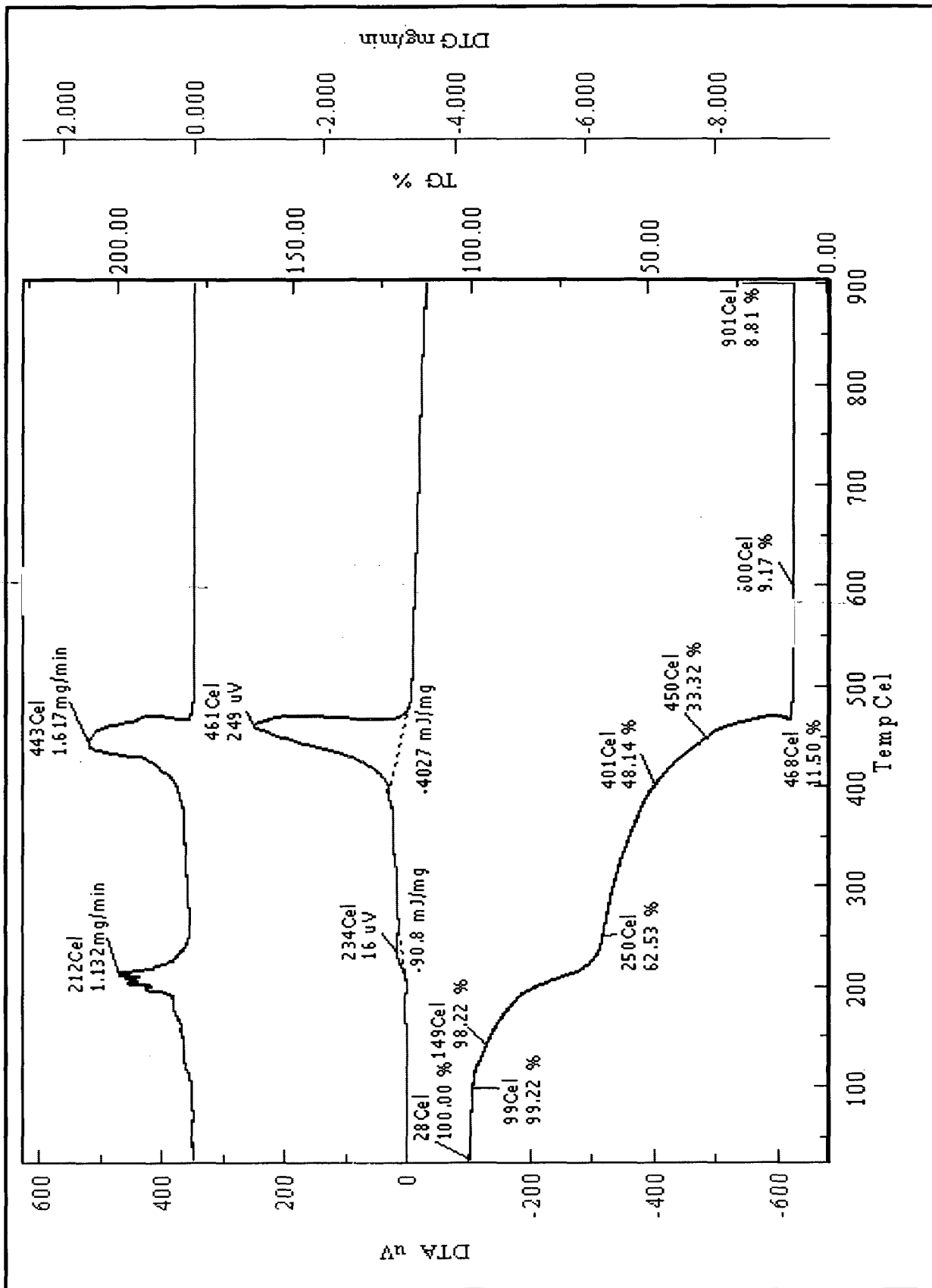


Fig 4.29 DTA-DTG-TG curve of $[\text{Fe}(\text{3-OCMe}_2\text{-5-Pr'pzH})_3] \cdot 2\text{NO}_2 \cdot \text{OBz}$

5. CONCLUSION

5. CONCLUSION

The ligand 3,5-diisopropylpyrazole was prepared. The complexes of this ligand with iron (II) were prepared by reaction of the methanolic solution of ferrous chloride with 3,5-diisopropylpyrazole in a solution of dichloromethane. The oxidation of methine C-H bond present in the isopropyl group of the pyrazole ring was tried out using H_2O_2 as the oxidizing agent and the effect of the presence of various sodium p-X benzoates ($X = H, Cl, F, CH_3, OCH_3, CHO, CN, NO_2, NH_2$) was studied. The products were studied using IR spectroscopy and seen to contain an additional peak which was inferred to be due to iron-oxygen bond formed. The UV-Vis spectra of the compounds showed absorption in the range 220-245 due to the metal to ligand charge transfer while d-d transitions showed absorption in the range 370-470. The thermal studies showed that the decomposition of the compounds mainly took place in two stages.

REFERENCES

REFERENCES:

1. Labinger J. A. and Bercaw J. E., "Understanding and exploiting C-H bond activation", *Nature* **417**, 507 (2002)
2. Arndtsen B. A., Bergman R. G., Mobley T.A. and Peterson T. H., "Selective intermolecular carbon-hydrogen bond activation by synthetic metal complexes in homogeneous solution", *Acc. Chem. Res.* **28**, 154 (1995)
3. Gradassi M. A. and Green N.W., "Economics of natural gas conversion processes", *Fuel Proc. Tech.* **42**, 65 (1995)
4. Marcela A., Torres E., "Enzymatic activation of alkanes : constraints and prospectives", *Appl. Cata. A: Gen* **272**, 1 (2004)
5. Notomista E., Lahm A., Di Danto A. and Tramontano A., "Evolution of bacterial and archeal multicomponent monooxygenases", *J. Mol. Evol.* **56**, 435 (2003)
5. Duetz W.-A., van Beilen J. B. and Witholt B., "Using proteins in their natural environment: potential and limitations of microbial whole-cell hydroxylations in applied biocatalysis", *Curr. Opin. Biotech* **12**, 419 (2001)
7. van Beilen J. B. and Funhoff E. G., "Expanding the alkane oxygenase toolbox: application", *Curr. Opin. Biotech* **16**, 308 (1005)
8. Murrell J. C., Gilbert B., McDonald I.R., "Molecular biology and regulation of methane monooxygenase", *Arch. Microbiol* **173**, 325 (2000)
9. Shanklin J., Achim C., Schmidt H., Fox B.G. and Münck E., "Mössbauer studies of alkane ω -hydroxylase: Evidence for a diiron cluster in an integral-membrane enzyme", *Proc. Natl. Acad. Sci.* **94**, 2981 (1997)
10. Schmid A., Sonnleitner B. and Witholt B., "Medium chain length alkane solvent-cell transfer rate in two-liquid phase, *pseudomonas oleovorans* cultures", *Biotech. and Bioengg.* **60**, 10 (1998)
11. Ratajczak A., Geißdorfer W. and Hillen W., "Expression of alkane hydroxylase from *Acinetobacter* sp. Strain ADP 1 is induced by a broad range of n-alkanes and requires the transcriptional activator AlkR", *J. Bacteriology* **180**, 5822 (1998)

12. Whyte L. G., Smits T. M. H., Labbé D., Witholt B., Greer C. W. and van Beilen J. B., "Gene cloning and characterization of multiple alkane hydroxylase systems in *Rhodococcus* strains Q15 and NRRL B-16531", *Appl. Environ. Microbiol.* **68**, 5933 (2002)
- 13 Tani A., Ishige t., sakai Y. and Kato N., "Gene structures and regulation of the alkane hydroxylase complex in *Acinetobacter* sp. Strain M-1", *J. Bacteriol.* **183**, 1819 (2001)
14. Marin M. M., Yuste L. and Rojo F., "Differential expression of the components of the two alkane hydroxylases from *Pseudomonas aeruginosa*" *J. Bacteriol.* **185**, 3232 (2003)
15. Stevenson J. A., Westlake A. C. G., Whittock C. and Wong L. L., "The catalytic oxidation of linear and branched alkanes by cytochrome P450_{cam}", *J. Am. Chem. Soc.* **118**, 12846 (1996)
16. Hill F. F., Venn I. and Lukas K. L., "Studies on the formation of long chain dicarboxylic acids from pure n- alkanes by a mutant of *Candida tropicalis*", *Appl. Microbiol. Biotechnol.* **24**, 168 (1986)
17. Peters M. W., Meinhold P., Glieder A. and Arnold F. H., "Regio- and enantioselective alkane hydroxylation with engineered cytochromes P450 BM-3", *J. Am. Chem. Soc.* **125**, 13442 (2003)
18. Groves J. T., Nemo T. E. and Myers R. S., "Hydroxylation and epoxidation catalyzed by iron-porphine complexes. Oxygen transfer from iodosylbenzene", *J. Am. Chem. Soc.* **101**, 1032 (1979)
19. Sherry A. E. and Wayland B. B., "Metalloradical activation of methane", *J. Am. Chem. Soc.* **112**, 1259 (1990)
20. Wayland B. B., Ba S. and Sherry A. E., "Activation of methane and toluene by rhodium porphyrin complexes", *J. Am. Chem. Soc.* **113**, 5305 (1991)
21. Sakuri H., Hataya Y., Goromaru T. and Matsuura H., "A model system for drug metabolism in isolated hepatocytes; oxidation of cyclohexene by metalloporphyrin complexes", *J. Mol. Catal.* **29**, 153 (1985)

22. Ostovic D. and Bruce T. C., "Mechanism of alkene epoxidation by iron, chromium and manganese higher valent oxo-metalloporphyrins", *Acc. Chem. Res.* **28**, 154 (1995)
23. Collman J. P., Hegedus L. S., Norton J. R. and Finke R. G., Principle and applications of organotransition metal chemistry Ch. 7, 2nd edn (Univ. Science, Mill Valley, 1987)
24. Sheldon R. A. and Kochi J. K., Metal catalyzed oxidations of organic compounds Ch. 4 (Academic, New York, 1981)
25. Fryzuk M. D. and Johnson S. A., "The continuing story of dinitrogen activation", *Coord. Chem. Rev.* **200 – 202**, 379 (2000)
26. Lavrushko V. V., Lermontov S. A. And Shilov A. E., "Formation of methyl platinum complex in the reaction of methane with chloroplatinic acid", *React. Kinet. Catal. Lett.* **15**, 269 (1980)
27. Janowicz A. H. and Bergman R. G., "C-H activation in completely saturated hydrocarbons: direct observation of $M + R-H \rightarrow M(R)(H)$ ", *J. Am. Chem. Soc.* **104**, 352 (1982)
28. Sen A., Lin M., Kao L. C. and Huston A. C., "C-H activation in aqueous medium. The diverse roles of platinum (II) and metallic platinum in the catalytic and stoichiometric oxidative functionalization of organic substrates including alkanes", *J. Am. Chem. Soc.* **114**, 6385 (1992)
29. Lin M. and Sen A., "Direct catalytic conversion of methane to acetic acid in an aqueous medium", *Nature* **368**, 613 (1994)
30. Watson, "Methane exchange reactions of lanthanides and early-transition-metal methyl complexes", *J. Am. Chem. Soc.* **105**, 6491 (1983)
31. Bromberg S. E., Yang H., Asplund M. C., Lian T., McNamara B. K., Kotz K. T., Yeston J. S., Wilken M., Frei H., Bergman R. G. and Harris C. B., "The mechanism of a C-H bond activation reaction in room-temperature alkane solution", *Science* **278**, 260 (1997)
32. Periana R. A. and Bergman R. G., "Isomerization of hydridoalkylrhodium complexes formed on oxidative addition of rhodium to alkane C-H bonds.

- Evidence for the intermediacy of η^2 -alkane complex”, *J. Am. Chem. Soc.* **108**, 7332 (1986)
33. Backlund M., Ziller J. and Farmer P. J., “ Unexpected C-H activation of Ru(II)- dithiomaltol complexes upon oxidation”, *Inorg. Chem* **20**, 1000 (2007)
34. Uhl W., Vinogradov A. and Grimme S., “C-H bond activation by hyperconjugation with Al-C bonds and chelating coordination of the hydride ion”, *J. Am. Chem. Soc.* **129**, 11259 (2007)
35. Paneque M., Taboada S. and Carmona E., “C-H and C-S activation of thiophene by rhodium complexes: Influence of the ancillary ligands on the thermodynamic stability of the products”, *Organometallics* **15**, 2678 (1996)
36. Paneque M., Poveda M. L., Salazar V., Carmona E. and Ruiz-Valero C., “Unexpected reactivity of 2,5-dimethylthiophene towards $\text{Tp}^{\text{Me}_2}\text{Ir}(\text{C}_2\text{H}_4)_2$ ”, *Inorg. Chim. Acta* **345**, 367 (2003)
37. Pittard . K. A., Lee J. P., Cundari T. R., Gunnoe T. B. And Petersen J.L., “Reaction of $\text{TpRu}(\text{CO})(\text{NCMe})(\text{Me})$ ($\text{Tp} = \text{hydridotris}(\text{pyrazolyl})\text{borate}$) with heteroaromatic substrates: stoichiometric and catalytic C-H activation”, *Organometallics* **23**, 5514 (2004)
38. Bharath A ., Santra B. K., Munshi P. and Lahiri G. K., “Cobalt-mediated selective C-H bond activation. Direct aromatic hydroxylation in the complexes $[\text{Co}\{\text{o-OC}_6\text{H}_3(\text{R})\text{N}=\text{NCH}_4\text{N}\}_2]\text{ClO}_4\cdot\text{H}_2\text{O}$ (R = H, o-Me/Cl, m-Me/Cl or p-Me/Cl). Synthesis, spectroscopic and redox properties”, *J. Chem. Soc., Dalton Tans.*, 2643 (1998)
39. Ito J., Shiomi T. and Nishiyama H., “Efficient preparation of new-rhodium- and iridium-[bis(oxazoliny)-3,5-dimethylphenyl] complexes by C-H bond activation: applications in asymmetric synthesis”, *Adv. Synth. Catal.* **348**, 1235 (2006)
40. Burling S., Paine B. M., Nama D., Brown V. S., Mahon M. F., Prior T. J., Pregosin P. S., Whittlesey M. K. and Williams J. M. J., “C-H activation of ruthenium N-heterocyclic carbene complexes: application in a catalytic tandem reaction involving CC bond formation from alcohols”, *J. Am. Chem. Soc.* **129**, 1987 (2007)

41. Sakakura T., Sodeyama T., Sasaki K., Wada K. And Tanaka M., "Carbonylation of hydrocarbons via C-H activation catalyzed by RhCl(CO)(PMe₃)₂ under irradiation", *J. Am. Chem. Soc.* **112**, 7221 (1990)
42. Bolig A. D. and Brookhart M., "Activation of sp³ C-H bond with cobalt(I): catalytic synthesis of enamines", *J. Am. Chem. Soc.* **129**, 14544 (2007)
43. Chen M. S. and White M. C., "A predictably selective aliphatic C-H oxidation reaction for complex molecule synthesis" *Science* **318**, 783 (2007)
44. Shilov A. E., "Chemical models of metallo-enzymes", *J. Mol. Catal.* **47**, 351 (1988)
45. Lipscomb J. D., *Annu. Rev. Microbiol* **48**, 371 (1994)
46. Sono M., Roach M. P., Coulter E. D. and Dawson J. H., *Chem. Rev.* **96**, 2841 (1996)
47. Bernhardt R., "Cytochromes P40 as versatile biocatalysts", *J. Biotech.* **124**, 128 (2006)
48. Williams P. A., Cosme J., Ward A., Angove H. C., Vinkovic D. M. and Jhoti H., "Crystal structure of human cytochrome P450 2C9 with bound warfarin", *Nature* **424**, 464 (2003)
49. Feiters M. C., Rown A. E. and Nolte R. J. M., "From simple to supramolecular cytochrome P450 mimics", *Chem. Soc. Rev.* **29**, 375 (2000)
50. Shaik S., de Visser S. P., Ogliaro F., Schwarz H. and Schröder D., "Two-state reactivity mechanisms of hydroxylation and epoxidation by cytochrome P-450 revealed by theory", *Curr. Opin. Chem. Bio.* **6**, 556 (2002)
51. Deeth R. J. and Dalton H., "Methane activation by methane monooxygenase: free radicals, Fe-C bonding, substrate dependent pathways and the role of the regulatory protein", *J. Bio. Inorg. Chem.* **3**, 302 (1998)
52. Siegbahn P. E. M., Crabtree R. H. and Nordlund P., "Mechanism of methane monooxygenase - a structural and quantum chemical perspective", *J. Bio. Inorg. Chem.* **3**, 314 (1998)
53. Sazinsky M. H. and Lippard S. J., "Correlating structure with function in bacterial multicomponent monooxygenases and related diiron proteins", *Acc. Chem. Res.* **39**, 558 (2006)

54. Murray L. J. and Lippard S. J., "Substrate trafficking and dioxygen activation in bacterial multicomponent monooxygenase", *Acc. Chem. Res.* **40**, 466 (2007)
55. Zhang J., Zheng H., Groce S. L. and Lipscomb J. D., "Basis for specificity in methane monooxygenase and related non-heme iron-containing biological oxidation catalysts", *J. Mol. Catal. A* **251**, 54 (2006)
56. http://en.wikipedia.org/wiki/Methane_monooxygenase
57. Samuelsson B., Dahlen S. E., Lindgren J. A., Rouzer J. A. and Serhan C. N., "Leukotrienes and lipoxins: structures, biosynthesis, and biological effects", *Science* **237**, 1171 (1987)
58. Schilstra M. J., Veldink G. A. and Vliegthart J. F. G., "The dioxygenation rate in lipoxygenase catalysis is determined by the amount of Iron (III) lipoxygenase in solution", *Biochemistry* **33**, 3974 (1994)
59. Nelson M. J., "Evidence for water coordinated to the active site iron in soyabean lipoxygenase-1", *J. Am. Chem. Soc.* **110**, 2985 (1988)
60. Jonas R. T. and Stack T. D. P., "C-H bond activation by a ferric methoxide complex: a model for the rate determining step in mechanism of lipoxygenase", *J. Am. Chem. Soc.* **119**, 8566 (1997)
61. Costas M., Chen K and Que Jr. L., "Biomimetic nonheme iron catalysts for alkane hydroxylation", *Coord. Chem. Rev.* **200-202**, 517 (2000)
62. Barton D. H. R., Hay-Motherwell R. S. and Motherwell W. B., "Further studies on the activation of the C-H bond in saturated hydrocarbons", *Tetrahedron* **24**, 1979 (1983)
63. Kokusen H., Sohrin Y., Kihara S. and Matsui M., "Complex formation reaction of polypyrazolylborates with divalent metal ions in aqueous solution studied by solvent extraction technique", *Anal. Sci.* **7**, 7 (1991)
64. Szécsényi K. M., Leovac V. M., Jaćimović Ž. K., Češljević V. I., Kovács A., Pokol G. and Gál S., "Transition metal complexes with pyrazole-based ligands", *J. Therm. Ana. Calori.* **63**, 723 (2001)
65. Sheldon R. A. and Dakka J., "Heterogeneous catalytic oxidations in the manufacture of fine chemicals", *Cata. Today* **19**, 215 (1994)

66. Clerici M. G. and Ingallina P., "Oxidation reactions with in situ generated oxidants", *Cat. Today* **41**, 351 (1998)
67. Cho J., Furutachi H., Fujinami S., Tosha T., Ohtsu H., Ikeda O., Suzuki A., Nomura M., Uruga T., Tanida H., Kawai T., Tanaka K., Kitagawa T. and Suzuki M., "Sequential reaction intermediates in aliphatic C-H bond functionalization initiated by a bis(μ -oxo)dinickel(III) complex", *Inorg. Chem.* **45**, 2873 (2006)
68. Hikichi S., Komatsuzaki H., Akita M. and Moro-oka Y., "Aliphatic C-H bond oxygenation by the CoIIIOOX species with the hindered hydrotris(pyrazolyl)borate ligand (X = Co(II), alkyl, H)", *J. Am. Chem. Soc.* **120**, 4699 (1998)
69. Parshall G. W., "Intramolecular aromatic substitution in transition metal complexes", *Acc. Chem. Res.* **3**, 139 (1970)
70. Dehand J. and Pfeffer M., "Cyclometallated compounds", *Coord. Chem. Rev.* **18**, 327 (1976)